A Study on the effect of β-adrenergic Stimulation on the Electrophysiology of the Isolated Heart

Annabel Sarah Campbell, B.Sc (Hons), MRes

Submitted in fulfillment of the degree of

Doctor of Philosophy

To

Institute of Cardiovascular and Medical Sciences

School of Medical, Veterinary and Life Sciences

University of Glasgow

March 2017

Abstract

Background

A coordinated heart beat relies on the propagation of a rapid depolarising event throughout the atria and ventricles and the subsequent coupling of this electrical signal to a transient contraction in every atrial and ventricular cardiomyocyte. The rate of propagation, known as conduction velocity (CV) is mainly determined by cellular expression of Na channels and gap junctional proteins (connexins), however there is emerging evidence that both proteins may be functionally regulated by intrinsic signaling processes. Previous studies indicate that stimulation of the β-adrenergic pathway increases CV, but little consistent data exists on the magnitude, associated adrenoreceptor pharmacology or time course of the effect. This study investigates the effect of β-AR stimulation – using either the β-agonist isoproterenol (ISO) or by directly raising cAMP via addition of Forskolin (Fsk) and/or 3-Isobutyl-1-methylxanthine (IBMX) - on ventricular CV in the intact rat heart. The aim was to measure the response of CV to β-AR stimulation and investigate the mechanisms behind this response. Action potential (AP) and intracellular Ca^{2+} measurements were also made to determine the effect of β-AR stimulation on cellular electrophysiology over the same time-course as the CV response to β-AR stimulation.

Methods

Adult male Wistar rats (250-350g) were euthanized by cervical dislocation and excised hearts retrogradely perfused with modified Tyrode's solution. CV measurements were taken using a custom-built probe, consisting of bipolar stimulating and recording electrode pairs placed flat against the epicardium of the left ventricle (LV). The CV probe also incorporated a fibre-optic light guide, allowing ratiometric measurements of voltage and intracellular Ca^{2+} from the LV epicardium.

Results and Conclusions

β-AR stimulation increased LV longitudinal CV by approximately 10%. This increase in CV was found to be cAMP mediated. This effect was not due to changes in Ca^{2+} handling alone and although an increase in AP amplitude (APA) suggested that I_{Na} was increased, the magnitude was thought insufficient to explain the change in CV. This suggested a potential role for gap junction conductance (GJC) in mediating CV changes. This view was supported by preliminary data indicating the magnitude of the response was larger when measuring transverse CV: transverse conduction involves proportionally more GJC than longitudinal conduction.

β-AR stimulation was confirmed to increase CV, a response mediated via β_1AR subtype, and which required an increase in cAMP: cAMP was increased by activation of adenylyl cyclase (AC) with forskolin (Fsk) or through inhibition of phosphodiesterases (PDEs) by IBMX. The increase in CV was shown to be mediated through the cAMP sensitive kinase, PKA; another cAMP target, Epac, appeared not have a role in this pathway.

Understanding the regulation of CV by β-AR stimulation is crucial to understanding sympathetic regulation of the heart and may lead to further understanding of the interplay between downregulated β-AR signaling and arrhythmia generation in the diseased heart.

Table of Contents

List of Figures

Acknowledgements

There are too many people who have been important to completing this thesis to name everyone, so I'll try and name as many as I can.

Firstly, to both my supervisors, Professor Godfrey Smith and Professor George Baillie, I am very grateful for the chance to work on this project and for all the help and advice I have received. I am especially grateful to Professor Smith, who has been a huge support and inspiration throughout - I honestly can't thank you enough.

I also need to thank Dr. Francis Burton, who has helped with almost every aspect of the project, from the initial setup of the experiments to writing the analysis programs and dealing with my many requests. Thank you!

I'd also like to thank the technical staff, Aileen Rankin and Michael Dunne, whose knowledge, expertise and friendship have been invaluable throughout this project.

I'd like to thank my colleagues and officemates, Dr. Karen McGlynn, Dr. Allen Kelly and Dr. Andrew Allen. You've helped with literally everything, not least keeping me sane.

I really have to thank all of the Smith lab, who have always helped me out when I've needed it. We are lucky to have such a great lab.

Thanks to my Mum and Dad, who have supported my long stint at university and have been there for me every step of the way, and to my wee sister for the motivational phone calls from halfway across the world.

I don't think I can adequately express the contribution my fiancé, Omar, has made. You know I couldn't have done it without you, thank you.

And lastly to my dog Leon, who slept on my feet during most of this write-up and always kept me going.

Author's Declaration

The experimental work described in this thesis was carried out by myself and has not beenpresented as part of any other degree. Some results during the period of research havebeen presented in abstract form and are detailed below.

A. S. Campbell, S.R. Johnstone, G. S. Baillie, G. L. Smith: β-Adrenergic modulation of myocardial conduction velocity: Connexins vs. sodium current. J. Mol. Cell. Cardiol. 77, 147–154. doi:10.1016/j.yjmcc.2014.09.030

A. S. Campbell, F. L. Burton, G. S. Baillie, and G. L. Smith: Action Potential Conduction Velocity is Increased by Raised Intracellular cAMP in the Intact Rat Heart via a CaMKII Mediated Pathway. Abstract - Biophysical Society annual meeting San Francisco, California. *Biophysical Journal* 2014 **106(2).**

A. S. Campbell, F. L. Burton, G. S. Baillie, and G. L. Smith: Changes in conduction velocity and action potential characteristics with increases of intracellular cyclic adenosine monophosphate in the intact rat heart. Abstract - EHRA Europace 2013 meeting Athens. Volume: 15 suppl 2

Abbreviations

2P 2-photon

6Bnz N6-benzoyladenosine-3',5'-cyclic monophosphate

8CPT 8-(4-chlorophenylthio)-2'-O-methyladenosine-3',5'-cyclic monophosphate,

AC Adenylyl cyclase

AM Acetoxymethyl ester

ANS Autonomic nervous system

APA Action potential amplitude

APD Action potential duration

BDM 2,3-butanedione monoxime

CaA Calcium transient amplitude

CaD - Ca^{2+} transient duration

CaMKII Ca^{2+}/calmodulim-dependent protein kinase II

cAMP Cyclic adenosine monophosphate

CGP CGP 20712A

Ch1 Channel 1

CV Conduction velocity

CV_L Point of highest CV

CV_T Transverse conduction velocity

Cx Connexin

dbcAMP Dibutyryl cAMP

DI Diastolic interval

EBZ Epicardial border zone

Epac Exchange protein directly activated by cAMP

ERP Effective refractory period

Fsk Forskolin

GJ Gap Junction

GJC Gap junctional conductance

GPCRs G-protein-coupled receptors

IBMX 3-Isobutyl-1-methylxanthine

I_{Ks} The slow inward K^+ current

I_{Na} Voltage-sensitive sodium current

ISO Isoproterenol

LED Light-emitting diode

LTCC L-type Ca^{2+} channel current

LV Left ventricle

MAPK MAP kinase

ME Microelectode

Na_v 1.5 Voltage sensitive Na channel

NRCMs Neonatal rat cardiac myocytes

PKA Protein kinase A

PLB Phospholamban

PLCε Phospholipase Cε

PMT Photomultiplier tube

Rap Ras-related protein

RyR2 Ryanodine receptor

SERCA2 Sarcoplasmic/endoplasmic reticulum Ca^{2+} ATPase

SpcAMPs Adenosine- 3', 5'- cyclic monophosphorothioate, Sp-isomer; a specific activator of cAMP dependent protein kinases

TAct Time until activation

TGN Trans-golgi network

TRise The time between 10 and90% of the upstroke

β-AR β-adrenoreceptors

1. Introduction

1.1 The heart as a functional syncytium

A coordinated heart beat relies on the propagation of a rapid electrical depolarising event, the action potential (AP), throughout the atria and ventricles and the subsequent coupling of this electrical signal to a transient contraction in every atrial and ventricular cardiomyocyte. Adult cardiomyocytes are elongated cells approximately 0.12mm long and 0.02mm in diameter. The contractile proteins within the cells are arranged longitudinally and the associated longitudinal mechanical force is transmitted to adjacent cells via complex bridging structures at the end of cells known as intercalated discs. These structures contain protein complexes called zona-adherins that provide mechanical cell-to-cell linkages (Giepmans, 2004) and specialised structures, termed gap-junctions (GJs),that allow the electrical coupling of adjacent cells by linking adjacent surface membranes with a protein channel. Clusters of GJs (called plaques) appear at the intercalated disc and to a lesser extent along the lateral membranes of the heart cells (Palatinus et al., 2012; Verheule et al., 1997).

1.2 The Cardiac AP

1.2.1 The Ventricular AP

The cardiac AP is the membrane potential (E_m) waveform which leads to the raise in intracellular [Ca^{2+}] that ultimately leads to contraction of the myocyte. It is created by the interplay of the many different ion channels and transporters present in the myocyte, and it has different properties in different regions of the heart. As this thesis focuses on conduction within the myocardium, this introduction will focus on the properties of the ventricular AP.

The ventricular AP has a stable resting E_m of -80mV and is primarily maintained by I_{K1} channels (Levick, 2000). The resting cardiac myocyte is preferentially permeable to K and E_m is therefore close to the equilibrium potential (or Nernst potential) for K^+: it is not exactly the Nernst potential for K^+ (-89mV) as the cardiac myocyte contains many ion channels and is not impermeable other ions (Bers, 2001; Kaneshiro, 2011). The ventricular AP has a rapid upstroke driven largely by activation of voltage sensitive Na^+ channels which reaches between +30-50mV, followed by the characteristic 'notch' and a prominent plateau phase (Bers, 2001). The AP is triggered by current spread from neighbouring activated

myocardium: this current spread is passive and occurs primarily through gap junctions, as discussed in section 1.8. This causes the depolarisation of the E_m to a threshold where enough Na^+ channels are activated that $I_{Na}>I_K$ (Kléber and Rudy, 2004).

The long APD of the ventricular AP is due to the plateau phase: the plateau phase is a phase in the AP where the E_m does not change rapidly. It maintains depolarisation, preventing reactivation of Na^+ and Ca^{2+} channels and therefore preventing electrical re-excitation (Bers, 2001).

An outline of the rabbit ventricular AP taken from Bers 2001 and the main ionic currents behind it is shown below (Fig. 1.2.1; Bers, 2001). There are 4 main phases to the AP which are outlined below:

Phase 0: Rapid upstroke

Passive spread of current from activated regions depolarises the membrane and leads to activation of voltage sensitive Na^+ channels ($Na_v1.5$), causing a rapid increase in I_{Na} and depolarising of E_m to ~30-50mV. Depolarising E_m also inactivates I_{K1} and activates voltage sensitive Ca^{2+} channels (Ca_L). At the AP peak, I_{Na} is at its maximum activation and I_{Ca} is at 43% of maximum.

Phase 1: Early Repolarisation

This is characterised by the 'notch' seen in the cardiac AP. $Na_v1.5$ channels rapidly inactivate (this is further explained in 1.2.3) and I_{to} and $I_{Ca(Cl)}$ are activated. Sarcoplasmic reticulum Ca^{2+} release causes inactivation of I_{Ca}.

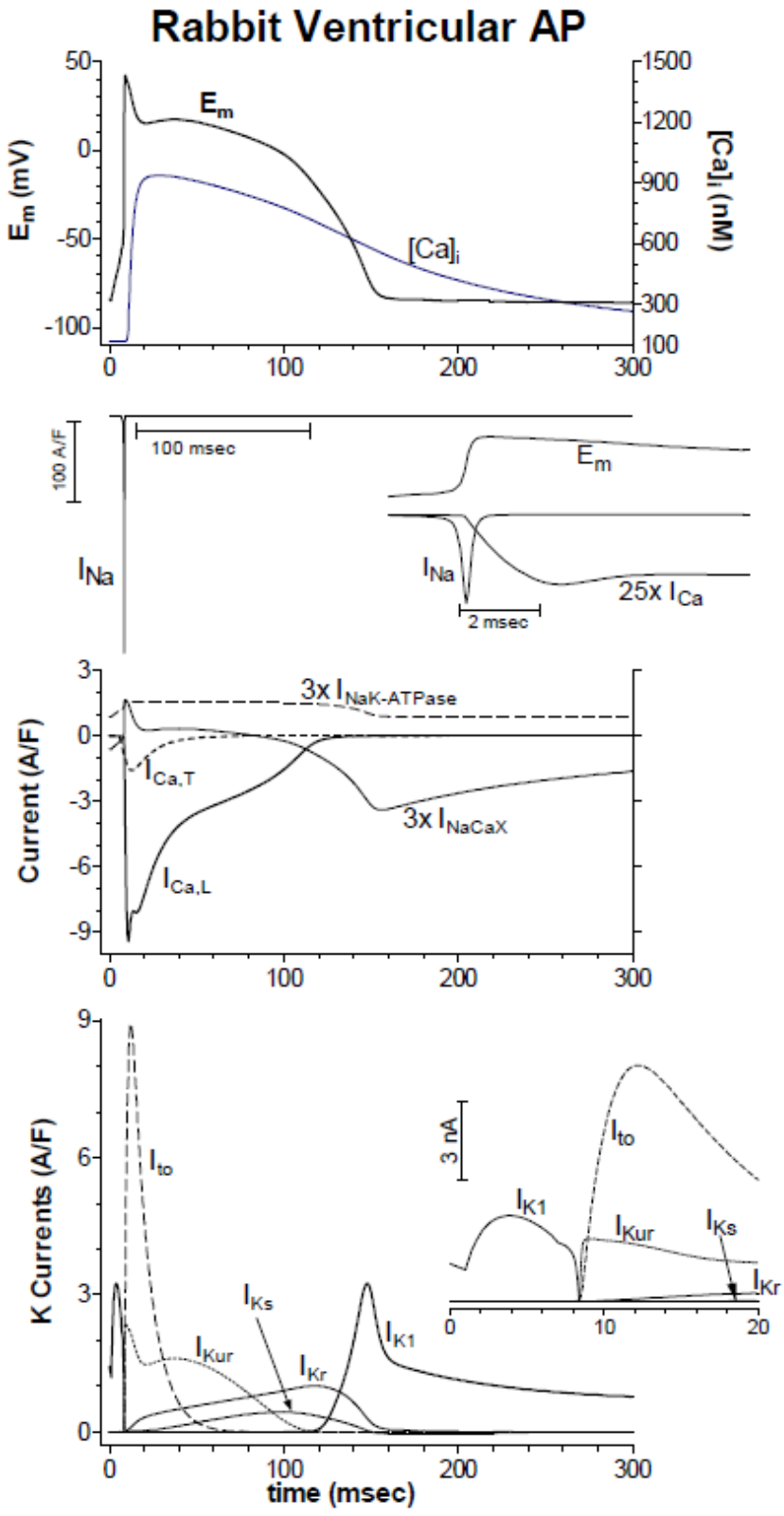

Figure 1.2.1: Calculated E_m, ionic currents and $[Ca]_i$ during a rabbit AP, taken from Bers, 2001.
This figure shows the rabbit ventricular AP alongside the ionic currents which generate the AP.

Phase 2: Plateau Phase

E_m does not change rapidly during the plateau phase. This phase is governed primarily by a combination of inward I_{CaL} and outward delayed rectifier K^+ currents (I_{Kur}, I_{Ks} and I_{Kr}),: the net influence of this is that there is little change in overall E_m.

Phase 3: Late Repolarisation

During late repolarisation, E_m rapidly repolarises back to resting E_m. As repolarisation increases, I_{Kr} increases, accelerating repolarisation. At more negative E_m, I_{Kr} inactivates and I_{K1} reactivates (at around -30mV). $I_{Na/Ca}$ acts in the direction of Ca^{2+} extrusion, due to high intracellular [Ca^{2+}].

1.2.2 Cardiac Ion channels

The waveform of the cardiac AP is determined by of ion channels and transporters, the activity of which alter E_m. Ions carry a charge and therefore cannot easily cross the hydrophobic lipid bilayer and require membrane translocators – in the form of ion channels, transporters or exchangers – to cross the cell membrane. Ion channels are complex protein channels in the cell membrane that provide an aqueous pore which allows the diffusion of ions across the cell membrane along their electrochemical gradient. The movement of ions across the membrane is ionic current, dennoted as 'I' (Aidley, 2008; Jalife et al., 2009; Kaneshiro, 2011).

Ion channels are characterised by two main properties:

i) Gating: the ability to exist in an opened or closed state. This occurs in response to appropriate stimulus: this stimulus can be electrical (voltage-gated); chemical (ligand gated) or mechanical (stretch). Switching between an open and closed state requires a conformational change in the channel which alters the conductance of the channel, denoted as 'g' (Catterall, 2012; de Lera Ruiz and Kraus, 2015) An example of voltage gating – the voltage-gated Na^+ channel – is explained below (1.2.3).

ii) Selectivity: ion channels discriminate between different species of ion, allowing the diffusion of particular ions across the membrane (Catterall, 2012). Again, a detailed example of ion channel selectivity is discussed below using $Na_v1.5$ as an example.

1.2.3 The Voltage Sensitive Na channel

The amplitude and shape of the AP is a major determinant of conduction in the heart, particularly phase 0: the upstoke (this is further discussed in 1.6). I_{Na} and the availability of Na^+ channels are a major determinate of membrane excitability and form the 'source' for cardiac propagation (Kléber and Rudy, 2004). Therefore, for this thesis it is important to understand the structure and function of the voltage-gated Na^+ channel ($Na_V1.5$). Voltage-gated Ca^{2+} channels and some K^+ channels share a similar structure to $Na_V1.5$ (Bers, 2001).

Voltage-gated Na^+ currents were originally discovered in the giant squid axon by Hodgkin and Huxley in 1952 (Hodgkin and Huxley, 1952). Na^+ channels were found to have 3 states: closed (resting); open conducting; inactivated.

The voltage-gated Na^+ channel is composed of one α subunit and 1 or 2 β subunits. There are nine subtypes of α subunit: $Na_V1.5$ is the α subunit expressed in cardiac tissue. $Na_V1.5$ is a single chain polypeptide 260kDa in size. It contains 4 homologous domains arranged in a pseudotetramic structure: DI-DIV. Each of these domains contains 6 transmembrane domains (S1-S6) (Catterall, 2012).

As previously discussed in 1.2.2, $Na_V1.5$ is a voltage gated channel. It is in the closed state at the resting membrane potential of -80mV. On depolarisation, the Na^+ channel opens. The voltage sensors of the Na^+ channel is composed of transmembrane α segments S1-4. The four voltage sensing domains are arranged around the central aqueous pore. The S4 domain is positively charged and lies at the centre of the pore. On depolarisation, it is believed that the S4 domain moves towards the extracellular surface (Yang et al., 1996): the voltage sensitive domains are flexible as they contain a positively charged arginine and lysine for every third amino acid (Catterall, 1988). Linkers between the voltage sensitive segments and the pore confer a conformational change to the pore, switching the channel into the 'open' state. This allows the movement of Na^+ down its electrochemical gradient into the cell – this gradient is established by the Na-K ATPase (de Lera Ruiz and Kraus, 2015).

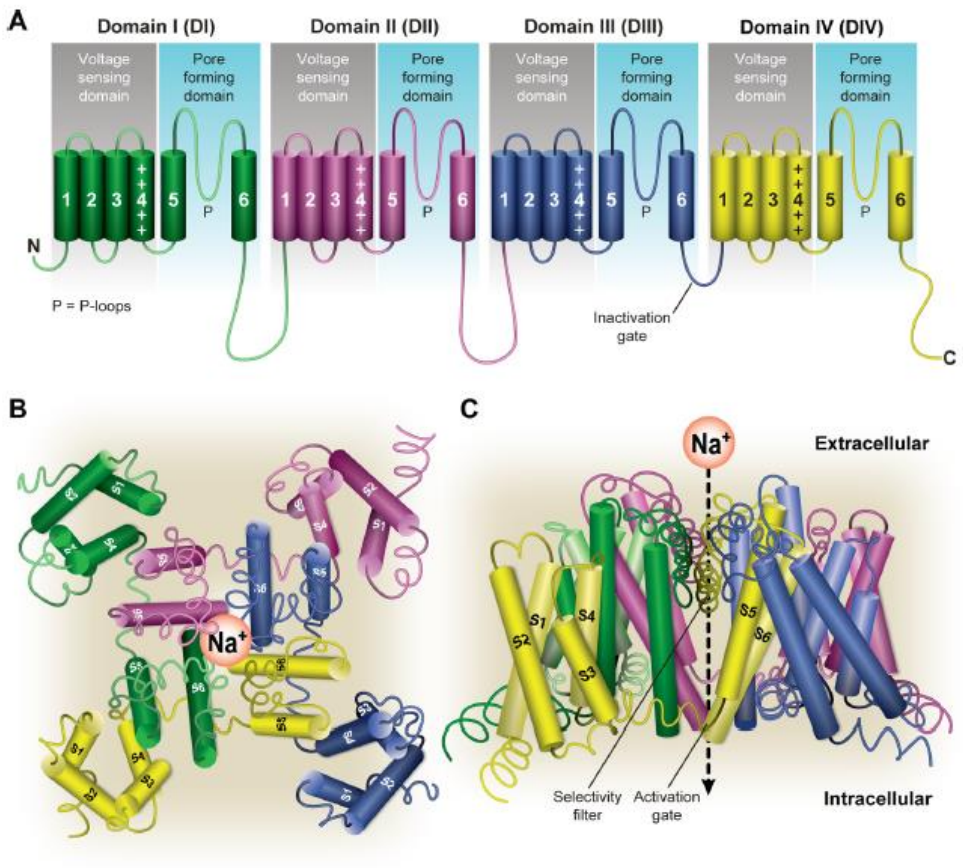

Fig. 1.2.3: Na_V channel architecture (Lera Ruiz de and Kraus, 2015)
(A) *Topology of the human Na_V α subunits.* ***(B)*** *Extracellular view of the open-channel conformation crystal structure of Na_VMs, a marine bacterium from Magnetococcus sp.* ***(C)*** *Side view of the open-channel conformation crystal structure of bacterial Na_VMs, showing the selectivity filter and activation gate.*

During depolarisation, inactivation of the Na^+ channel occurs rapidly due to the inactivation gate. This consists of the intracellular loop connecting DIII and DIV: this loops forms a 'hinged lid' which is believed to fold into the centre of the pore during inactivation. This cause the 'rapid' inactivation of Na^+ channels (Catterall, 2012; de Lera Ruiz and Kraus, 2015).

Membrane repolarisation is required for the reactivation of $Na_V1.5$ – therefore Na^+ channels are inactive during the AP and a second activation of the myocyte cannot be elicited (absolute refractory period). The rate at which Na^+ channels recover depends on how negative the E_m is. Therefore, the more negative the E_m, the faster the recovery of Na^+ channels and the higher the Na^+ channel availability (Bers, 2001).

The pore itself is composed of the S5 and S6 transmembrane helices and the extracellular connecting pore loops. The pore confers the ion selectivity of the Na^+ channel. Ion

selectivity in part relies on steric hindrance: the narrowest part of the pore is 3.5x5.1Å and allows hydrated Na^+ ions to pass through the channel. However, this cannot entirely explain ion selectivity, otherwise smaller ions would be able to pass freely through the Na^+ channel. It also relies on liganding of ions to specific sites on the pore where energy conditions favour the binding of the ion to which the channel is permeable (Aidley, 2008). An extracellular outer ring screens for Na^+ and repels it towards a highly Na^+ selective location within the pore. This is formed of the hydroxyl groups of aspartate and glutamate (de Lera Ruiz and Kraus, 2015).

1.2.4 Species differences in the cardiac AP

The animal model used in this thesis is the rat. The rat is a well-established model and widely used model for studying cardiac electrophysiology. However, there are differences between the electrophysiology of the rat compared with larger mammals. These are particularly apparent in the AP shape and duration: rat APs lack the notch and plateau phase seen in humans and larger mammals such as rabbit and dog (Fig 2.1.2). The rat has a much greater I_{to} than larger mammals, leading to rapid early repolarisation. The extent of this early repolarisation eliminates the plateau phase seen in larger mammals (Bers, 2001). Late repolarisation is also different in rats compared to larger mammals due to the contribution of I_{Ks} and I_{Kr}: these currents are much smaller in the rat and contribute far less to repolarisation (Varró et al., 1993). This is particularly important when considering the effect of β-AR signalling on the AP, as β-AR increases I_{Ks} and therefore shortens the AP in large mammals – this is not observed in rat due to the rat AP's rapid repolarisation (Walsh et al., 1988; Walsh and Kass, 1988).

However, for studying propagation of the AP, the rat is still a valid model. $Na_V1.5$ is highly conserved across species, and the upstroke of AP is the component most likely to contribute to CV. Ventricular CV is between 60cm/s and 80cm/s longitudinally with little variation between species (Draper and Mya-Tu, 1959). Connexins – the proteins from which gap junctions are composed – are also conserved across species. It is well established that the main Cx in the ventricle is Cx43, and although there is differential expression of Cx43 the atria, Cx43 is similarly expressed in the ventricle in human and other mammals, including rat (Gros and Jongsma, 1996; van Kempen et al., 1995; Vozzi et al., 1999). This makes the rat a suitable model for the study of ventricular CV.

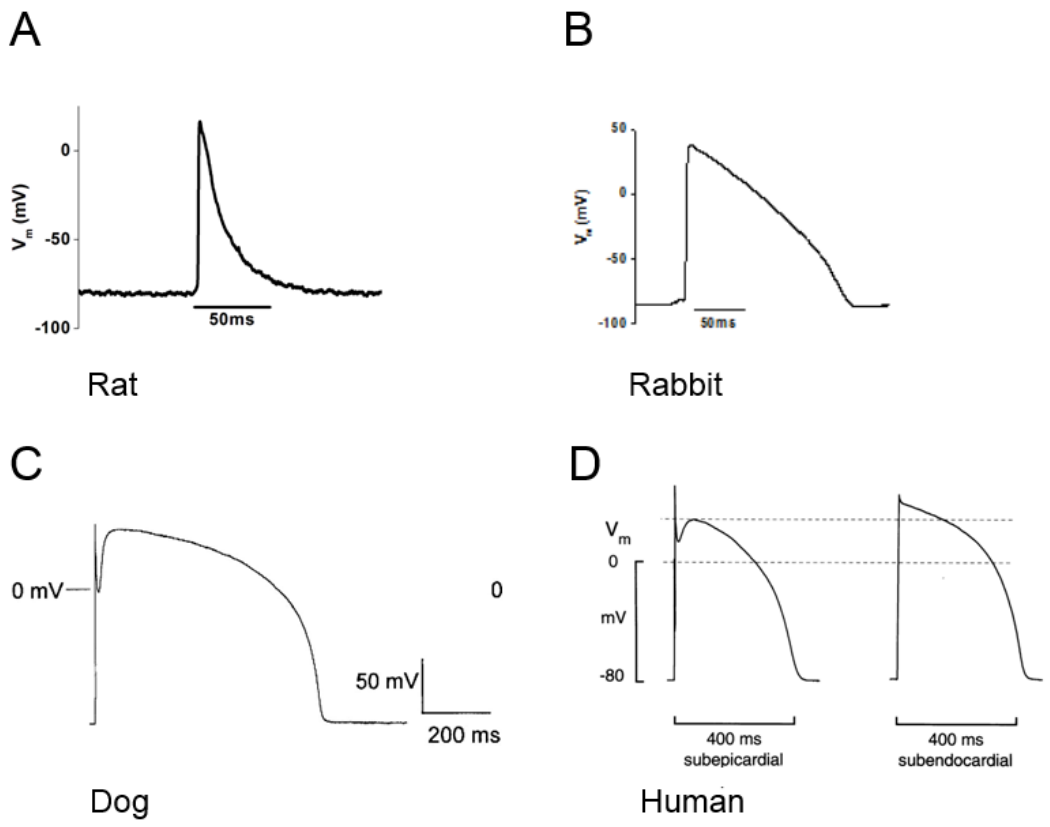

Fig 1.2.4 APs across species.

*Example APs recorded from rat **A)** and rabbit **B)** recorded by ME in lab. **C)** Example dog ventricle AP recorded in isolated cells (Kääb et al., 1996). **D)** Example human APs recorded from isolated human cells (Näbauer et al., 1996).*

1.3 Conduction of Action Potentials in the Ventricle

Cardiac APs propagate along the length of a single cardiomyocyte at approximately 100cm/sec (Cheng et al., 1999); this speed is dictated by the AP shape, particularly the leading phase, and the electrical cable properties of the cell, including the electrical resistance due to the intracellular space (approximately 5MΩ for a cell 0.12mm long)(Rohr, 2004). The resistance of the link between cells provided by the GJs within the intercalated disc is a factor of ~10^4x higher than a comparable length of continuous cytosol (Rohr, 2004). However, the distance that GJs span between cells is ~10^{-4}x the length of the cell, thus the resistance between adjacent cells (5MΩ) is comparable to the resistance along the length of one cardiomyocyte (5MΩ). On this basis, the overall resistance of a series of

cardiomyocytes linked end-to-end is only ~2X that of a single cell of equivalent length and therefore the conduction velocity (CV) is ~1/$\sqrt{2}$ X 100cm/sec, i.e. approximately 70cm/sec. As demonstrated using computational models (Jongsma et al., 1999; Shaw and Rudy, 1997), the dependence of CV on the conductance of GJs is non-linear, with CV being proportional to GJ conductance to the power 0.28: i.e. doubling of GJ conductance would increase CV by approximately 12%. This analysis applies to longitudinal conduction model, where the intercellular resistance is equally distributed between intercalated disc and intracellular resistances. However, conduction transverse to the fibre axis has a larger contribution from intercalated disc resistances relative to the cytoplasmic component for an equivalent distance. Therefore, the effect of changes in overall GJ conductance on CV may be larger in the transverse axis.

A second determinant of CV is the amplitude and shape of the cardiac AP. In particular, CV depends on the rate of depolarisation, which is approximately sigmoidal in time course, rising from 10% to 90% of maximum in 1-2ms with a maximum rate of rise (dV/dtmax) of ~0.1V/msec. Computational modelling has shown that CV is proportional to dV/dtmax (and AP amplitude) raised to the power ~0.5 (Cohen et al., 1981) i.e. doubling dV/dtmax would increase CV by approximately 22%.

Recently studies have shown high levels of Na channels (type NaV 1.5) in the regions of the intercalated disc near connexins. This raises the possibility that Na current flow at one membrane surface could generate negative potential in the narrow gap between cells at the intercalated disc and the subsequent electric field could influence membrane potential of the adjacent cell (Kucera et al., 2002). The same arguments apply to the movement of potassium within the limited extracellular space; this type of transmission between cells (i.e. not involving net ion current flow between cells) is termed ephaptic and the role of this form of cell-to-cell transmission relative to that mediated via gap-junctions is not known (Veeraraghavan et al., 2014). Some studies suggest that ephaptic transmission between adjacent cells is a significant consideration when coupling via gap-junctions is below normal e.g. under ischaemic conditions, in the presence of connexin-blocking drugs (Veeraraghavan et al., 2012) or after significant down-regulation of connexin expression.

The ventricular wall has a complex 3D structure containing bundles of cardiac myocytes surrounded by a connective tissue sheath and arranged in regular sheets termed “laminae”, with the myocytes within these laminae connected end-to-end. On the epicardial surface, these sheets are arranged such that the fibre orientation (long-axis of

the cells) is parallel with the surface and runs approximately 90^{o} to the vertical axis. This angle changes progressively in the myocardial layers between epicardial and endocardial surfaces. By the mid-myocardium, fibre orientation is approximately vertical and by the endocardial surface fibre orientation has turned by another 90^{o} (Gilbert et al., 2011). During a normal cardiac cycle, the activation sequence of the free wall of the right and left ventricles consists of an initial rapid conduction of the AP over the endocardial surface via the Purkinje fibre network followed by propagation through the wall of the ventricle from endocardial to epicardial surfaces via cardiomyocyte-to-cardiomyocyte conduction. As longitudinal fibre orientation runs parallel to the surface of the heart, the conduction from endo to epicardium is at a direction transverse to the fibre axis (Gilbert et al., 2012): The speed of transverse propagation (i.e. 90^{o} to the fibre axis) is approximately 1/2 that along the fibre axis (longitudinal propagation) (Roberts et al., 1979); this is thought to be due to the greater number of gap-junctions (per unit length) transverse to the fibre axis. Therefore, propagation velocity for this final phase of ventricular activation surface is slow (approximately 35cm/sec). For example, in a human left ventricle wall (1-1.5cm in thickness), propagation will take 0.03-0.05s, i.e. a major fraction of the total QRS duration (0.06-0.1s).

Analysis of the timing of different phases of the electrocardiogram indicate significant shortening of the QRS duration during exercise, which is explained in terms of decreased ventricular activation time due to increased CV (Goldberger et al., 1994; Pilhall et al., 1993). These studies showed a decrease of QRS duration by approximately 10% during mild exercise (heart rate approximately 140bpm) in normal healthy adults. The QRS duration is a parameter that can be influenced by a series of factors other than ventricular CV e.g. Purkinje fibre propagation velocity and position and geometry of the heart, but the contribution of increased ventricular CV due to the influence of autonomic nervous system has not been properly investigated.

Interventions which increase heart rate do so through reciprocal changes in activity of the parasympathetic and sympathetic nerves and therefore the effects on the ventricular electrophysiology could be via decreased parasympathetic as well as increased sympathetic activity (Brack et al., 2013b). Furthermore, sympathetic nerves release other neurotransmitters such as neuropeptide Y as well as norepinephrine (Potter, 1988). Thus examining the physiology of autonomic influences is complex; this study is focused on the potential effects of activation of adrenoreceptors on ventricular electrophysiology as one

of the dominant influences on the heart, but it should be recognised that the physiological response is more complex.

1.4 The effect of adrenergic stimulation on ventricular conduction velocity in the intact heart

Most reports of direct measurement of ventricular CV during adrenergic stimulation were published in the 1950s and 60s. These studies were carried out exclusively in dog and looked at the CV response to superfusion of epinephrine and norepinephrine. They showed increased AV-node CV and shortening of its functional refractory period by 40% in response to epinephrine *in vivo*, alongside an increase in ventricular CV (Krayer et al., 1951; Siebens et al., 1953). Decreased ventricular conduction time over the right ventricular epicardial surface in response to epinephrine has also been noted in dog (Mendez et al., 1964), though this study did not differentiate between changes in Purkinje fibre and myocardial conduction. As these studies adminstered catelcholamines *in vivo*, effects of epinephrine remote from the heart can occur making the direct effect of epinephrine on the heart less clear (Siebens et al., 1953; Williams et al., 1972) rather than a direct effect on the heart. In subsequent measurements on isolated dog heart-lung preparations, only small and inconsistent increases in ventricular CV were recorded following epinephrine administration (Swain and Weidner, 1957).

Research has also been carried out looking at direct stimulation of the sympathetic nervous system of the heart. Stimulation of the left stellate ganglion caused an increase in intraventricular CV of approximately 6% (Wallace and Sarnoff, 1964) suggesting direct effects of sympathetic innervation to the heart. A more recent study on isolated rabbit heart with an intact sympathetic innervation described an instantaneous decrease in conduction delay of approximately 30% during sympathetic nerve stimulation but the conduction pathway would have included both ventricle and Purkinje fibres (Ng et al., 2007). As mentioned above, it is important to consider that stimulation of the sympathetic nervous system may also include the activation of pathways other than the β-adrenergic pathway. However, this thesis will focus on the specific effects of the β-AR pathway on conduction.

More recently, the effect of β-stimulation on Purkinje fibre electrophysiology recorded an increase in CV of ~10% without any significant change in the Vmax of the AP upstroke (Gintant and Liu, 1992; Munger et al., 1994). However, due to the relatively short time involving Purkinje fibre conduction, a 10% increase in CV would be anticipated to have a

small effect on the QRS duration, which is primarily influenced by propagation through the myocardium.

In summary, the few studies directly measuring CV within the ventricular myocardium indicate an increased CV during activation of the β-AR pathway, but little consistent data exists on the magnitude, associated adrenoreceptor pharmacology or time course of the effect.

1.5 β-Adrenergic signalling in the heart

Sympathetic nerves release norepinephrine which binds to predominately β-adrenoreceptors (β-ARs), sub-types β1 and β2, causing an increase in force of contraction (positive inotropy) and rate of relaxation (positive lusitropy). The summation of all these effects results in a rapid increase in pump function via increased heart rate and increased force of contraction. In normal human ventricular muscle, β1-ARs are the predominant form (~70% β1:30% β2) (Mendez et al., 1964) and are expressed in both cell surface and T-tubular membranes (Nikolaev et al., 2010). β1-adrenergic receptors are linked via G_s proteins to adenylyl cyclase (AC), and ligand binding to these receptors leads to activation of AC and production of the second messenger, cyclic adenosine monophosphate (cAMP). Protein kinase A (PKA) is activated by cAMP and has many targets in the heart, including multiple ion channels and components of EC-coupling (Hicks et al., 1979; Lehnart and Marks, 2007; Marx et al., 2000; Yue et al., 1990). cAMP also signals via the exchange proteins activated by cAMP (Epac) (Bos, 2006, 2003; Métrich et al., 2008) and by binding directly to ion channels activated by Camp (DiFrancesco and Tortora, 1991). Desensitisation of cAMP signals is undertaken by a superfamily of enzymes known as phosphodiesterases that hydrolyse the second messenger (Baillie et al., 2007).

It is important to consider that multiple signalling pathways use cAMP as an intracellular messenger, for example prostaglandin E1 causes an increase in cellular cAMP concentrations comparable to that seen following β-AR stimulation (Hayes et al., 1979), but the effects of the independent addition of the two agonists on cardiac function is not the same. This data suggested and subsequent studies have gone on to show that cAMP and its effector proteins are compartmentalised within the cell (Baillie, 2009; Vila Petroff et al., 2001). This results in agonist-specific increases of cAMP within certain discrete microdomains, allowing local cAMP -mediated effects (Fischmeister et al., 2006; Mongillo et al., 2004; Zaccolo et al., 2001).

1.6 The effect of β-stimulation on the upstroke of the ventricular action potential.

The amplitude and shape of the cardiac AP is a major determinant of CV, particularly phase 0: the AP upstroke (Buchanan et al., 1985; Kléber and Rudy, 2004). This phase of the AP is caused by activation of voltage dependent sodium channels. These channels are substrates for phosphorylation by PKA (Catterall, 1988; Rossie and Catterall, 1987) and several studies have shown that β-AR stimulation causes an increase in the magnitude of the voltage-sensitive sodium current (I_{Na}) and the AP dV/dt_{max} (Frohnwieser et al., 1997; Lu et al., 1999; Matsuda et al., 1992; Schreibmayer et al., 1994; Wang et al., 1996). Other work has demonstrated that I_{Na} is increased by the action of Ca/CaM-dependent protein kinase II (CaMKII) (Jost et al., 2005). β-AR signalling also influences AP duration (APD) and the relationship between APD and the diastolic interval (restitution). However, the regulation of APD by β-AR signalling is complex; the slowly activating delayed rectifier K^+ channel (I_{Ks}) is a substrate for phosphorylation by PKA; in large mammals, but not rats and mice, β-AR stimulation increases I_{Ks} which promotes APD shortening (Jost et al., 2005; Volders et al., 2003). In whole hearts, sympathetic nerve stimulation or addition of β-agonists increases the steepness of the slope of the APD restitution curve and reduces the effective refractory period (Ng et al., 2007; Taggart et al., 2003). Therefore, the effects of β-AR on the upstroke of the AP are a combination of direct effects on I_{Na} and indirect effects via the diastolic interval that are difficult to predict and have not been measured systematically.

The availability of I_{Na} during the AP upstroke is also limited by the duration of the preceding diastolic interval (DI). The normal positive chronotropic response associated with B-AR stimulation would naturally shorten the DI and hence reduce I_{Na} reactivation. But as described above, APD will shorten both due to the intrinsic rate dependence and the activation of I_{Ks}, both effects helping to maximise the DI and recovery of I_{Na} at higher heart rates.

By examining the relationship between I_{Na}, dV/dt_{max} and CV, estimates can be made of the maximal possible effects of β-AR stimulation of CV via I_{Na}. The measured maximal effect of isoprenaline on I_{Na} reported is variable but on average isoprenaline increased the current by 30-40% (Frohnwieser et al., 1997; Lu et al., 1999; Matsuda et al., 1992; Schreibmayer et al., 1994; Wang et al., 1996). The relationship between I_{Na} and dV/dt_{max} is approximately linear (Cohen et al., 1984; Kléber and Rudy, 2004); according to both theoretical and experimental studies a 40% increase in I_{Na} would increase dV/dt_{max} by approximately 20%.

Several studies have shown that in intact ventricle dV/dt_{max} is proportional to CV^2(Buchanan et al., 1985; Cohen et al., 1984), therefore an estimate of the maximal effect on CV following β-AR stimulation of I_{Na} is an increase of only 4-5%. This requires experimental validation, but it suggests a limit in the extent to which CV may be increased solely through changes in I_{Na}. These results assume that the myocardium can be described by a continuous cable, but work by Spach has shown that relationship between dV/dt_{max} and CV is more complex on the surface of the myocardium (Spach and Dolber, 1986). Recently this relationship was examined using AP measurements in all 3 dimensions of the myocardium. The study concluded that dV/dt_{max} was unaffected by propagation direction deep within the myocardium and that AP rise time was dictated by a balance between I_{Na} and the downstream axial current developed by the myocardium (Kelly et al., 2013).

Given the well documented effects of β-AR stimulation on the amplitude of the L-type Ca^{2+} channel current (LTCC), it is relevant to consider the role of this ionic conductance in determining propagation velocity. Under normal conditions, the role of I_{Na} is dominant; but under conditions of reduced excitability - e.g. chronic depolarisation when I_{Na} may be reduced to <30% of control values - LTCC activity makes a significant contribution to the upstroke of the AP and therefore CV. Therefore, modulation of this by β-AR stimulation may result in a marked increase in velocity as amplitude of LTCC is increased (Kléber and Rudy, 2004; Shaw and Rudy, 1997).

1.7 The effect of adrenergic signalling on intracellular resistance.

Low resistance channels between adjacent caridiomyocytes were first identified in 1975 by Silvio Weidmann's group (Weingart et al., 1975). Measurement of intracellular conductances/resistances during adrenergic stimulation is technically difficult and only a few studies have examined this directly. Intercellular conductance between pairs of neonatal cardiac myocytes increased rapidly by approximately 50% on addition of isoprenaline or dibutyryl cAMP (dbcAMP) (Burt and Spray, 1988). Other studies simply inferred intracellular resistance from CV measurements and examined the effects of more long-term stimulation. For example, a large increase in conduction velocity (~25%) in response to 24 hrs incubation with dbcAMP was reported in cultured rat neonatal cells (Darrow et al., 1996). This was accompanied by an increase in both Cx43 and Cx45 expression within the first 4 hours of exposure to dbcAMP and a causal link was suggested since no significant change in dV/dt_{max} was observed. However, more recent studies using a similar protocol on rat neonatal cardiomyocytes showed an increase in CV and dV/dt_{max} in

response to ISO (de Boer et al., 2007). This suggests I_{Na} is increased alongside any potential changes in intercellular resistance and therefore the potential role of β-AR mediated changes in gap junction conductance are difficult to assess.

1.8 Gap junctions and Connexins

Gap junctions are composed of clusters of thousands of GJ channels (Bruzzone et al., 1996). These consist of two opposing connexon hemichannels docked end to end, one provided by each of the adjacent cells (Maeda and Tsukihara, 2011; Segretain and Falk, 2004). The connexons form a channel which allows the diffusion of ions and proteins up to 1000Da in size, and provide a low resistance pathway for the propagation of electrical impulses between adjacent cells (Verheule et al., 1997).

Each connexon is made up of six connexin subunits: connexins (Cx) are proteins with four transmembrane domains, two extracellular loops and a long intracellular C terminal tail (Bruzzone et al., 1996; Maeda and Tsukihara, 2011; Segretain and Falk, 2004). The Cxs are arranged in a cylinder surrounding a central hydrophilic pore which is tilted along its axis (Unwin and Zampighi, 1980; Yeager, 1998). It has been suggested that sliding or tilting of the subunits may close the pore, though 'ball and chain' type gating mechanisms have also been suggested for some Cx isoforms (Maeda and Tsukihara, 2011). There are at least 21 different isoforms of Cx and connexons can be homo- or heteromeric, consisting of more than one type of Cx (Giepmans, 2004). Cxs are ubiquitously expressed in a number of tissues, electrically and chemically coupling cells throughout the body. Cxs play roles in cell signalling (Bedner et al., 2003; Bruzzone et al., 1996), embryonic development (Wei et al., 2004), and electrically couple neurons, cardiac myocytes and retinal cells. Cxs are synthesised and assembled into the GJ hemi-channels, connexons, in the endoplasmic reticulum (Segretain and Falk, 2004). It has been suggested that Cx43 is an exception to this and is assembled in the trans-golgi network (TGN) (Vanslyke et al., 2009). Connexons are then transported through the golgi stacks to the TGN, where they can be stored or transported to the plasma membrane in vesicles. Cx assembly into connexons occurs before the proteins reach the plasma membrane, allowing incorrectly folded or assembled connexons to be transported to the endoplasmic reticulum for degradation, before insertion into the membrane (Bruzzone et al., 1996). Docking of two connexons, one from each of the adjacent cells, forms the gap junction channel (Yeager, 1998). This occurs through hydrogen bonding between residues of the extracellular loops: these amino acids are highly conserved in different Cx isoforms (Maeda and Tsukihara, 2011).

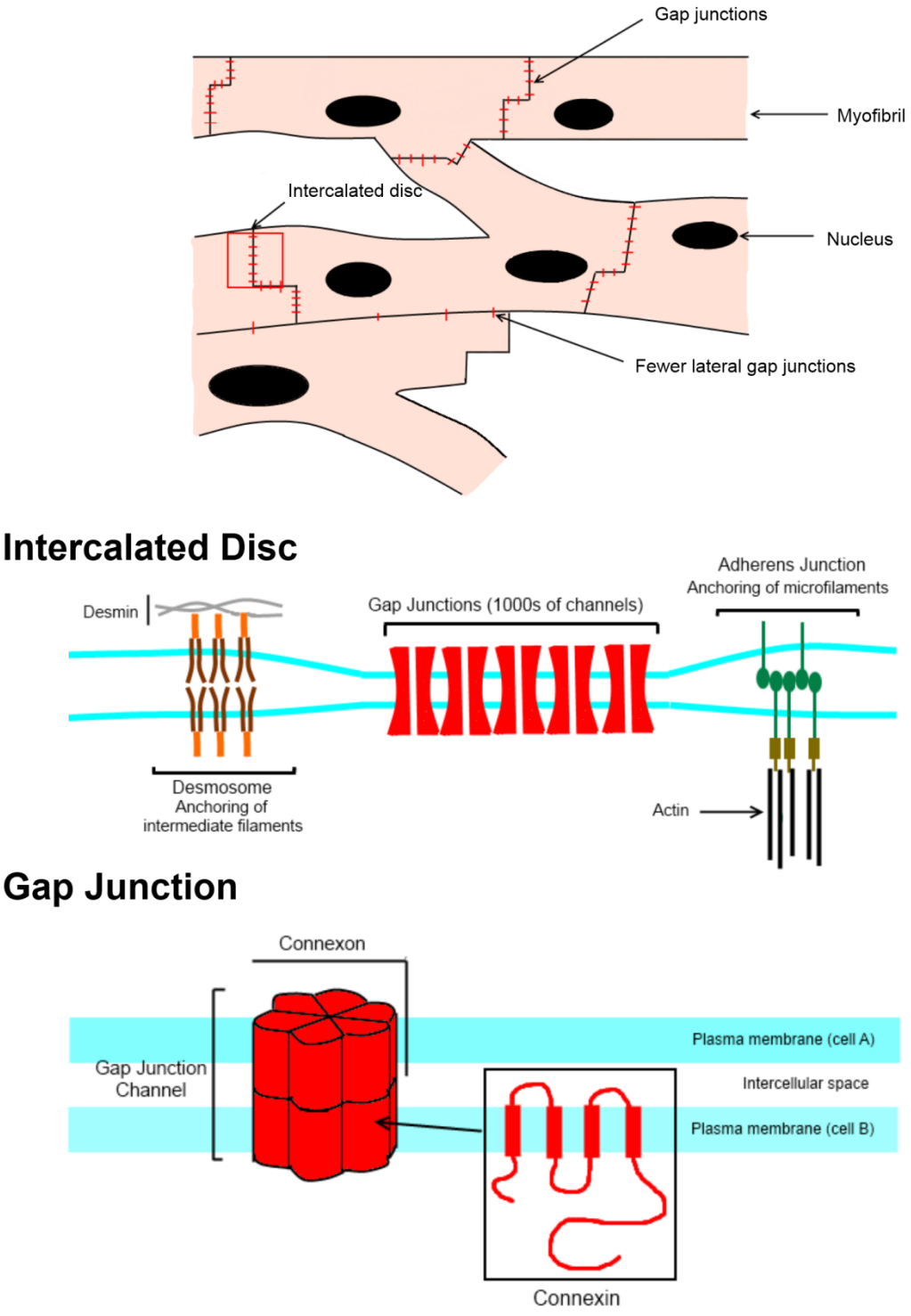

Figure 1.8.1. Gap junctions and the intercalated disc:
Diagram showing the organisation of cardiac myocytes and their communication via the intercalated disc. The intercalated disc contains GJs plaques - made up of 1000s of GJ channels - through which adjacent cells communicate, alongside physical junctions, such as desmosomes and adherens junctions. GJ channels themselves are composed of connexon dimers, with one connexon provided by each of the adjacent cells. Each connexon is composed of 6 connexins.

Once gap junction channels are formed, they cannot be separated into individual connexon hemi-channels (Goodenough and Gilula, 1974). This means the entire channel is internalised for degradation. Both the lysosomal and proteosomal pathways play a role in degradation of connexons (Dunn et al., 2012; Segretain and Falk, 2004). It has been suggested that active proteosomal degradation may play a role in the degradation of phosphorylated Cxs (Beardslee et al., 1998) and that gap junctional conductance (GJC) can be regulated at the level of Cx turnover (Musil et al., 2000).

1.9 Regulation of connexins

Physiologically, GJ function in cardiac muscle is regulated via altering Cx levels, localisation and opening of GJ channels. Cx43 turnover in the heart is dynamic: studies using radioactive labelling have demonstrated that Cx43 has a half life of only 1-2hrs (Beardslee et al., 1998; Laird et al., 1991). The short half-life of Cx43 allows dynamic regulation of Cx expression, synthesis and degradation, which may rapidly alter levels of Cx at the intercalated disc: this may, therefore, influence GJC. Cx43 is also post-translationally modified by various intracellular kinases; this allows rapid regulation of Cx43 channel formation and behavior (Lampe and Lau, 2004).

Cx open probability is altered by intracellular Ca^{2+} and H^{+} concentrations (Ek-Vitorín et al., 1996, p.; Liu et al., 1993) and by various forms of post-translational modification (Johnstone et al., 2012). Cx43 is a phosphoprotein, which is phosphorylated at multiple different sites on the C-terminal tail by kinases including PKA, PKC, PKG and MAPK (Lampe and Lau, 2004; Márquez-Rosado et al., 2012; Solan and Lampe, 2009). Mass spectrometry has also shown that Cx is variably phosphorylated throughout its lifetime (Chen et al., 2013) and its phosphorylation state has been suggested to play a role in almost every aspect of Cx life-cycle and function (Jongsma et al., 1999).

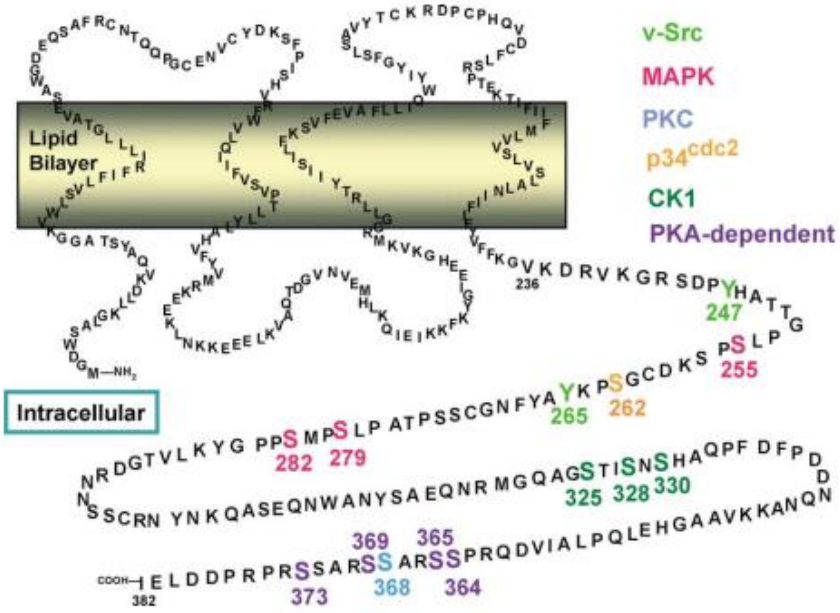

Figure 1.9.1. Schematic of Cx43 and known regulatory sites
Diagram showing the C terminal tail of Cx43 and previously established phosphorylation sites located in this region (Lampe and Lau, 2004).

Multiple signalling cascades play a role in the regulation of Cx43. PKC and MAPK have been shown to increase the probability of Cx being in a 'closed' state, reducing GJC (Johnstone et al., 2012), and have also been shown to play a role in Cx internalisation and degradation (Saffitz et al., 2000). The role of PKA mediated phosphorylation, and therefore β-AR mediated regulation of Cx43, is less clear: Cx43 has multiple PKA consensus sites in its C-terminal tail but the protein is considered a relatively poor substrate for PKA (TenBroek et al., 2001).

1.10 Connexins in the heart

In the heart, the main isoforms of Cx expressed are Cx 43, Cx 40, Cx 37 and Cx 45 (Vozzi et al., 1999). Cx43 is the most abundant Cx and is expressed in all four chambers: it is the main Cx expressed in the ventricles, though Cx37, Cx40 and Cx45 are also expressed at lower levels (Vozzi et al., 1999). Cx40 is expressed mainly in the cardiac conduction system, at levels at least three-fold higher in the nodal and His-Purkinje system than in the ventricle, and also in the atrial myocardium (Kanter et al., 1993). Highest levels of Cx40 are found in the right atria, followed by the left atria and lower expression levels exist in the ventricles (Vozzi et al., 1999). Cx40 forms channels which have higher unitary conductance than Cx43, and higher expression levels of Cx40 may contribute to the distinct conduction properties of the His-Purkinje system (Beblo et al., 1995; Johnstone et al., 2009; Kanter et al., 1993).

Cx45 is also expressed primarily in the conduction system and is found at very low levels in the myocardium (Vozzi et al., 1999).

1.11 Potential signalling pathways for gap junction regulation.

As regulation of the ventricular gap junction protein Cx43 may play an important role in the regulation of CV, recent studies have looked at the way β-AR stimulation may affect Cx43. There are multiple ways GJC could be regulated: through an increase in permeability of gap junction channels, an accumulation of gap junctions in plaques at the intercalated disc or through changes in Cx expression (Giepmans, 2004; Salameh and Dhein, 2011). Regulation by cAMP plays a role in the assembly of Cx43 GJs, with the gap junction plaques shown to be dynamic structures which increase in size in response to increases in cAMP (Holm et al., 1999). TenBroek et al. demonstrated that the cAMP analogue, 8-br-cAMP, increased assembly of Cx43 gap junctions and that the C-terminal tail of Cx43 was required for the reassembly of GJs, with a negative charge on Ser364 improving assembly (TenBroek et al., 2001). However, as they observed little Cx43 phosphorylation in response to PKA, they suggested that increased assembly of Cx43 gap junctions occurs indirectly through a kinase pathway other than PKA (TenBroek et al., 2001). This conclusion was supported by a subsequent report in which cAMP increased dye-transfer and plaque size in Novikoff heptoma cells, but these changes were not seen in the presence of inhibitors of trafficking (Paulson et al., 2000a).

Other studies suggest that regulation of Cx43 is responsible for changes in GJC in response to raised cAMP (Salameh and Dhein, 2011). Treatment of neonatal rat cardiac myocytes (NRCMs) with isoproteronol (ISO) over 24hrs increased Cx43 expression and subsequently increased GJC (Salameh et al., 2006). Transcription of Cx43 in communication deficient cell line – the rat Morris hepatoma cell line – is increased ~40 fold in response to cAMP elevation (Mehta et al., 1992). Changes in expression are reported to occur after longer (24hr) exposures to raised cAMP, which may explain why some studies report no GJC response to acute cAMP concentration increases (Kwak et al., 1995; Neyton and Trautmann, 1985). It has also been suggested that chronic elevation of cAMP may lead to upregulation of MAP kinase (MAPK) pathways, increasing Cx43 expression indirectly (Kanter et al., 1993; Saffitz et al., 2000). Conversely, some studies which report increases in GJC or CV in response to raised cAMP report no changes in Cx43 expression even after prologoned exposure to cAMP (de Boer et al., 2007; TenBroek et al., 2001).

There is some conflict as to whether cAMP and β-AR mediate acute changes via permeability and assembly of gap junctions, or slower changes through the upregulation of gap junction expression. It is possible that both possibilities could occur via distinct cAMP-mediated signaling pathways. Somekawa et al. measured gap junctional permeability by measuring dye-transfer between adjacent cells in neonatal cardiac myocytes (Somekawa et al., 2005). They showed an increase in dye-transfer in response to increased cAMP, accompanied by both increased accumulation of Cx at the intercalated discs and an increase in the size of gap junction plaques. Activation of PKA by the PKA specific activator N^6-benzoyladenosine-3′,5′-cyclic monophosphate (6Bnz) also led to an increase in dye transfer between cells, but with little change in levels of Cx at the intercalated discs. An alternative to the classical PKA pathway is cAMP mediated activation of Epac. The Epac specific activator 8-(4-chlorophenylthio)-2′-O-methyladenosine-3′,5′-cyclic monophosphate (8CPT) led to an increase in dye transfer through increased accumulation of Cx at the intercalated discs (Somekawa et al., 2005). This suggests that cAMP can regulate GJC through both PKA and Epac dependent pathways.

In summary, there is considerable evidence that connexin function can be altered by β-AR stimulation and raised intracellular cAMP, both in the short-term (via phosphorylation or connexin assembly) or long-term (via altered turnover or expression). The majority of these reports use neonatal cardiac preparations to facilitate studies of intracellular pathways and few studies examine the functional consequences in terms of CV or electrophysiological characteristics. Therefore, the role of these pathways in the acute effects of β-AR stimulation on CV in the adult heart remains uncertain.

1.12 The interaction between conduction velocity and action potential duration to cause re-entrant arrhythmias.

APD and CV are important parameters in determining the propensity to re-entrant arrhythmias in the mammalian heart. Under normoxic conditions, the APD is the main determinant of the effective refractory period (ERP) i.e. the time limit after which an area of myocardium can be re-excited. This period multiplied by the CV gives a measure of the electrical “wavelength” of the myocardium. This concept, originating approximately 100 years ago was used to predict the likelihood of re-entrant arrhythmias, i.e. the smaller the electrical wavelength, the more likely that re-entrant arrhythmias would occur within a fixed geometry. Since then several studies have indicated that electrical wavelength is a good predictor of propensity to tachy-arrhythmias (Weiss et al., 2000). In the case of

increased sympathetic nervous system activity, the shortened AP and ERP would be pro-arrhythmic unless there was a commensurate increase in CV. However, the extent to which mediated changes in CV are able to stabilise ventricular electrophysiology in either atrial or ventricular tissue is at present unclear.

Increased sympathetic activity may also modulate arrhythmic activity in the heart by altering the frequency of triggered activity, i.e. non-sinus spontaneous depolarisation in either the atria or ventricle which can initiate sustained arrhythmic activity. Early studies suggest that sympathetic activity increases the frequency of triggered activity, making the occurrence of arrhythmias more likely (Han et al., 1964). Thus, the effect of increased sympathetic activity on the vulnerability of the heart to arrhythmic activity is complex.

1.13 Changes in ventricular conduction in cardiac disease

Poor contractility and susceptibly to arrhythmias characterises heart disease from a variety of different causes. Uncoupling of GJs occurs acutely in ischaemic myocardium and profoundly slows conduction into an ischaemic area (Kléber et al., 1987; Severs et al., 2004). In the surviving myocardium, over longer time periods, gap junctions remodel during heart failure in humans (Severa et al., 2004; Smith et al., 1991) and in animal models of cardiac disease (Matsushita et al., 1999; Smith et al., 1991). Cx43 expression is reduced (Wang and Gerdes, 1999) causing both an overall slowing and increased heterogeneity of CV (Kojodjojo et al., 2006; Peters, 2006). There is also an increased lateralisation of Cx43 in cells at the epicardial border zone (EBZ) of infarcts in canine hearts (Peters et al., 1997). Some studies suggest transverse coupling is decreased to a greater extent than longitudinal coupling in infarcted hearts (Cabo et al., 2006; Yao et al., 2003). It also suggests that Cx43 which has relocalised to lateral membranes may not form functional gap junctions (Cabo et al., 2006). Additionally, reduced Na current also occurs in heart disease and would also contribute to a slowing of CV (Lue and Boyden, 1992; Pu et al., 1998). In inducible models of ischemia, Cx43 redistribution to lateral regions plays a significant role in post-ischemic arrhythmias, facilitated through reduction in PKC-epsilon phosphorylation of Cx43 (O'Quinn et al., 2011). Experimentally increasing phosphorylation of Cx43 at PKC sites (Cx43-S368) in mouse hearts reduces lateralisation and can limit post-infarct arrhythmias (Jozwiak and Dhein, 2008; O'Quinn et al., 2011).

Changes in β-AR signalling are also known to occur in heart failure, typically down-regulation of β1-ARs (to ~50% of control) occurs in response to a chronic increased activity of sympathetic nerves that normally occurs post myocardial infarction (Lohse et al., 2003a).

The proportion of β1:β2 changes to ~50:50 and there is recent evidence in a rat HF model for the loss of the selective of expression β2-ARs in the T-tubular network and subsequent loss of localised cAMP production on selective β2-AR stimulation (Nikolaev et al., 2010). Other aspects of the adrenoceptor pathway are altered in hypertrophic myocardium, including the uncoupling of the remaining receptors from G_s via increased activity of β-AR kinases (Lohse et al., 2003a). Changes in β-AR signalling in heart failure could reduce adrenergic regulation of I_{Na} and/or Cx43 which may attenuate the normal increase in CV that accompanies increase in heart rate. Potentially the limited CV response may affect both the inotropic response and contribute to the generation of arrhythmias.

1.13.2 Cardiac arrhythmias

Normal electrical conduction in the heart involves an AP originating from the sino-atrial (SA) node, conducted through the atria via the atrio-ventricular (AV) node down to the Purkinje fibres and then to the ventricles. Abnormality in the properties of ionic currents can lead to abnormal impulse generation and/or propagation which further leads to electrical disorder in the ventricles. This thesis will focus on the mechanism of arrhythmia generation termed re-entry, as alterations in CV can lead to the generation of re-entry arrhythmias.

Re-entry

Re-entry is the circulation of the cardiac impulse causing repetitive excitation of the heart. It depends upon the occurrence of unidirectional block, causing activation to occur in one direction only. For the arrhythmia to be maintainted, the size of the circuit must exceed the recovery period of the tissue within the circuit. Features which contribute to this are: a large circuit, slow CV or a short effective refractory period (ERP) (Jalife et al., 2009). This can be summarized by the 'wavelength' theory. CV x ERP is defined as the cardiac wavelength. A lower wavelength promotes the generation and maintenance of re-entrant circuit arrhythmias, due to slow CV or a shorter ERP. Therefore, a lower CV could contribute to arrhythmogenesis and in principle, a higher CV could be anti-arrhythmic.

Uncoupling of GJs has been demonstrated to occur in ischaemic regions of the heart (Kléber et al., 1987), which profoundly reduces CV. In surviving regions of the heart, remodeling of gap junctions has been shown to occur in heart failure in humans (Severs et al., 2004; J. Smith et al., 1991) and in animal models (Matsushita et al., 1999). Alongside this, β-AR signaling, particular β_1ARs, has also been demonstrated to be down-regulated in heart failure (Lohse et al., 2003a; Nikolaev et al., 2010). Therefore, understanding the

regulation of CV by β-AR stimulation in heart failure could be key to understanding the changes in disease which lead to the generation of arrhythmias.

1.14 Hypothesis and Aims

Ventricular CV depends on multiple factors, including tissue excitability and intercellular resistance, both of which are potentially modifiable via β-AR stimulation. Despite the key role of ventricular CV in the electrical stability of the mammalian heart, little is known of how it is influenced by the activity of the autonomic nervous system. This introduction has focused on the literature associated with the potential for β-AR stimulation to modulate CV. *In vivo* and *in vitro* studies on whole hearts suggest that sympathetic nerve stimulation increases ventricular CV, but there is uncertainty over the magnitude of this response and little data that would allow the electrophysiological mechanism to be distinguished. *In vitro* studies on isolated cardiac muscle preparations report increases in GJC in response to β-AR stimulation or increasing intracellular cAMP, but the intracellular mechanisms are still unclear to explain both rapid (within 1 minute) or more long term (within several hours) effects on gap junction function. An additional issue is that many of these latter studies are carried out in neonatal cardiac myocytes in which the localisation of Cx is very different to that in adult ventricular myocytes.

Hypotheses:

i) An increase in ventricular CV is a component of the adrenergic response
ii) This increase in CV is mediated by changes in gap junctional conductance
iii) Increased CV in response to adrenergic stimulation is mediated via β-1 adrenergic receptors
iv) Ventricular CV is increased by raised cAMP via a PKA-dependent mechanism

The overall aim of this PhD was to measure and quantify the effects of β-AR activation on CV and determine the relative contribution of changes in AP rise time and intercellular resistance to the response in adult ventricle.

The individual aims of the project were:

i) To develop a method by which CV can be measured in the intact rat ventricular myocardium on a scale which is primarily influenced by changes in cell-cell communication
ii) To determine if β-AR stimulation altered CV in the intact rat heart and to determine if this was a cAMP mediated response

iii) To develop a method by which APs and Ca^{2+} transients can be simultaneously measured from the site at which CV is recorded using fluorescent dyes, Di-4-ANEPPS and Fura-4-AM

iv) To record the effect of β-AR stimulation on the ventricular AP and Ca^{2+} transient over the same time course as the CV response and determine if changes in cardiac electrophysiology cause the change in CV

v) To examine the effect of Ca^{2+} on CV by altering extracellular Ca^{2+} and using the L-type Ca^{2+} channel inhibitor, Nifedipine

vi) To investigate the signalling pathway responsible for the change in CV via inhibitor studies

vii) To determine if a change in CV in response to β-AR stimulation is primarily mediated by gap junctions

2. General Methods

2.1 Modified Tyrode's Solution

93mM NaCl, 20mM NaHCO3, 1mM Na2HPO4, 1mM MgSO4.7H2O, 5mM KCl, 20mM Na^+ acetate, 25mM glucose. Solution contained 1.8mM $CaCl_2$ unless otherwise stated. The solution was filtered through a 5µm filter (Millipore) and continuously bubbled with a gaseous mixture containing 95% O2 and 5% CO2 to maintain pH 7.4

2.2 Preparation: Langendorff perfused rat heart

Adult, male Wistar Han rats (Envigo, UK) were used in these experiments. These rats were weight-matched at 250-300g. All procedures were carried out in accordance with the Animals Scientific Procedures Act (ASPA, 1986). Rats were euthanized by cervical dislocation and the hearts excised and placed in chilled modified Tyrode's solution. The hearts were Langendorff perfused with oxygenated modified Tyrode's solution gassed with 95% oxygen and 5% CO_2 to maintain oxygenation and pH7.4. Hearts were perfused at a constant flow rate – rather than constant pressure – of 12ml/min using a peristaltic pump. Pressure was continually monitored using an inline pressure monitor, and typical pressure readings were between 40-60mmHg. The perfusate was maintained at a temperature of 37°C.

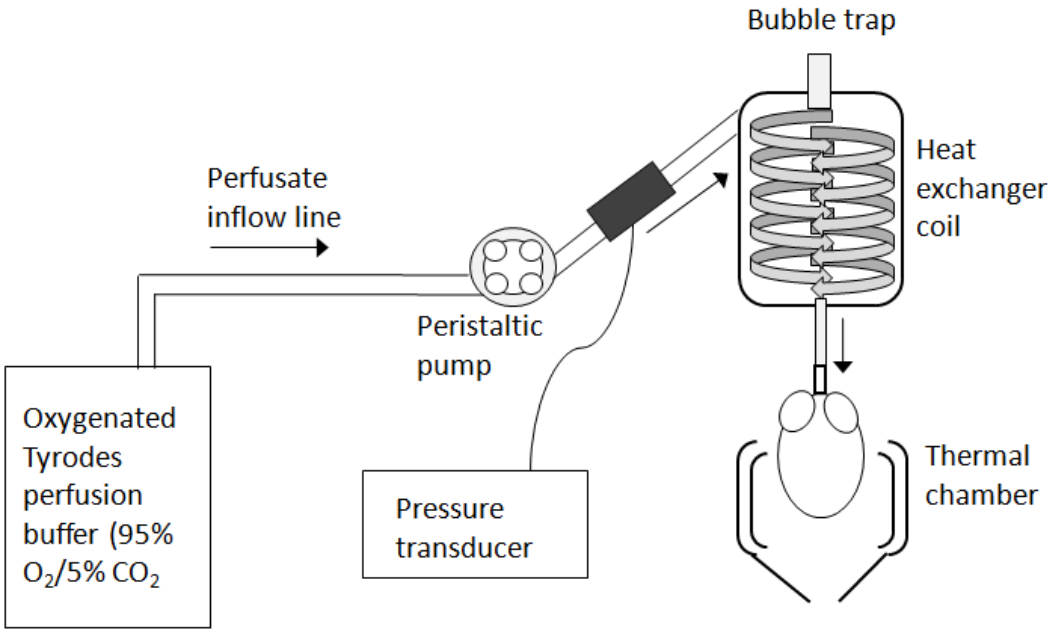

Fig. 2.2.1 Diagram of the Langendorff setup
Oxygenated Tyrode's was retrogradely perfused through the rat aorta and then to the coronary arteries. A peristaltic pump was used to keep the flow of Tyrode's at a constant rate. A bubble trap and heat exchange coil protected the heart from air bubbles - which would block the blood vessels of the heart - and kept the Tyrode's solution at 37°C at the point it reached the heart. The heart was cannulated and suspended from the aorta, allowing it to contract freely. A pressure transducer was used to record the pressure in the system.

2.3 Conduction Velocity Recordings

Electrode Design and Analysis

Measurements were taken using custom electrodes, consisting of silver bipolar stimulating electrodes and two sets of silver bipolar recording electrodes in fixed positions. Channel 1 (Ch1) recording electrodes were positioned a fixed distance apart from Channel 2 (Ch2) recording electrodes and set in epoxy. These electrodes were placed flat against the epicardium of the LV (Fig. 2.3.1A). CV was recorded by pacing continuously on the epicardium at a fixed interval and recording the signals from the Ch1 and Ch2 recording electrodes continuously at a sampling rate of 20kHz. The difference in time between the peaks on the Ch1 and Ch2 electrodes was taken as the difference in time between activation of the LV at each pair of electrodes. As the distance between these electrodes was known, CV could be calculated using CV=Distance/time. Heart rate was recorded in unpaced hearts by measuring the time difference between peaks on a single channel.

Recordings were made using software written in house: ACQ1 (Dr. Francis Burton, University of Glasgow).

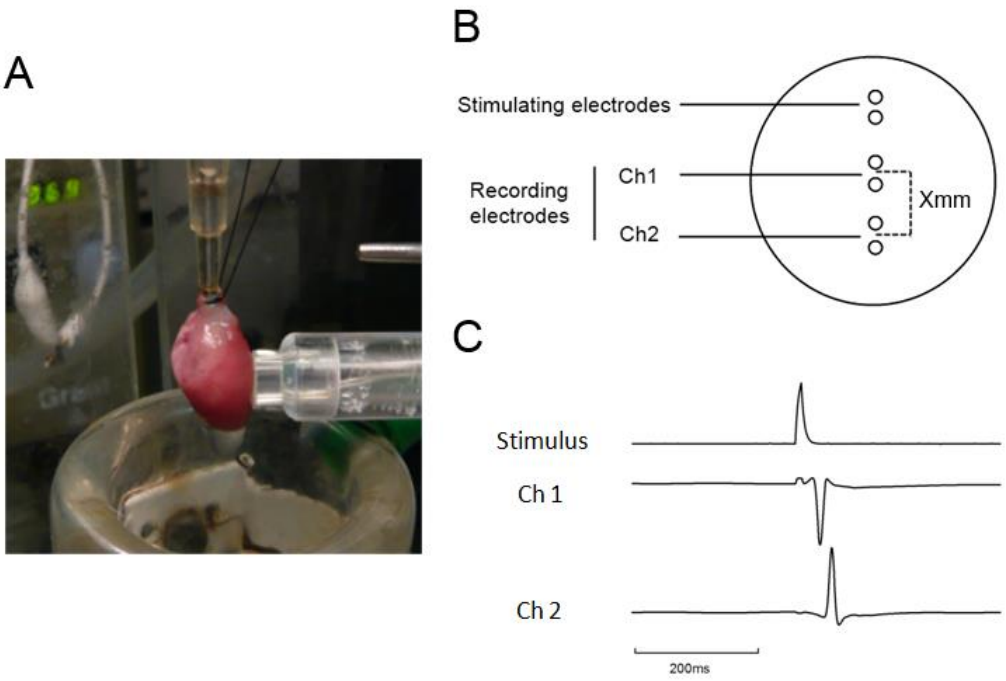

Fig. 2.3.1 Electrode Design.
A) *Photo of setup showing positioning of the electrode on the surface of the LV.* ***B)*** *Diagram of electrode design, showing the stimulating electrodes and two sets of recording electrodes which are all set in epoxy. Xmm is the distance between electrode pairs and is between 1 and 1.6mm, as several different electrodes were made and used during these experiments.* ***C)*** *Example traces taken from an experiment showing the stimulus artefact and the peaks on the Ch1 and Ch2 recording electrodes.*

Traces were analysed using a program written in house (Dr. Francis Burton, University of Glasgow) in MATLAB (Mathworks). The software detects the peaks in the traces and calculates the delay between each pair of peaks, creating a continuous trace of the conduction delay (Fig. 2.3.2). This allows detection of small changes in CV and shows the exact time point at which these changes occur. Our system was limited to a digitization rate of 20kHz – this limited the resolution of the conduction delay (Fig. 2.3.2 B), producing a trace which fluctuates between two values when in reality the actual value will lie between the two recorded delays. Adjacent averaging of 30 sequential points of the conduction delay traces was used to minimise the impact of this.

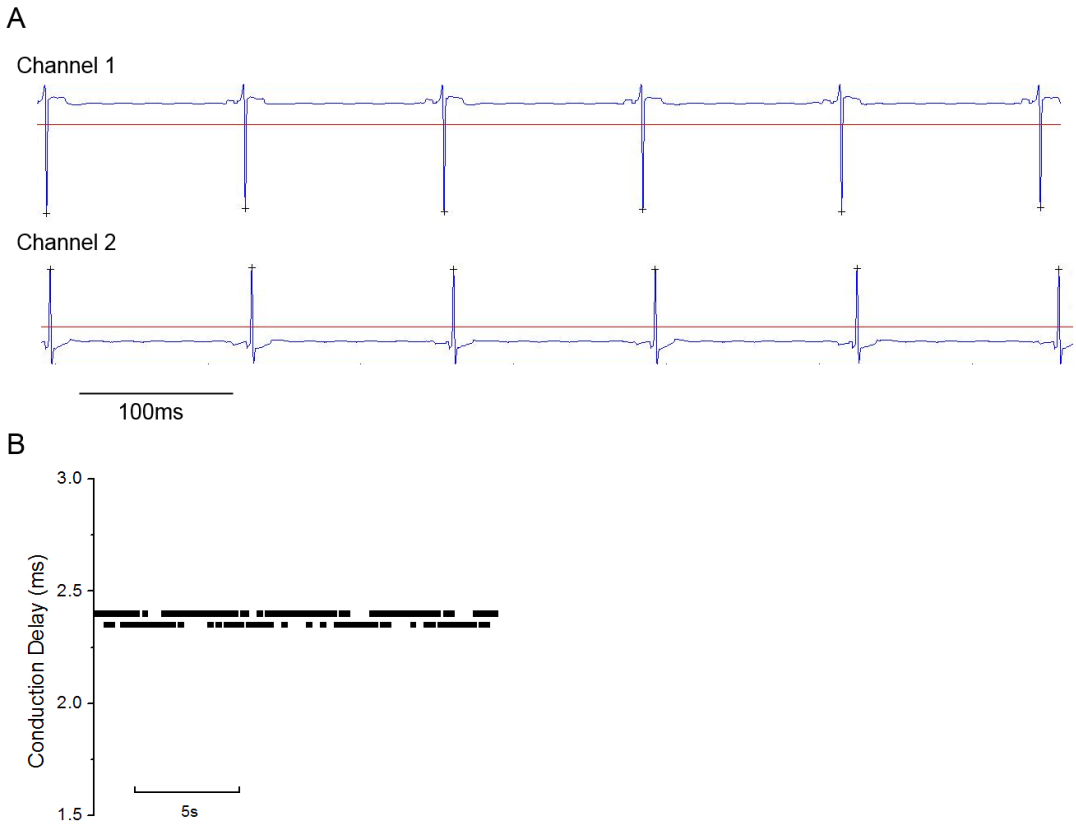

Fig. 2.3.2 Analysis Program
A) *Example trace from section of experiment. Program detects trace peaks (black +) from the Ch1 and Ch2 electrodes. This allows a continuous conduction delay (ms) to be calculated* ***B)****. Note the digitisation rate (20KHz) limits the resolution of the conduction delay (0.05ms) and the subsequent CV calculation.*

Fibre Orientation

Position of the electrode relative to fibre orientation leads to differences in conduction velocity: CV is roughly twice the CV in the longitudinal orientation (parallel to the fibre orientation) than in the transverse orientation (perpendicular to fibre orientation). To confirm that we were able to detect changes in CV relative to fibre orientation, the electrodes were rotated through 360^{o} with CV recorded at 30^{o} intervals. As it was not possible in this setup to identify fibre orientation, longitudinal CV was estimated by rotating the electrode until the fastest CV was observed: this was termed longitudinal CV. The electrode was then rotated 90^{o} to record transverse CV. This was termed 0^{o} for the diagram shown below (Fig. 2.3.3). From the 0^{o} point, the electrode was rotated in a clockwise direction and an individual CV recording was made at each 30^{o} interval. CV was

found to be approximately 50% faster at 90^{o} vs. 0^{o}, representative of the difference between longitudinal and transverse CV due to fibre orientation.

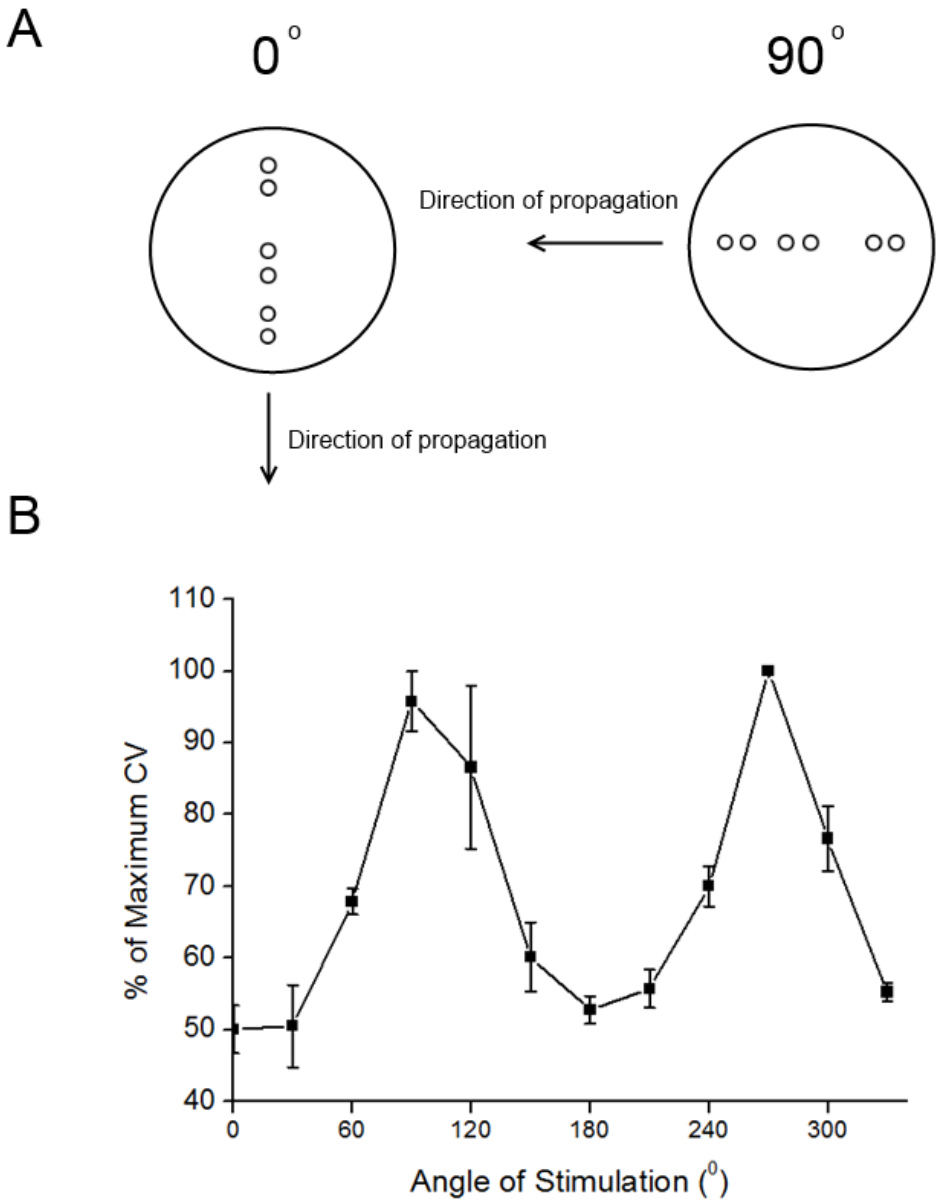

Fig. 2.3.3 360^{o} recording of CV on the rat LV.
A) *Diagram showing the angle of the electrodes and the direction of propagation at 0^{o} and 90^{o}.* ***B)*** *Range of CVs recorded from 3 rats across 360^{o} shown as a % of the max CV recorded.*

To minimize variation in CV between different hearts, CV was recorded at as close to longitudinal CV as possible. At the beginning of each CV experiment, the electrodes are rotated through various angles to locate the fastest CV (minimum conduction delay).

2.4 Microelectrode Recordings

Sharp microelectrode (ME) measurement of V_m is the 'gold standard' method by which intracellular APs are recorded. APs were measured from epicardial myocytes of the LV at the same region as CV recordings in previous experiments. This allowed us to measure the effect of β-AR stimulation on the AP to ascertain if changes in cellular electrophysiology could explain recorded changes in CV.

ME AP recordings were carried out on horizontal Langendorff, with the heart positioned so that the LV surface faced up. Preparations were submerged in a specially designed Perspex water bath maintained at 37^{o}C, containing modified Tyrode's solution (see 2.1). Sharp glass microelectrodes of between 40-50MΩ were pulled (Flaming/Brown Pipette 97 Micropipette Puller Sutter Instruments, Novato, CA) and filled with 1M KCl. Silver Chloride (AgCl) wire was used in the micropipettes – the Ag wire was galvanically chlorided in lab. The potential difference between the microelectrode and a Ag/AgCl reference electrode (commertially bought) placed in the water bath was recorded. ME recordings measured using an Axoclmap 2B amplifier and digitally recorded at 28kHz. A HS2A headstage (10x gain) with an input impedence of 500MΩ was used. An ECG was recorded using Ag/AgCl disc electrodes and AP recordings were made using WinEDR (Dr John Dempster, University of Strathclyde, UK). The heart was LV paced using bipolar platinum electrodes.

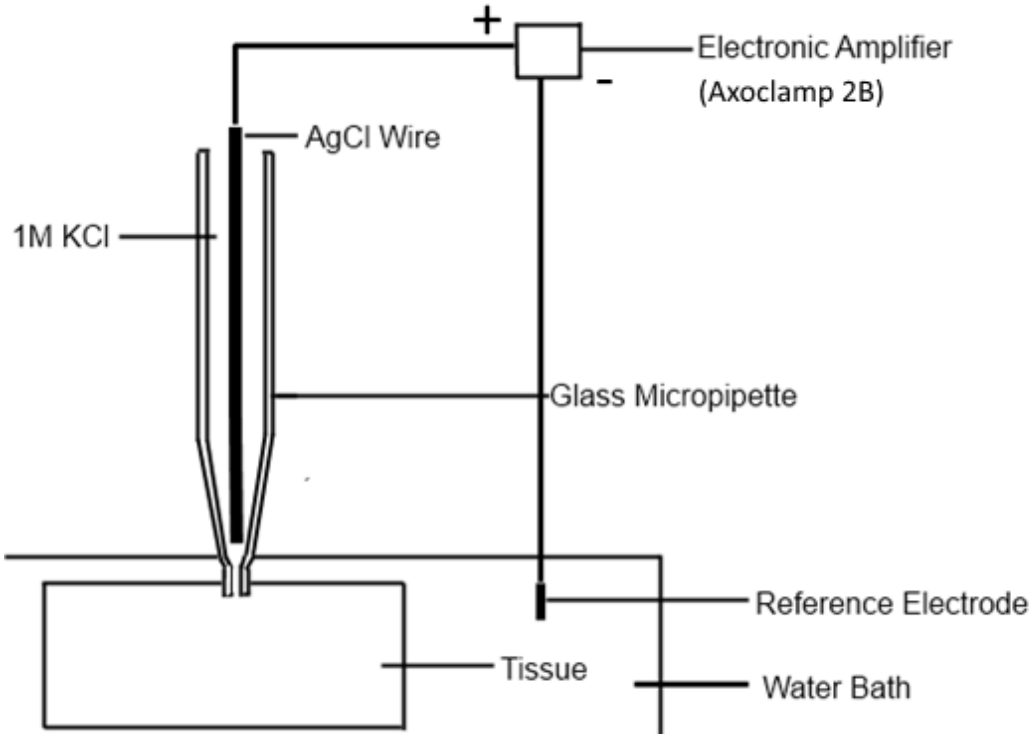

Fig. 2.4.1 Diagram of ME setup.
Potential difference between the glass microelectrode and the waterbath reference electrode were recorded using WinEDR (Dr John Dempster, University of Strathclyde, UK).

2.5 Optrode recordings

Although ME recordings allowed us to record APs from the site at which we recorded CV, it was not possible to record CV and AP measurements simultaneously on this setup. Also, to obtain a continuous ME recording of APs was technically challenging, even in a mechanically quiescent heart. Therefore, a system was designed which allowed the simultaneous recording of CV, optical APs and optical Ca^{2+} transients from the same site on the LV. Electrodes with a similar design as previous setups (Fig. 2.3.1 B) were set into the centre of a fibre optic lightguide, which allowed the transmission and collection of light from sites directly adjacent to the CV recording electrodes (Fig. 2.5.1 A). The fibres of the fibre optic light guide were fixed in place in crescent shapes to either side of the CV recording electrodes, which each side containing five individual fibre optic fibres; this covered two areas of 4mm by 2mm which were 4mm apart.

Fluorescence was recorded simultaneously at 2 wavelengths (550nm and 650nm) using photomultiplier tubes (PMTs) to allow ratiometric measurements of voltage using Di-4-ANEPPS. The 470nm LED was switched on for 5s at a time every 30s. This recorded a train of 60 APs, which would later be averaged during the analysis process to give a mean AP from this time-point.

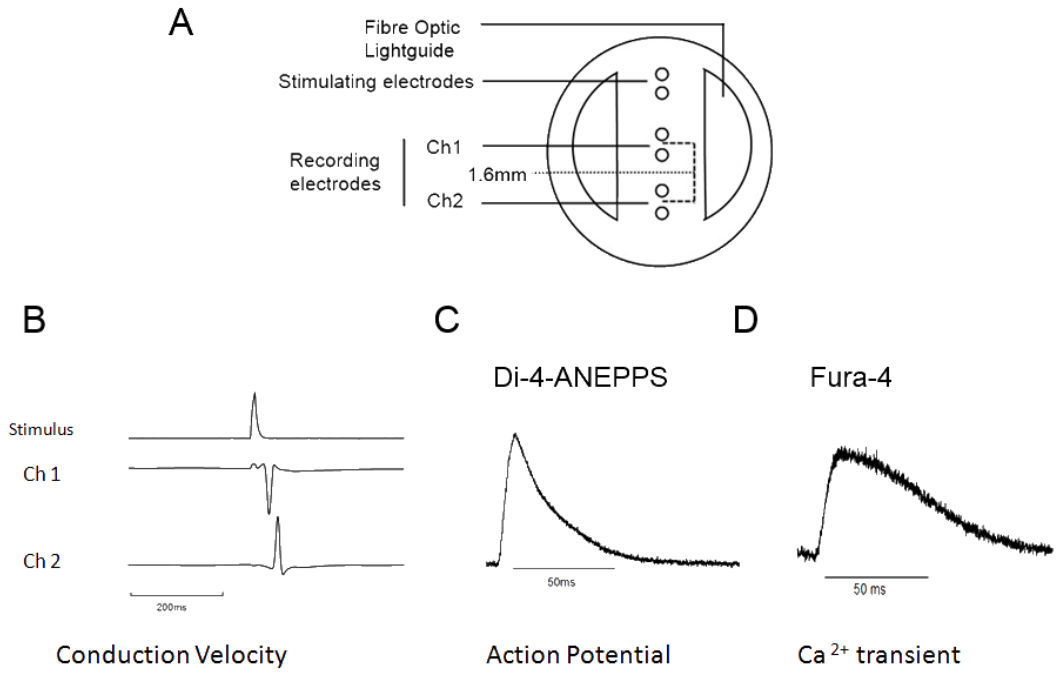

Fig. 2.5.1 Diagram of optrode setup.
A) The 'optrode' incorporates the CV electrodes from the previous setup and includes a fibre optic lightguide which allows the excitation of fluorescent dyes and collection of light from the heart. **B)** CV recordings can be made in the same way as shown in section 2.2. **C)** An example averaged AP taken from recordings made using the optrode and the voltage-sensitive dye, Di-4-ANEPPS. **D)** An example averaged Ca^{2+} transient recorded with the optrode and the Ca^{2+} sensitive dye, Fura-4.*2.5.1 Voltage Sensitive Dye: Di-4-ANEPPS*

To record APs using the optrode, voltage sensitive dyes were used. These are dyes which respond rapidly to changes in membrane potential, which alters their fluorescence; this change is extremely fast and allows the recording of changes in electrical potential within milliseconds.

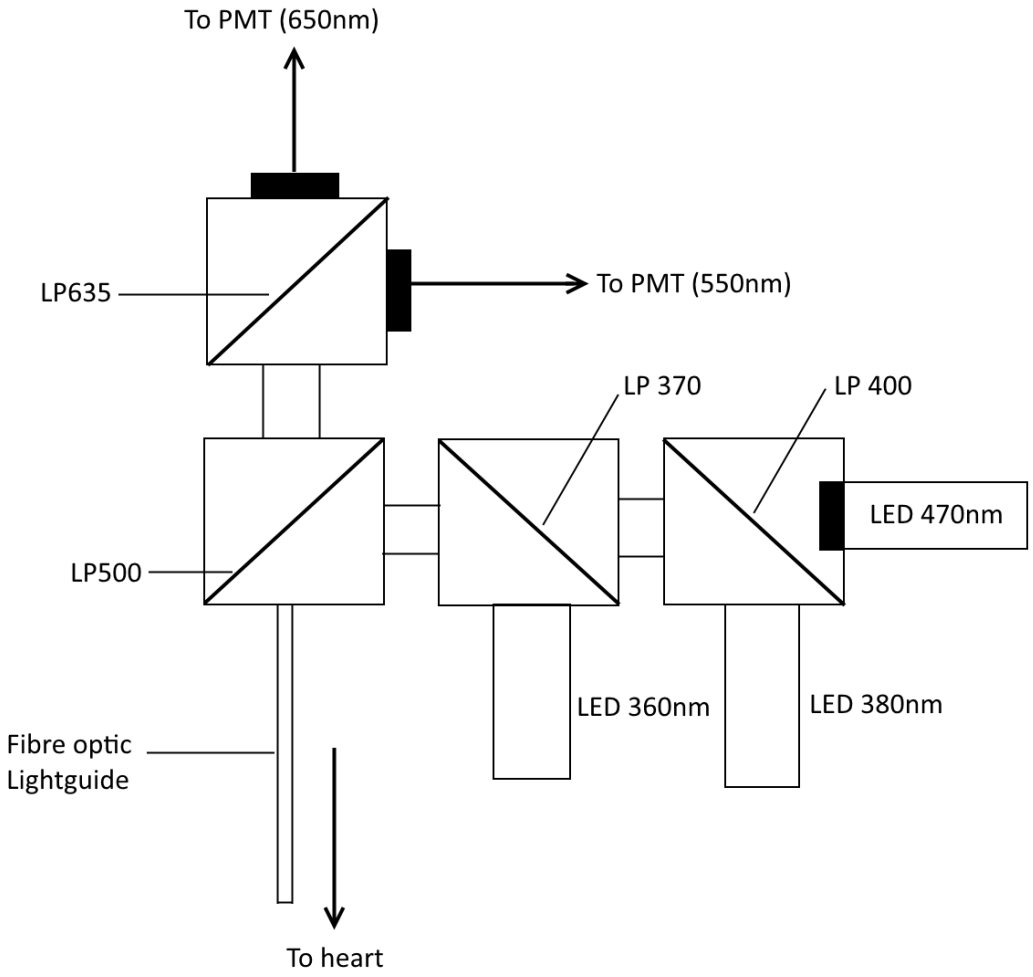

Fig. 2.5.2: Diagram of optrode light path
Diagram showing the set-up for the optrode recordings. LP = long pass filter. LED = light emitting diode. Light from the LEDs would pass through a series of long pass filters to reach the fibre optic light-guide which would shine light on to the heart. Emission from the flouroescent dyes would be collected by the light-guide and pass through the LP500 filter to the PMTs. There the LP535 filter would split the emission between the 550nm and 650nm PMTs.

The dye used in this study is Di-4-ANEPPS (Biotium, UK), an ANEP ratiometric dye. Di-4-ANEPPS is not fluorescent until membrane bound, but when in the membrane its peak excitation wavelength is 470nm and its peak emission is at 600nm (Fig 2.5.2 A). Fig. 2.5.2 B shows the Di-4-ANEPPS emission spectrum in an adult rabbit cardiac myocytes. The black line shows emission of the dye in normal Tyrode's and the red dotted line shows emission in high potassium (K^+), which depolarises the cardiac cell membrane. The change in membrane potential caused by the high K^+ causes a spectral shift in fluorescence: this spectral shift is extremely small and can be seen more clearly in Fig. 2.5.2 C.

Fig. 2.5.2 B shows the relative change in fluorescence of Di-4-ANEPPS in normal Tyrode's and Tyrode's containing high K^+. The change in fluorescence peaks at two different wavelengths. Emission was split and recorded on two separate PMTs set to 550nm and 650nm, which made it possible to take a ratio of the fluorescence at each wavelength. Calculating the ratio helps reduce the artifact associated with movement during the recording. Di-4-ANEPPS bleaches in the presence of light – i.e. the fluorescence of the dye decreases with the time exposed to excitation light. As the emitted fluorescence recorded on at the two channels will decrease to the same relative extent due to bleaching, taking a ratio also reduces the effect of bleaching on the signal level.

50µL Di-4-ANEPPS (2mM stock concentration) was diluted in 2ml of modified Tyrode's (50µM) and added slowly as a bolus over 10s, using a syringe cannula as close to the heart as possible (Fig. 2.7.1). Due to the flow-rate of 12ml/min, this equated to an approximate concentration at the heart of 25µM. This method of Di-4-ANEPPS administration had been optimized in previous work carried out in the lab. A light-emitting diode (LED) that emitted light at 470nm was used to excite the dye. To minimize the effect of bleaching, the 470nm LED was turned on at either 30s or 1min intervals throughout these experiments for 5s at a time to record a train of APs that were subsequently averaged prior to analysis.

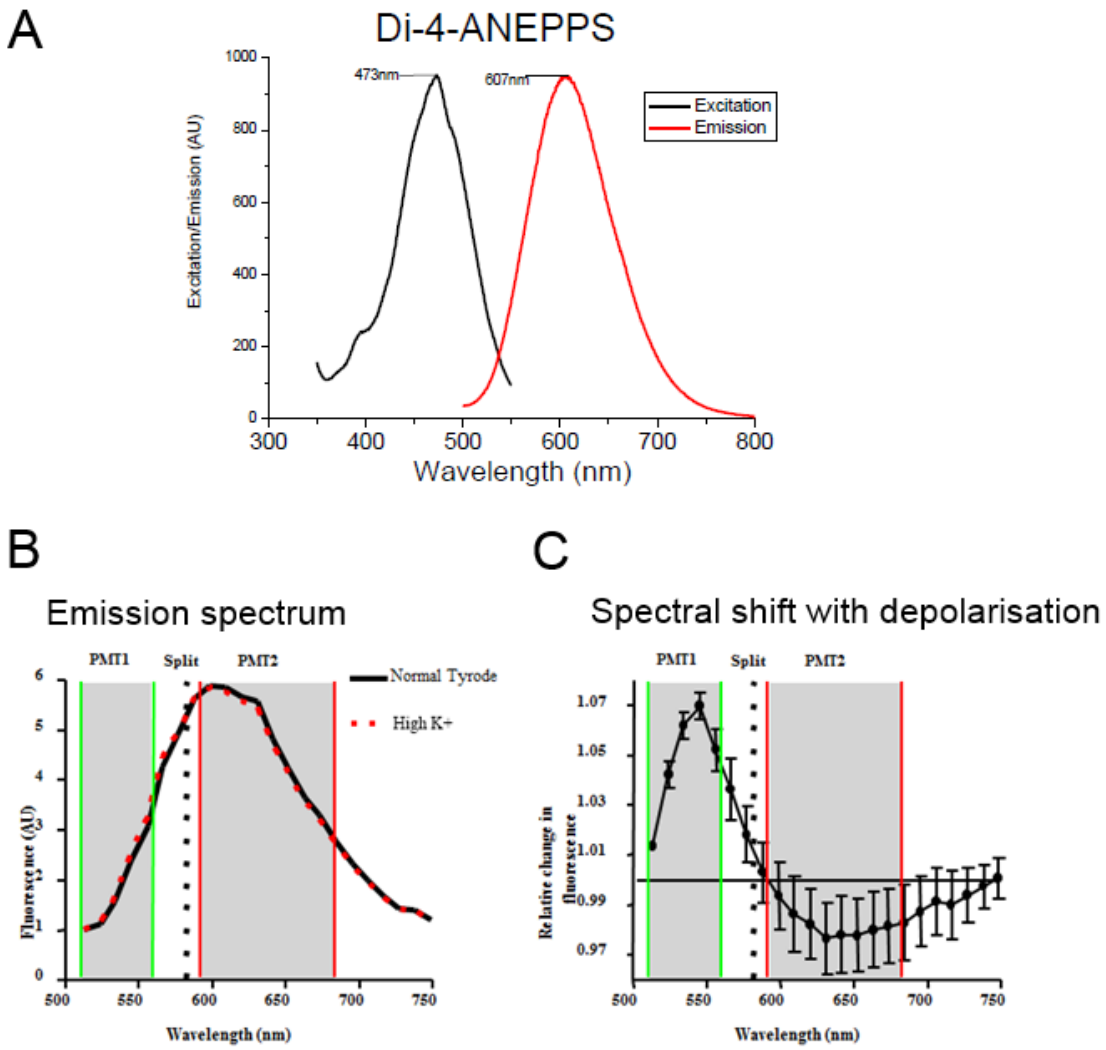

Fig 2.4.1.1 Excitation and Emission spectra of Di-4-ANEPPS (Recorded by Dr. Ole Kemi and Dr. Niall MacQuaide, University of Glasgow).
A) *Excitation and emission spectra of Di-4-ANEPPS. Peak excitation occurs at 473nm wavelength and peak emission is recorded at 607nm.* ***B)*** *Emission spectra of Di-4-ANEPPS in rabbit cardiac myocyte in presence and absence of high K^+. High K^+ depolarises the cell membrane and causes a spectral shift in Di-4-ANEPPS fluorescence.* ***C)*** *The spectral shift of Di-4-ANEPPS is shown; from this it is possible to see that there is a larger change in fluorescence at two wavelengths. By recording at both these wavelengths, a ratio can be taken.*

2.5.2 Ca^{2+} Sensitive Dye: Fura-4-AM

Fura dyes are calcium sensitive dyes used for measuring intracellular Ca^{2+} concentrations. They are aminopolycarboxylic acids which bind to free Ca^{2+} in the cytoplasm (Grynkiewicz et al., 1985). Fura-4 is a lower affinity version of Fura-2, with a kd of 800nM: although this means there is a lower sensitivity to diastolic levels of Ca^{2+}, it allows for better resolution of

peak Ca^{2+} recorded during Ca^{2+} transients. Fura-4 is designed to be excited sequentially at 340nm and 380nm, with emission from both being collected at 510nm. This allows for a ratiometric measurement to be taken as a result of the emitted fluorescence from the two excitation wavelengths. However, using an LED based system does not easily allow excitation at 340nm since current LEDs that emit at this wavelength are of very low power. Therefore in these studies, Fura-4 was excited with a 360nm light from a longer wavelength LED. This wavelength is termed the isosbestic point since it represents a Ca^{2+} insensitive sector of the excitation spectrum. This approach still yields a ratiometric measurement of Ca^{2+} since changes in fluorescence signal due to movement or other artefacts are minimized due to the fluorescence signal recorded at 360nm.

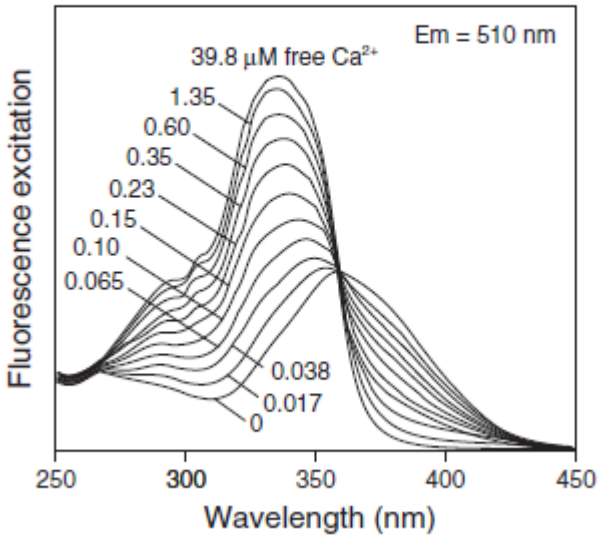

Fig.2.5.2 Fluorescence excitation spectra of Fura-2 in solutions containing from 0-39.8µM Ca^{2+} (taken from ThermoFisher Scientific).
Fluorescence excitation of Fura-2 at different concentrations of Ca^{2+}. The excitation of Fura-2 is the same as Fura-4; only the Kd of Fura-4 is different. The isosbestic point, at which fluorescence does not change in response to Ca^{2+} concentration, can be clearly seen at 360nm.

Background recordings of fluorescence were taken before adding Fura-4 to the heart. 30µM Fura-4-acetoxymethyl ester (Fura-4-AM, Molecular Probes, Life Sciences, UK) - a cell permeable form of Fura-4 - was perfused into the heart over 5min: this was done at half the normal perfusion rate to allow time for the Fura-4-AM to enter the heart; this also allowed us to use smaller volumes of Fura-4-AM. The heart was then left for a further 10min to allow the acetomethyl groups to be removed by intracellular esterases: this is

required for the functioning of Fura-4, but also prevents Fura-4 from diffusing back across the membrane. Further to this 2.5mM probenecid (Sigma Aldrich, UK) was perfused on with the Tryrode's solution to inhibit anion transport and prevent Fura-4 secretion.

Recordings were made by exciting with a 360nm optoLED for 5s and then immediately switching to a 380nm LED for an additional 5s. Fluorescence was collected at 450nm and recorded using the custom software ACQ1 (Dr Francis Burton, University of Glasgow). The signals were then background subtracted and ratioed using custom software created in house: ViewACQ (Dr. Francis Burton, University of Glasgow).

The recording of Ca^{2+} transients alongside APs and CV, using the optrode probe was a new technique developed in the lab. Fura-4 concentration, LED power and PMT settings were optimized over a series of experiments. Difficulties were encountered due to the low power of the 360 LED which generated a signal with low signal:noise. To reduce the impact of this noise on the Ca^{2+} transients, a section of each 360 recording was averaged and this average was used to calculate the ratioed Ca^{2+} transients: i.e. Ca^{2+} transient ration = mean 360 / 380 trace.

2.5.3 Near-simultaneous AP and Ca^{2+} recordings

Due to their overlapping emission wavelengths, it was not possible to record both AP and Ca^{2+} signals simultaneously. Instead a protocol was developed which allowed sequential measurements of APs and Ca^{2+} transients. An initial 5s recording was made by switching on the 470nm LED: this excited Di-4-ANEPPS and allowed the recording of 5s of APs. The LED would then immediately be switched off and the 360nm LED switched on for 5s: this allowed the recording of the isbestic point of Fura-4. Finally, the 360 LED would be switched off and the 380nm LED would be immediately turned on: this allowed the recording of the Ca^{2+} sensitive portion of Fura-4 emission. Although these recordings were not simultaneous, they did allow both APs and Ca^{2+} transients to be recorded optically in the same heart and at the same location on the epicardium. The short time window in which these were recorded also allowed comparison of Ca^{2+} transients and APs at similar time-points during drug addition. However, it is important to consider that Ca^{2+} transients were recorded a full 10s after the APs were recorded.

2.5.4 Analysis

Both APs and Ca^{2+} transients were analysed using custom software developed in house: RatioAverager (Dr. Francis Burton). Using this program, it was possible to average the signals recorded over 5s to a mean single AP or Ca^{2+} transient. Properties such as the rise

time between 10 and 90% of the upstroke (TRise), the amplitude and the duration of the transient could be measured.

2.6 Pacing Protocol

Bipolar platinum stimulating electrodes were encorportated into the CV electrode design (2.3.1B). Bipolar platinum 'hook' electrodes were used to pace the heart in ME experiments. The heart was paced epicardially on the LV in all experiments. The heart was stimulated using a square pulse 2ms in duration. These were generated using an isolated constant voltage stimulator (Digitimer, Ltd.) and interval was maintained using a digitimer developed in-lab. Threshold for pacing was found by gradually increasing the voltage (V) of the pulse until successful pacing of the heart was established. V was mainted at 1.5x threshold. Unless otherwise stated, hearts were paced at 8Hz to override the higher intrinsic rates seen in adrenergic stimulation.

2.7 Mechanical Uncoupler

The normal contraction of the heart can interfere with the recordings. Although it was possible to make CV recordings while the heart was contracting, the electrode was more likely to be moved by the contracting heart and therefore invalidate the experiment. It is also not possible to make optical AP or Ca^{2+} recordings while the heart is contracting normally, as this generates a large motion artifact that is not sufficiently cancelled by ratiometric measurements.

Mechanical couplers act by uncoupling the electrical signal from the physical contraction of the myocyte: this leaves the electrical signal unchanged, but prevents the heart from contracting during the experiment. Previously used uncouplers include 2,3-butanedione monoxime (BDM) and cytochalasin D. However, these uncouplers also have effects on intracellular Ca^{2+} handling, therefore making them imperfect for use in research (Kettlewell et al., 2004; Y. Liu et al., 1993).

A newer mechanical uncoupler, blebbistatin, is believed to have fewer non-specific interactions. It is an inhibitor of the ATPases associated with myosin II, and therefore prevents the normal cycling of the myosin head and its attachment to actin (Straight et al., 2003): this prevents cellular contraction. Federov et al. found that blebbistatin at 5-10µM eliminated contraction but had no effect on action potential morphology or intracellular calcium transients (Fedorov et al., 2007). However, Brack et al. found that blebbistatin at

5µM prolonged effective refractory period and caused AP prolongation in the intact rabbit heart (Brack et al., 2013a).

In this study 3µM blebbistatin was used to try to reduce the negative impact of blebbistatin on the electrical activity of the heart. It was perfused onto the heart for 25min prior to any experimental recordings, so that the heart could reach a steady state. Further to that, all control recordings were made in the presence of blebbistatin. All experiments were carried out in the presence of 3µM blebbistatin unless otherwise stated.

2.8 Drug Delivery

Various drug interventions were used throughout this study. Timing of drug delivery was important, so it was necessary that the drug entered the system as close to the heart as possible and also that a set drug concentration could be maintained over a chosen period of time. To do this, a syringe driver was set up adjacent to the Langendorff system. This was set up to perfuse drugs at 0.4ml per min. The syringe cannula passed through the top of the rubber bung in the heat exchange coil, down the central channel and the opening was positioned immediately before the aortic cannula. This tubing was primed with drug prior to the experiment, meaning that as soon as the syringe driver was turned on, drug was mixed and delivered directly into the coronary circulation. Passing through the heat exchanger ensured that the drug was heated to close to 37^{o}C and also allowed the drug to mix with the Tyrode's solution prior to reaching the aorta. A second tube through the heat exchanger coil was also used to deliver Di-4-ANEPPS to the coronary circulation.

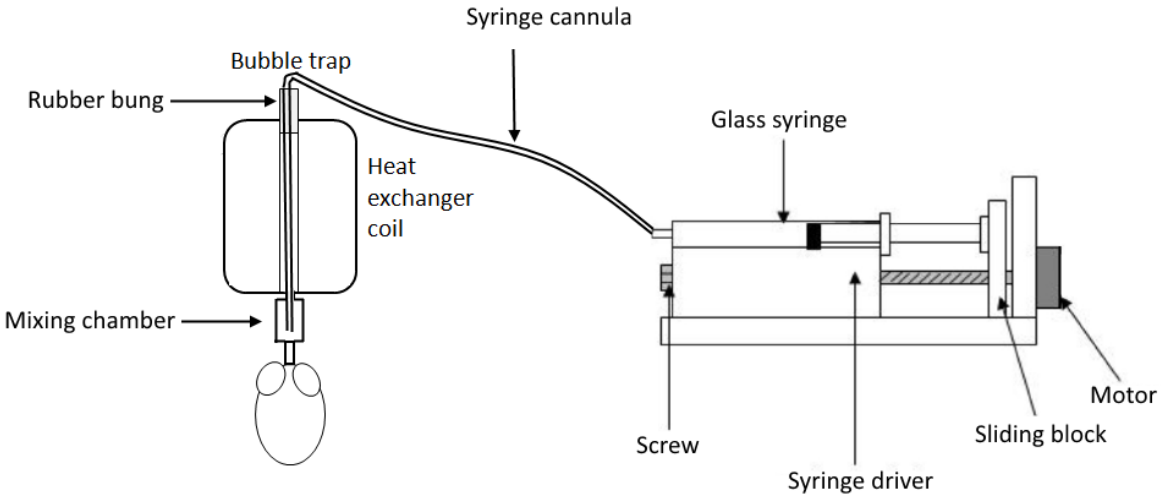

Fig. 2.8.1 Diagram of syringe driver and drug delivery.
Diagram showing the setup of syringe driver used to deliver drugs to the heart. Drugs were perfused on at a constant rate, to maintain a constant concentration for the duration of the experiment. A syringe cannula was used to ensure that drug was delivered as close to the coronary arteries of the heart as possible so that there was minimal 'dead space' in the system.

2.9 Analysis and Statistics

AP and Ca^{2+} transient data were exported from WinEDR (Dr. John Dempster, University of Strathclyde, UK) or ACQ1 (Dr. Francis Burton, University of Glasgow, UK) in the acq format. The section of trace pertaining to each time point was then exported as a ratio using ViewACQ (Dr. Francis Burton, University of Glasgow, UK). In the case of Ca^{2+} transient analysis, a section of the 360 trace (the isobestic point of Fura-4) was averaged, and this average was divided by the 380 trace; this reduced signal:noise, as noise was generated on the 360nm trace due to the low power of the 360nm LED. The ratioed transients were then averaged and analysed using RatioAverager (Dr. Francis Burton, University of Glasgow, UK). Example traces were exported using Origin (OriginLab Corporation, USA).

CV traces were recorded using ACQ1 and exported using ViewACQ. CV analysis was carried out using MATLAB (Mathworks, USA) and software generated in-lab. Example traces were generated in Origin.

Graphical and statistical analysis was carried out using GraphPad Prism (GraphPad Software, Inc., USA). Unless otherwise stated, graphs are presented as the mean with the standard deviation (s.d.) stated in the text. A student's *t*-test was used in single comparison

tests, whereas a non repeated measures ANOVA with Bonferroni's post-hoc test was used for multiple comparisons. A *P*-value of <0.05 was considered significant (* = $p<0.05$; ** = $p<0.01$; *** $p<0.001$).

3. β-adrenergic stimulation increases CV in the intact heart

3.1 Introduction

The autonomic nervous system (the ANS) is composed of the sympathetic and parasympathic branches. The sympathetic nervous system of the heart governs the 'fight or flight' response: it allows the heart to rapidly respond to stimuli to increase pump function and speed of contraction. The sympathetic nervous system acts through the binding of catecholamines to α- and β-adrenoreceptors, though in the normal adult myocardium the β-adrenorecptors (β-AR) are the dominant subtype.

The effect of β-AR stimulation on the heart is well established. β-AR increases heart rate - positive chronotropy - via an increase in I_f - an ion channel directly activated by cAMP (DiFrancesco and Tortora, 1991) - and on shortening the conduction delay in the SA (Hutter and Trautwein, 1956, 1955; Levick, 2000). β-AR stimulation also causes an increase in the force of contraction of the heart - positive inotropy. This is achieved primarily through an increase in the inward Ca^{2+} current and enhancing the intracellular Ca^{2+} store (Bers, 2001, 2002); this is dicussed in further detail in 4.1.2. β-AR stimulation also increases the rate at which the heart relaxes following contraction - positive lusitropy. This is due to the increased uptake of Ca^{2+} from the cytoplasm by SERCA (Bers, 2002) and also due to an increase in the slow outward K^+ channel, I_{Ks} (Walsh et al., 1988).

The effect of β-AR on the speed of myocardial conduction however, has not been well studied. The majority of studies on the effect of β-AR stimulation on CV were primarily carried out in the 1950s and 60s. Initial experiments carried out in *in vivo* dog hearts showed an increase in ventricular CV (Krayer et al., 1951; Siebens et al., 1953) in response to epinephrine, however later experiments carried out in the isolated dog heart-lung preparations showed only a small and inconsistent increase in CV (Swain and Weidner, 1957). While Krayer et al. attribute the increase in CV to an increase in serum K^+ caused by the action of epinephrine on the liver, Wallace and Sarnoff demonstrated that stimulation of the left stellate ganglion caused an increase in CV of approximately 6% (Wallace and Sarnoff, 1964), suggesting that sympathetic stimulation was having a direct effect on CV in the heart. More recent studies on isolated rabbit heart with intact sympathetic innervation demonstrate an increase in CV of 30% in response to sympathetic nerve stimulation (Ng et al., 2007). However, these studies included conduction via both the ventricle and Purkinje

fibres. So, though there is evidence that β-AR stimulation increases myocardial CV, there are few studies which measure ventricular CV directly and they do not address the mechanism or time-course of this response.

Using the electrode design shown in Fig. 2.2.3, it was possible to measure conduction delay on the epicardial surface over a limited distance (between 1 and 2mm) that ensures only local conduction is sampled. Therefore, it was possible to directly record conduction delay from myocardial conduction without involving the cardiac conduction system. The initial aim of this study was to measure the effect of β-AR stimulation on CV, confirming the increase in CV previously recorded and measuring the time-course and amplitude of this response.

The drug used initially to stimulate the β-AR was isoproterenol: ISO is a full agonist of all 4 types of the β-receptors on the heart.

This study also aims to determine the signaling pathways responsible for the increase in CV. One of the possible second messengers involved in β-receptor signaling in the heart is cyclic adenosine monophosphate (cAMP). To ascertain whether this was a cAMP-mediated response, drugs which raise cAMP were used: the activator of adenylyl cyclase, forskolin (Fsk), and the PDE inhibitor 3-Isobutyl-1-methylxanthine (IBMX) were used to raise intracellular cAMP.

The effect of β-AR on heart rate is previously well documented (DiFrancesco and Tortora, 1991; Hutter and Trautwein, 1956). In a separate set of experiments, heart rate was also recorded to ensure that the dose of ISO used was having the expected effect on the heart, to compare the time course of the CV and HR responses and to determine if the heart reached a steady state during drug perfusion.

3.2 Methods

3.2.1 Drug concentrations

100nM of isoproterenol hydochloride (ISO) was dissolved in deionoised water (Sigma Aldrich, UK). 30μM Fsk and 100μM IBMX (both Sigma Aldrich, UK) were used to achieve a near maximal response, based on previous studies (Mehta et al., 1992; Paulson et al., 2000b; Zhai et al., 2012). Both drugs were dissolved in DMSO. Finally, the combination of 1μM Fsk and 100μM IBMX was chosen as the combination of drugs to maximally raise cAMP in further work: Fsk gave the most consistent and stable results, however, Fsk is known to have some non-specific effects at high concentrations, so the lower

concentration of Fsk alongside a PDE inhibitor was chosen as the most effective and specific drug intervention.

All experiments were carried out in the presence of 3µM blebbistatin, unless otherwise stated.

3.2.2 Drug delivery

Recordings were taken of both heart rate and CV for 5mins prior to drug addition to ensure that the heart had reached a steady state and to allow for a control recording. The control point for the graphs was taken as 30s prior to drug addition. The drug was perfused on for a total of five minutes until the response approached a steady state; in initial experiments drugs were added for 3mins (data not shown) but this was not long enough for the response to reach a steady state. Recordings continued for 5 minutes following drug perfusion to record the 'wash-off' of the response. However, as it appeared the CV response had a very slow wash off period, in subsequent experiments the wash-out period was not recorded.

In the protocol to determine the ISO dose response curve, CV was taken as the maximal CV response. Each concentration was recorded separately on different hearts, as prolonged exposure to ISO may induce a desensitization response which would reduce the heart's response to ISO.

3.2.3 Heart Rate Recordings

Interval was recorded continuously throughout the experiment using the same electrodes as used for the CV recordings:Interval was recorded as the time between peaks on a single channel - the trace recorded from a single pair of electrodes. Heart rate was calculated from interval as beats per minute.

3.2.4 Conduction Velocity Recordings

Conduction delay was recorded continuously through the experiment, as described in the methods (Fig. 2.2.1; Fig. 2.2.2) and CV was calculated from the conduction delay (v=d/t). The heart was paced continuously at 130ms (approx. 8Hz) to prevent the increase in intrinsic HR caused by β-AR stimulation from disrupting pacing. The heart was paced on the epicardium of the left ventricle.

Results

3.3 CV response to IBMX in presence and absence of blebbistatin

The mechanical uncoupler blebbistatin was used to uncouple the electrical activity from the contraction of the heart in all CV experiments. This means that the heart remains still during recordings, which allows for more reliable and consistent CV recordings and is also required for the AP and Ca^{2+} recordings carried out in later experiments.

As it was possible to make CV recordings without the use of a mechanical uncoupler, the CV response to IBMX was recorded both in the presence and absence of blebbistatin to ensure that blebbistatin was not having a non-specific effect on CV.

100µM IBMX increased CV 11.5±2.5% in the absence of blebbistatin ($p<0.05$, n=3) and by 9±1.9% in the presence of blebbistatin ($p<0.05$, n=4). The difference between the responses in the presence and absence of blebbistatin was not significant (Fig 3.3.1).

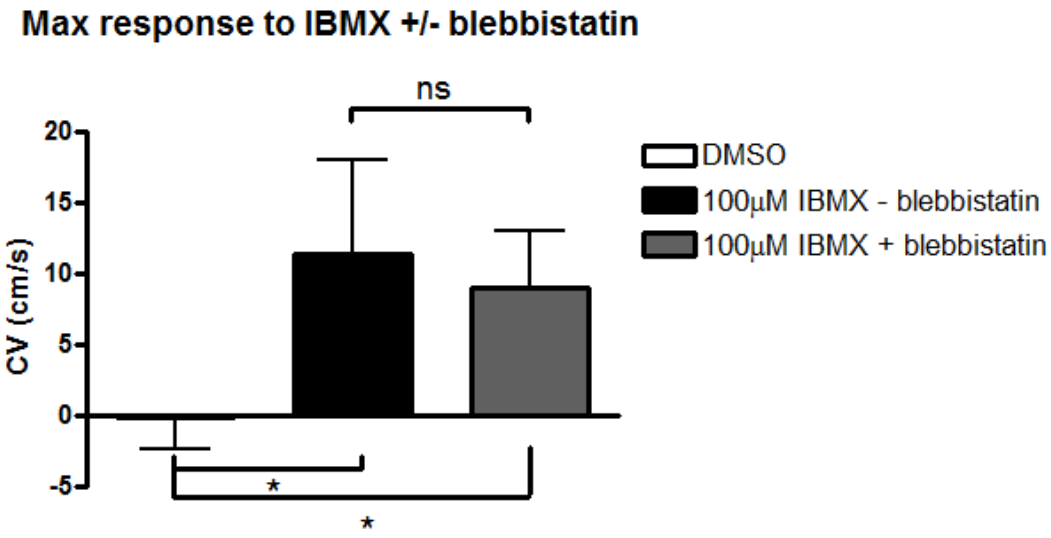

Fig. 3.5.1 There is no significant difference between the CV response to IBMX in the presence and absence of 3µM blebbistatin.

White bar indicates DMSO control, black represents treatment with 100µM IBMX in the absence of blebbistatin and grey shows hearts treated with 100µM IBMX while also continuously perfused with 3µM blebbistatin. CV was taken as the max response to IBMX. IBMX significantly increased CV in the presence and absence of blebbistatin ($p<0.05$, n=4). Data are shown as mean±s.d. There was no significant difference between the IBMX response in the presence and absence of blebbistatin. (=$p<0.05$)*

3.4 The β-receptor Agonist ISO Increases Left Ventricular Conduction Velocity in the Intact Rat Heart

HR was measured continuously as 100nM ISO was perfused onto the heart. ISO caused a rapid increased in mean HR from 270±50bpm to 360±80bpm (Fig 3.4.1 C). Mean heart rate in the control was recorded as 250±30bpm. Due to the high degree in variation in heart rate between individual hearts, % change in heart rate was calculated. The max response of HR to ISO was on average a 30±20% ($p<0.05$ n=4) above control values. There was no significant change in the time control (Fig. 3.4.1 E). Following drug perfusion, the heart rate response began to wash out within five minutes, returning to 6±14% above the control heart rate recording.

Left ventricular CV increased in response to treatment with 100nM ISO: CV increased from 72±9cm/s to 78±10cm/s at its highest point (Fig. 3.4.1 D). The response was slow, with highest CV recorded after perfusion with ISO had stopped. The time control fluctuated between 66±10cm/s and 68±10 cm/s. This was probably due in part to limitations with the digitisation rate, as described in Fig. 2.2.2. Again, due to the high degree of variation in CV between different hearts, % change in CV was calculated. A change in CV - at its highest point - of 8±4% was recorded ($p<0.01$, n=4). No significant change was recorded in the time control (Fig. 3.4.1 F). This is in line with previous experiments looking at the effect of sympathetic stimulation on CV (Wallace and Sarnoff, 1964) but demonstrate that the increase in CV is due to changes in myocardial CV and not other segments of the conducting system. The CV response to ISO did not return to normal within the 5min washout period: CV remained at 7±4% above control recordings at the end of the experiment.

A dose response to ISO was carried out to ensure that the maximal response to ISO was being recorded. Concentrations between 0.1nM and 100nM were used. A near maximal response was recorded at 10nM: ~11.3±1.7cm/s at 10nM (SEM, n=4), vs. 11.8±1.4cm/s at 100nM (SEM, n=5), so higher concentrations of ISO were not used (Fig. 3.4.2).

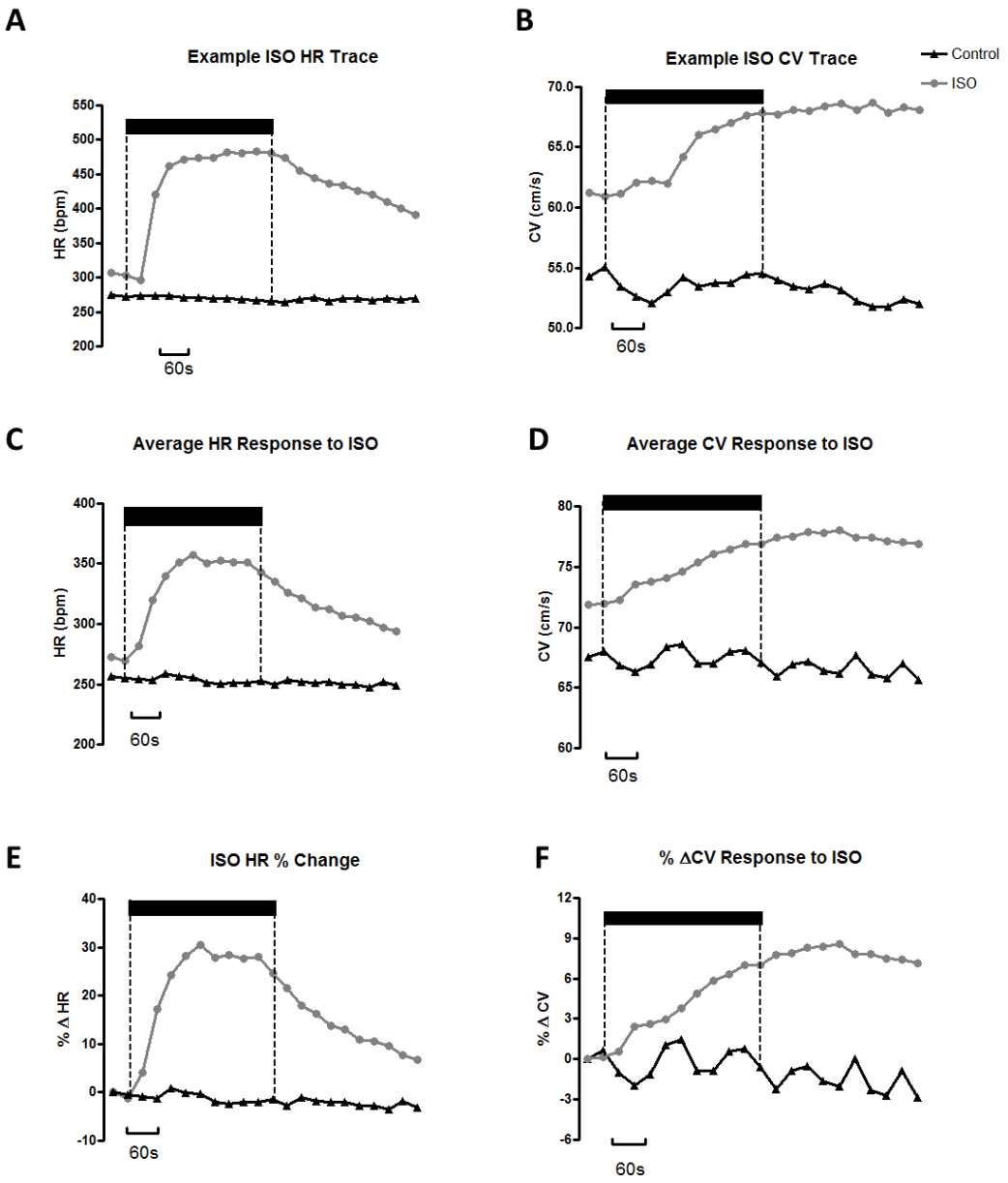

Fig 3.4.1 Effect of 100nM isoproterenol (ISO) on heart rate (HR) and CV in the intact rat heart
Time control is shown in black and the ISO trace in grey. Black bar and dotted lines indicate time over which ISO was perfused onto the heart. Data shown is mean at individual time points. ***A)*** *Example traces showing the effect of ISO on HR.* ***B)*** *Example traces showing the effect of ISO on CV.* ***C)*** *Average HR response to ISO. Error bars represents SE.* ***D)*** *Average CV response to ISO (n=4).* ***E)*** *%Δ in HR in response to ISO. Increase in HR in response to ISO became significant (p<0.05, n=4) at 120s. At 300s the change was no longer significant (n=4).* ***F)*** *%Δ in CV in response to ISO. Increase in CV became significant at 210s (p<0.05, n=4). At 330s-600s p<0.01 (n=4).*

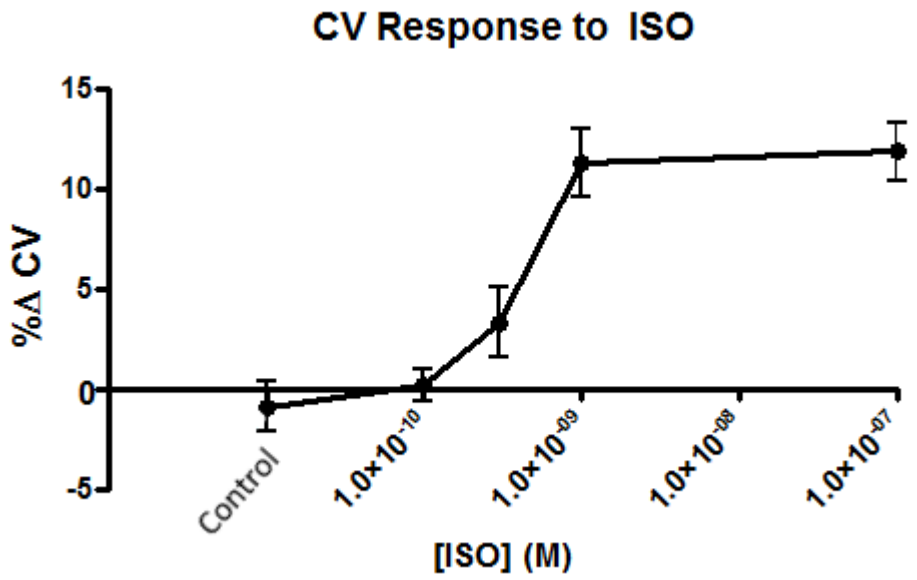

Fig 3.3.2 Dose response of CV to ISO.
Graph showing the dose response of CV to ISO. Data displayed as mean with bars to represent standard error (SEM). ISO was perfused on over 5 minutes and the peak CV recorded during that time was recorded as the CV response at that concentration. n=4 at Control, $1x10^{-10}$, and $3x10^{-10}$. n=2 at $1x10^{-9}$. n=5 at $1x10^{-7}$M.

3.5 Treatment with Forskolin and IBMX Increases Left Ventricular CV in the Intact Rat Heart

30µM Fsk caused a rapid increase in HR in the intact rat heart: heart rate was increased from 280±200bpm to 420±30bpm (Fig. 3.5.1 C). Fig. 4.4.1E shows an increase in HR of 50±20% at its highest point ($p<0.001$, n=4). There was no significant change in the DMSO control. Fsk did not appear to wash out, with heart rate remaining at 30±7% above the resting heart rate at the end of the 5min washout period.

30µM Fsk increased left ventricular CV: CV increased from 75±8cm/s to 85±11cm/s (Fig. 3.5.1 D). This was a change of 13±2% (Fig. 3.5.1 F) and was significantly different from the DMSO control ($p<0.001$, n=4). There was no significant change in the DMSO control. Again, the CV response did not return to normal within the washout period, with CV remaining at 9±6% higher than the control. However, this results was no longer significant when compared to the DMSO control (n=4), suggesting a high degree of variability.

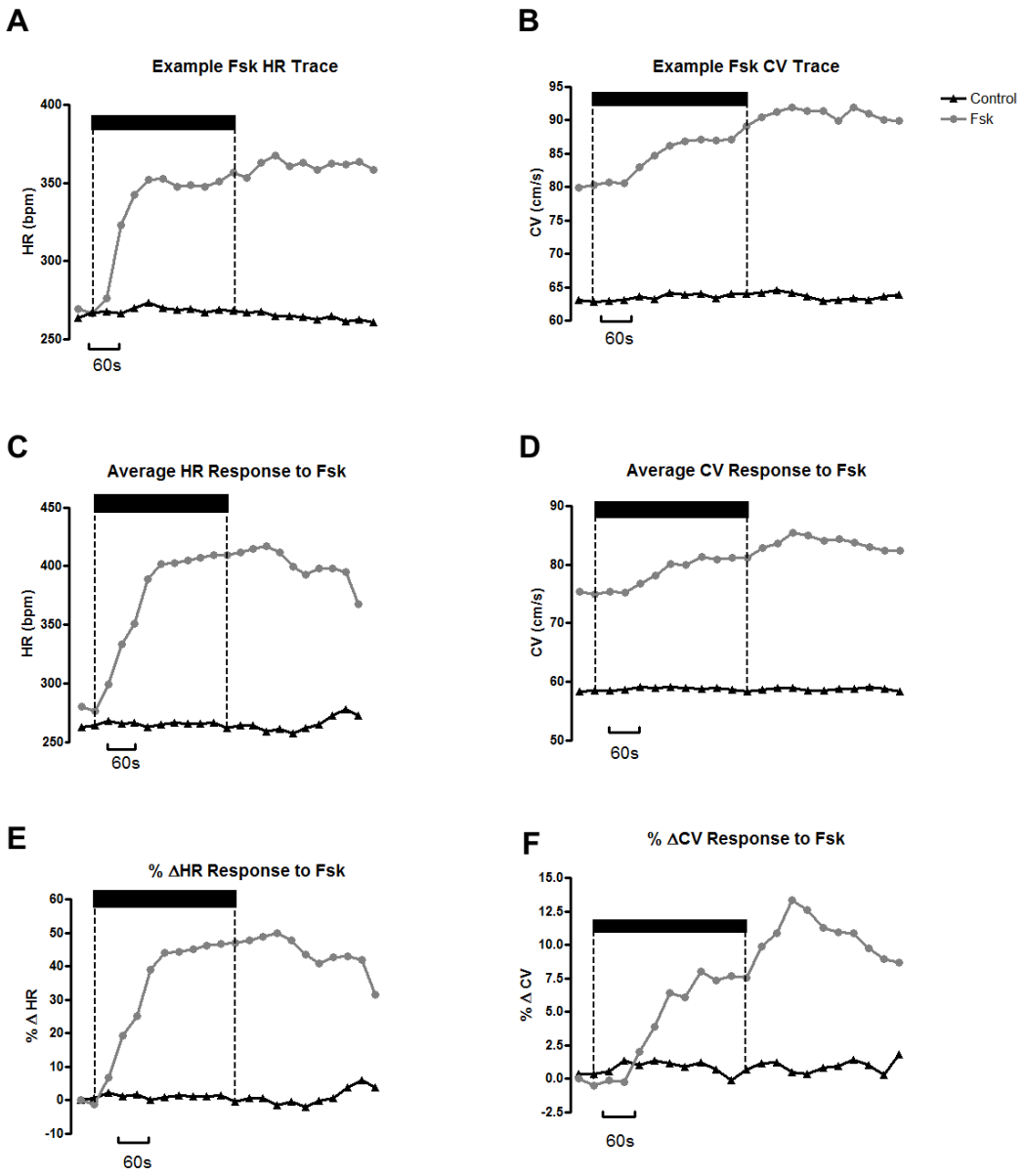

Fig 3.5.1 Effect of 30μM forskolin (Fsk) on heart rate (HR) and CV in the intact rat heart.
Black bar and dotted lines indicate time over which Fsk was perfused into the heart. Data are shown as mean at individual time points. ***A)*** *example traces showing the effect of Fsk on HR.* ***B)*** *example traces showing the effect of Fsk on CV.* ***C)*** *Average HR response to Fsk. Error bars represents SE.(n=4) D) Average CV response to Fsk (n=4).* ***E)*** *%Δ in HR in response to Fsk. Increase in HR in response to Fsk became significant (p<0.05) at 90s (n=4). At 120s-570s p<0.001.* ***F)*** *The %Δ in CV in response to Fsk. Increase in CV became significant at 210s (p<0.01). At 330s-540s p<0.001 (n=4).*

These results show the raising cAMP, independent of β-AR stimulation, increases CV in the intact rat heart.

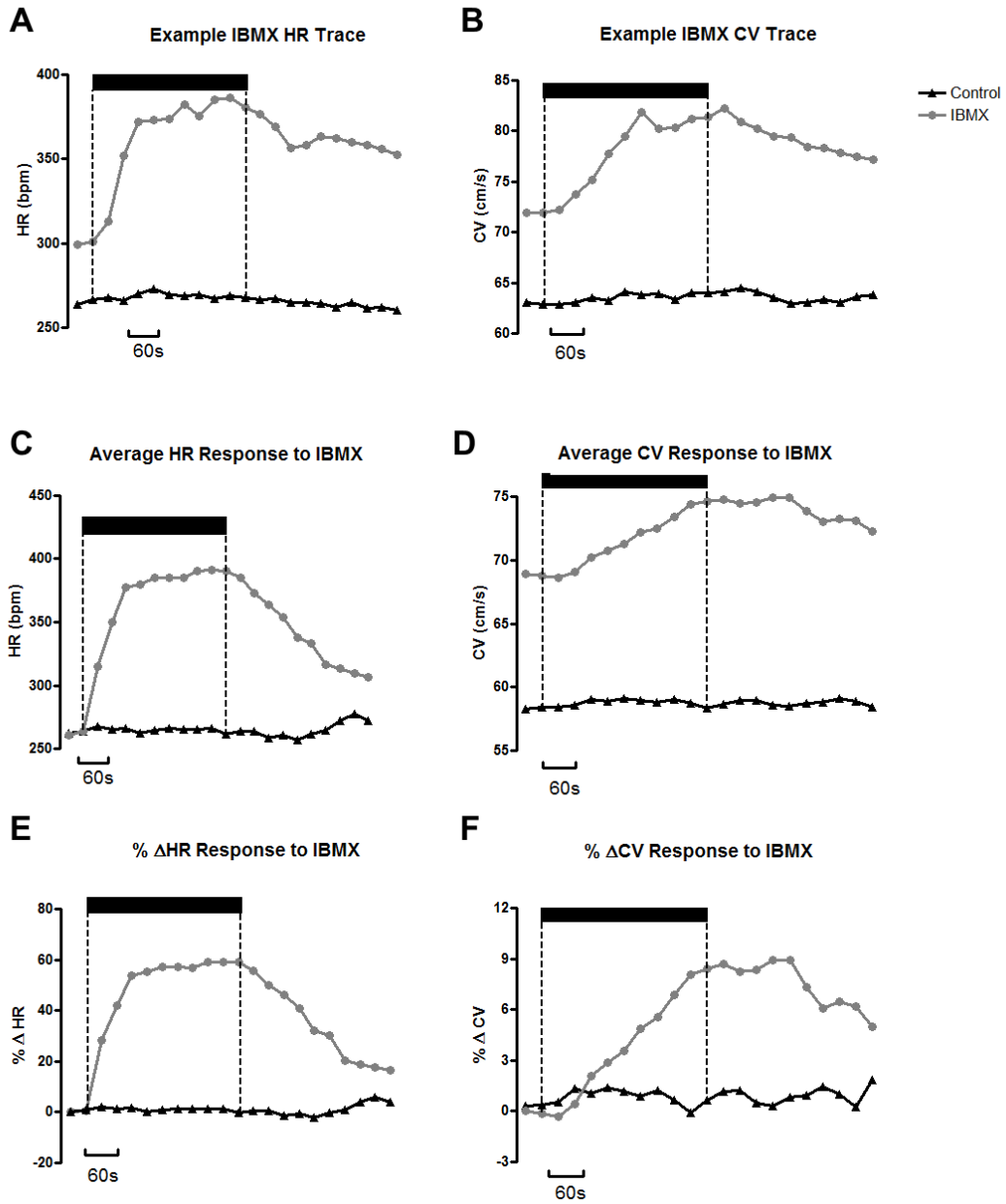

Fig 3.5.2 Effect of 100μM 3-Isobutyl-1-methylxanthine (IBMX) on HR and CV in the intact rat heart. *Black bar and dotted lines indicate time over which IBMX was perfused into the heart. Data are shown as mean at individual time points.* ***A)*** *example traces showing the effect of IBMX on HR.* ***B)*** *example traces showing the effect of IBMX on CV.* ***C)*** *Average HR response to IBMX. Error bars represents SE.(n=4)* ***D)*** *Average CV response to IBMX (n=6).* ***E)*** *%Δ in HR in response to IBMX. Increase in HR in response to IBMX became significant (p<0.05) at 240s-300s (n=4).* ***F)*** *%Δ in CV in response to IBMX. Increase in CV became significant at 270s-450s (p<0.05, n=6).*

The PDE inhibitor IBMX was used to confirm this result by raising cAMP in an independent fashion. IBMX is a global inhibitor of PDEs, which breakdown cAMP, and therefore inhibiting PDEs increases intracellular cAMP.

100µM IBMX increased HR from 260±80bpm to 390±200bpm (Fig. 3.5.2 C), which was an increase of 60±40% (Fig. 3.5.2 E). This increase was significant when compared to the DMSO control ($p<0.05$, n=4). Heart rate began to return to normal after perfusion of IBMX ceased, with heart rate returning to 16±7% above control within the five minute washout period.

Treatment with IBMX increased left ventricular CV in the intact heart. IBMX increased CV from 69±4cm/s to74±6cm/s (Fig. 3.5.2 D). Fig 3.4.2 F shows a maximal increase in CV of 9±4%, which was significant when compared to the DMSO control ($p<0.001$, n=4). CV began to decrease towards control values during the washout period: at the end of the five minutes, CV was 5±3% above control values. This was not significantly different from the DMSO control (n=4), suggesting a high degree of variability in both the control and the IBMX trace at this time-point.

These results confirm the Fsk results and show that raising cAMP increases LV CV in the rat heart.

Finally, a combination of a lower dose of Fsk with IBMX was used to raise cAMP (Fig. 3.5.3). 1µM Fsk and 100µM IBMX were perfused at the same time onto the heart for 5min. As the heart rate response for IBMX and Fsk had already been recorded, only CV was recorded for these experiments. Washout was also not recorded during these experiments.

Treatment with Fsk and IBMX raised CV from 61±7cm/s to 67±6cm/s (Fig. 3.5.3 B). This was an increase of ~9±1% at its highest point and was significant when compared to the DMSO control ($p<0.001$, n=4).

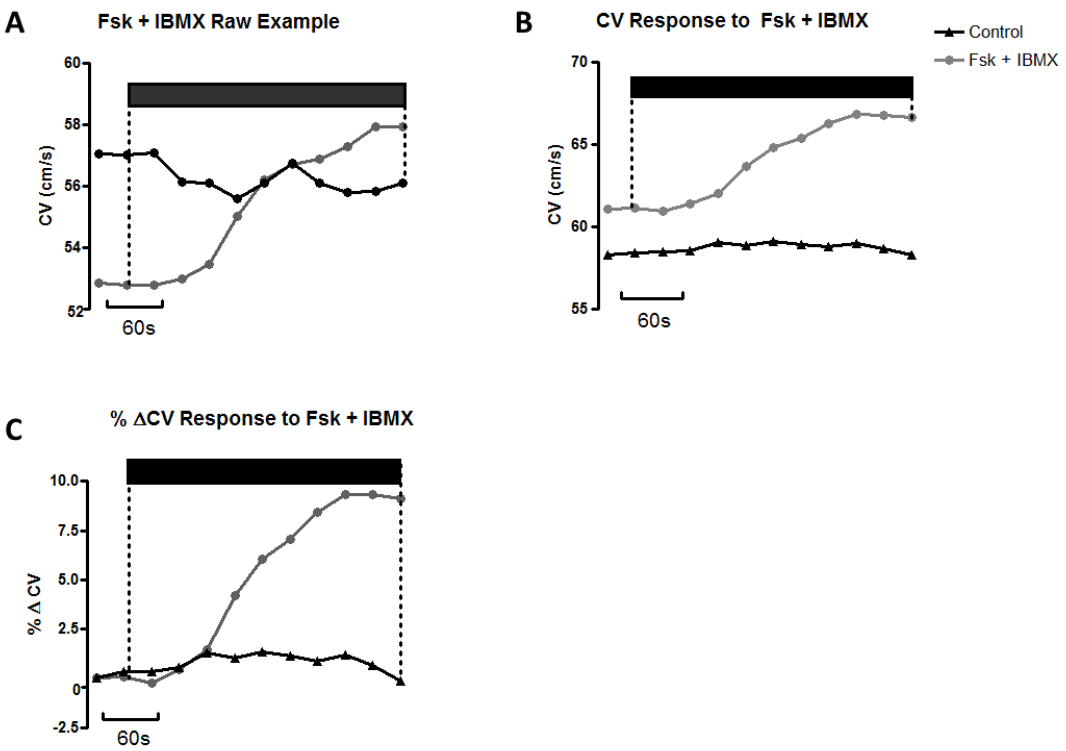

Fig 3.5.3 Effect of 1µM forskolin (Fsk) + 100µM 3-Isobutyl-1-methylxanthine (IBMX) on CV in the intact rat heart.

Black bar and dotted lines indicate time over which Fsk+IBMX was perfused into the heart. Fsk+IBMX was perfused on for five minutes. Data are shown as mean at individual time points. ***A)*** *Example traces showing the effect of Fsk+IBMX on CV.* ***B)*** *Average CV response to Fsk+IBMX. Error bars represents SE.(n=4)* ***C)*** *%Δ in CV in response to Fsk. Increase in CV became significant at 150s ($p<0.01$, n=4). 180s-300s $p<0.001$.*

3.6 Discussion

3.6.1 Summary

Previous studies looking at the effect of β-AR stimulation on myocardial activation time had reported a decreased ventricular conduction time in response to epinephrine (Krayer et al., 1951; Siebens et al., 1953; Swain and Weidner, 1957; Wallace and Sarnoff, 1964). These studies date from the 50s and 60s, and did not distinguish between changes in Purkinje fibre conduction or myocardial CV (Mendez et al., 1964; Swain and Weidner, 1957). Neither did they investigate the signaling pathways involved in these changes.

More recent studies have looked at the effect of raising cAMP on cell-cell conduction and intercellular resistance (Burt and Spray, 1988; Darrow et al., 1996; Somekawa et al., 2005). These studies have found that increasing cAMP can decrease intracellular resistance and suggest that these changes are gap junction mediated (Darrow et al., 1996; Somekawa et al., 2005). However, these studies were carried out in cell pairs or cultured cell lines and therefore cannot directly address the effect on CV.

This study has found that stimulation of β-AR with the non-specific β-agonist ISO increases CV in the intact heart. As the heart was paced on the epicardium within 1.6mm of the recording electrodes, it is assumed that this corresponds with an increase in myocardiul CV independent of the His-Purkinje system. This study also showed that raising cAMP, one of the second messengers of β-AR signaling, also increases CV. Raising cAMP was achieved by manipulating two distinct pathways; increasing cAMP synthesis and decreasing cAMP degradation, respectively. The results indicate that the change in CV is not due to non-specific effects of the drugs or due to effects specific to either adenylyl cyclase or PDEs.

3.6.2 Relevance To Heart Failure

The effect of β-AR stimulation on the heart has been extensively studied: particularly its effect on heart rate, force of contraction (positive inotropy) and on the speed of relaxation (positive lusitropy) (Hicks et al., 1979; Lehnart and Marks, 2007; Marx et al., 2000; Yue et al., 1990). Its effects on the heart are diverse and involve a range of secondary messengers (Hayes et al., 1979). Understanding not only the effect of β-AR stimulation on the heart, but also which intracellular pathways are involved, is important because any intervention on the β-AR signaling pathway will cause a range of different responses. It is well established that β-AR signaling is down-regulated during heart failure (Lohse et al., 2003a; Nikolaev et al., 2010), however β-AR stimulation increases mortality in heart failure patients, while β-blockers are extensively used in treatment of heart disease. Although β-blockers are used

successfully in heart failure to reduce cardiac work, it is clear that β-AR signaling is complex and upregulating specific effects of the β-AR may be beneficial to patients with cardiac disease. It has been demonstrated that there is compartmentalisation of β-AR signaling in the heart (Edwards et al., 2012), and therefore fully understanding these separate signaling pathways is crucial to developing more targeted and effective drugs for heart disease.

It is also important to understand the regulation of CV in the heart: the "electrical wavelength" of the myocardium - determined by the ERP multiplied by the CV - is used to predict the likelihood of re-entrant arrhythmias. This concept was first discussed by Thomas Lewis in 1920 (Lewis, 1920), and Smeets et al. further developed its application to examining re-entrant arrhythmias. A lower wavelength creates a smaller re-entrant circuit which is more likely to be created and sustained by conduction block or areas of inhomogeneity (Smeets et al., 1986). More recently, it has been demonstrated that a low wavelength is a predictor of tachy-arrhythmias (Weiss et al., 2000). A decrease in CV would lower the wavelength and therefore increase the chance of re-entrant arrhythmias in the heart. These changes in CV can occur both at an ischemic region in the heart due to intracellular acidosis affecting gap junction conductance (Kléber et al., 1987) or through remodeling of gap junctions during heart failure (Severs et al., 2004; J. Smith et al., 1991). Therefore, understanding normal regulation and modulation of CV may be important in treating heart failure in the future.

3.6.3 Limitations of Conduction Velocity Recordings

CV was recorded using a fixed set of electrodes placed on the surface of the LV myocardium. This set of electrodes was freely able to rotate through 360^{o}. As shown in fig. 2.2.3, CV varies depending on the rotation of the electrode on the myocardium: this is due to its position relative to the fibre orientation. To keep CV as consistent as possible throughout experiments, CV was recorded as close to longitudinal fibre orientation as possible However, it is not possible to observe fibre orientation in the intact Langendorff preparation without high magnification optics. Therefore, it was necessary to estimate when the CV was at longitudinal CV - this was determined as the fastest CV observed as the electrode was rotated through 360^{o}. This means there was an additional degree of variation in CVs recorded between different hearts.

There seemed to be variation between different hearts in these experiments: basal CV recordings ranged from ~40cm/s to ~80cm/s. This could be due to a number of external factors, the most of likely of these being due to differences in position of the electrode

relative to fibre orientation and also due to slight differences in temperature of solution between experiments - reducing temperature decreases gap junctional conductance (Bukauskas and Weingart, 1993). For this reason, %Δ CV was calculated for all experiments.

Any movement of the electrodes or preparation during the experiment would move the electrodes relative to fibre orientation and would cause a sharp peak or drop in CV. This would invalidate the experiment and for this reason some experiments had to be excluded from the results. This suggested the need for a mechanical uncoupler during these experiments to reduce the incidence of rapid discontinuities in the activation time recordings.

3.6.4 Drug Interventions

All drugs used in this study were perfused on via the method shown in fig. 2.6.1. Initially ISO was perfused on for 3mins (data not shown) however this was not long enough for the CV response to reach a near maximal response. 5min was then chosen for the incubation time. As seen in figs. 3.3.1 and 3.4.1, CV continued to increase following a 5min incubation period with both ISO and Fsk. Perfusion for more than 5mins was tried, however, the heart often became unstable during this time, sometimes developing arrhythmias. It was also a concern that incubation with ISO for a prolonged period would trigger the desensitization/β-arrestin response (Baillie et al., 2007; Lohse et al., 1992). Therefore, 5min was chosen as the optimal incubation time. Treatment with IBMX alone and with Fsk+IBMX appeared to reach near maximal response during the 5min perfusion with these drugs, therefore Fsk+IBMX was chosen as the intervention for future experiments raising cAMP.

4. Effect of β-adrenergic stimulation on the cardiac action potential and intracellular calcium transient

4.1 Introduction

Previous chapters have shown that β-adrenergic stimulation increases CV in ventricular muscle acutely. The main factors which affect ventricular CV are: cell size; gap junctional conductance (GJC) - due to either increased connexin or increased GJ permeability; and action potential shape. Specifically, the rate of rise (dV/dt_{max}) of the AP is a major determinant of CV: it is the source of the depolarising current which spreads between adjacent cells (Buchanan et al., 1985; Kléber and Rudy, 2004; Shaw and Rudy, 1997). The AP upstroke is also indirectly influenced by β-AR stimulation through changes in diastolic interval, via influences on heart rate and APD (Ng et al., 2007; Taggart et al., 2003). Therefore, changes in both dV/dt_{max} and APD may have an influence on CV.

There is no evidence to suggest the β-AR stimulation would alter cell size over short time periods (1-5mins). Therefore, to understand the mechanism by which β-AR stimulation increases CV, the most likely point at which to start would be either to look at the effect of β-AR stimulation on the cardiac AP or on GJC.

This chapter looks at the effect of β-AR stimulation on the cardiac AP using both microelectrode recordings and the voltage-sensitive dye, Di-4-ANEPPS. Ca^{2+} transients were also recorded using the Ca^{2+} dye, Fura-4-AM. The incorporation of an LED light-guide into the electrodes used to record CV allowed the recording of AP and Ca^{2+} alongside CV at the same point on the myocardium.

4.1.1 Effect of β-AR Stimulation on the Cardiac AP

β-AR stimulation has multiple effects on cardiac AP shape. The upstroke of the AP - caused by the activation of voltage dependent Na channels ($Na_v1.5$) is a major determinant of CV (Shaw and Rudy, 1997). Previous studies have shown that β-AR stimulation causes an increase in the magnitude of I_{Na} and AP dV/dt_{max} (Frohnwieser et al., 1997; Lu et al., 1999; Matsuda et al., 1992; Schreibmayer et al., 1994; Wang et al., 1996). However, in whole hearts sympathetic stimulation also increases the steepness of the slope of the APD restitution curve and reduces effective refractory period (ERP), which would in turn decrease the Na current (Ng et al., 2007; Taggart et al., 2003). Therefore, the effects of β-AR on g_{Na} is complex and its effects have not been extensively studied in the intact heart. β-AR stimulation also influences APD and therefore diastolic interval: in large mammals, β-

agonists increase I_{Ks}, causing shortening of the APD (Jost et al., 2005; Volders et al., 2003), preserving diastolic interval and maximizing time for Na channel recovery.

Understanding the extent of the effect of β-AR stimulation on I_{Na} could indicate whether this change is responsible for the corresponding increase in CV. Recording AP amplitude, the rise time of the AP (TRise) and calculating the rate of rise (dV/dt_{max}) will all give an indication of the behavior of I_{Na} in response to β-AR stimulation. When considering AP amplitude as an indicator of I_{Na}, it is important to consider the effect of Ca^{2+} on the AP amplitude: studies carried out in the frog heart have indicated that an increase in extracellular Ca^{2+} leads to an increase in the AP amplitude (Niedergarke and Orkand, 1966). Therefore, dV/dt_{max} and TRise - which is also used to indicate the rate of rise of the AP – are considered better indicators of I_{Na} then AP amplitude. Recording these changes at the same site and over the same time-course as the CV recordings is essential to understanding the effect of AP changes on CV. Our setup would not allow for microelectrode recordings at the site of the CV recordings, as the surface CV electrodes covered a large portion of the LV. Therefore, although the microelectrode is the more established method by which to measure cardiac APs - and allowed the calculation of dV/dt_{max} - the use of Di-4-ANEPPS and optical recordings of APs was a more valuable tool in understanding the impact of changes in AP on CV.

4.1.2 Effect of β-AR Stimulation Ca^{2+} Handling in the Heart

β-AR stimulation has a positive inotropic effect of the Ca^{2+} handling in cardiac myocytes. The L-type Ca^{2+} channel is a substrate for protein kinase A (PKA) - the main effector protein of β-AR signaling. On phosphorylation of the LTCC by PKA, I_{Ca} is increased (Bers, 2001; Reuter, 1987) increasing cytosolic Ca^{2+}, SR Ca^{2+} content and thereby increasing the amplitude of the Ca^{2+} transient (Bers, 2002). The ryanodine receptor (RyR2) is also a target of PKA - this increases RyR2 sensitivity to Ca^{2+} (Bers, 2001) further facilitates calcium-induced calcium release and therefore increases cytosolic [Ca^{2+}] (Bers, 2002). This increase in systolic Ca^{2+} is largely responsible for the positive inotropic response to β-AR stimulation.

The sarcoplasmic/endoplasmic reticulum Ca^{2+} ATPase (SERCA2) is also a target for PKA phosphorylation following β-AR stimulation. Phospholamban (PLB) - an inhibitory protein which inhibits SERCA2 in the unphosphorylated state - relieves inhibition of SERCA2 when phosphorylated by PKA (Bers, 2001). This increases reuptake of Ca^{2+} from the cytoplasm and generates the positive lusitropy caused by β-AR stimulation. It also contributes to

positive inotropy - a combination of increased systolic Ca^{2+} and increased uptake by SERCA2 increases the SR Ca^{2+} content (Bers, 2002).

Recording Ca^{2+} alongside APs and CV allows a better understanding of the effect of β-AR on the cardiac AP and provides another possible mechanism for changes in CV.

4.2 Methods

4.2.1 Microelectrode Recordings

Glass microelectrode recordings are the gold standard technique for measuring absolute transmembrane voltages. The sharp microelectrode technique was used to measure the electrical activity on a single cell as part of the intact myocardium, as previously carried out in this lab (Ghouri et al., 2015). This allowed recording of the AP at the same site and under similar conditions to the way CV recordings had previously been made.

As described in 2.3, the heart was Langendorff perfused and orientated horizontally with the left ventricle facing upwards. The heart was submerged in a specially designed Perspex waterbath containing Modified Tyrode's solution (93mM NaCl, 20mM NaHCO3, 1mM Na2HPO4, 1mM MgSO4.7H2O, 5mM KCl, 20mM Na^{+} acetate, 25mM glucose, 1.8mM Ca^{2+}Cl) maintained at 37^{o}C. The modified Tyrode's solution also contained 3µM blebbistatin to prevent contraction of the heart and allow ME recordings. Sharp glass microelectrodes were pulled from borosilicate glass capillary pipettes of between 40-50MΩ tip resistance and were fillled with 1M KCl and a Ag/AgCl wire. Recordings were digitised at a sampling frequency of 28kHz.

APs were recorded continuously where possible. However, as slight movement of the heart could disturb the microelectrode, this was often not possible. Therefore, recordings were made immediately prior to drug administration and at 1min, 3min and 5min during drug perfusion. Where possible an additional recording was made at 5min after drug 'wash-out.'

The heart was LV paced continuously at 130ms intervals, as in the CV recordings, using bipolar platinum electrodes. Drug delivery occurred through the same syringe driver/syringe cannula system described in 2.6, however due to differences in the horizontal Langendorff system, drug was delivered via a syringe port immediately adjacent to the aortic cannula. As in the CV recordings, this ensured drug was delivered directly to the coronary vasculature.

4.2.2 Optrode Recordings

The setup for the microelectrode recordings did not allow for the recording of CV during these experiments. To record AP and Ca^{2+} measurements alongside CV at the same site and time would allow better understanding of the interaction between these changes. Therefore, it was necessary to develop a method by which APs, Ca^{2+} transients and CV could be recorded simultaneously.

The electrodes used to record CV were set into the centre of a fibre optic light guide. This allowed the transmission and collection of light from sites directly adjacent to the site at which CV was being recorded (2.4). Di-4-ANEPPS is well established as a voltage-sensitive dye, which has been used in single cell in multicellular preparations (Fluhler et al., 1985; Ghouri et al., 2015; Nygren et al., 2003). It is described in more detail in 2.4.1.

Ca^{2+} sensitive dyes are also well established for use in recording intracellular Ca^{2+} transients. Fura dyes have been used in both single and 2-photon (2P) microscopy (Aistrup et al., 2009; Choi and Salama, 2000; Ghouri et al., 2015; Nishizawa et al., 2009). The dye used in these experiments was Fura-4-AM, a cell permeable version of Fura-4. This dye is discussed in more detail in 2.4.2.

The 'optrode' setup allowed the recording of signals from the region of myocardium directly adjacent to the site at which CV was recorded. These were not single cell recordings, but a sum of the electrical activity and Ca^{2+} signals from epicardial cells over a small - ~$1cm^3$ - region.

Background recordings were made prior to the addition of Fura-4-AM or Di-4-ANEPPS. 30µM Fura-4-AM in Tyrode's solution was perfused into the heart over 5min. The perfusion was then switched back to Tyrode's and the preparation was left for a further 10min to allow the acetoxymethyl groups to be removed by intracellular esterases and for the heart to reach a steady state. At the end of this time, 50µl Di-4-ANEPPS (2mM) was added as a bolus.

4.2.3 Drug Intervention

30µM Fsk was used in the microelectrode experiments, as in 3.4 treatment with Fsk appeared to create the largest response of the interventions used (Fig. 3.4.1). However, it was later decided that 1µM Fsk and 100µM IBMX used together was a better intervention which was more stable and had a lower risk of causing non-specific effects. Therefore, Fsk+IBMX was used in the optrode experiments.

In both the microelectrode and optrode experiments, drug was perfused on continuously for 5min using the method described in 2.6.

Results

4.3 Microelectrode Recordings

30µM Fsk was perfused into the heart for 5 min. Fig. 4.3.1A shows the time-course of these experiments alongside sections of example trace from each of the main time-points below.

The resting membrane potential was recorded as -80mV and did not appear to change throughout the experiment. Fsk did not significantly change TRise (rise time of the upstroke between 10-90. AP amplitude also did not change significantly (12.6±3.8%, mean±SEM, n=4; 4.3.1 B). The TRise is a good indicator of dV/dt_{max} and is used to represent this in the optrode experiments. However, with microelectrode recordings it was also possible to calculate dV/dt_{max}. Actual values of dV/dt_{max} are shown in Fig. 4.3.1 D, to demonstrate that these were within expected values and that there was little variation between experiments. There was also no significant change in dV/dt_{max}.

The greatest impact of Fsk was seen on the APD. APD is shown at 50%, 75% and 90% of the repolarisation. Fsk caused a rapid and significant increase in APD50, 75 and 90, increasing to near maximal response within the first minute of drug perfusion (Fig. 4.3.1 E). APD50 increased by 90±20% (mean±SEM, n=4) at the maximal point of the response. APD75 increased by 60±10% (mean±SEM, n=4) and APD90 increased by 30±10% (mean±SEM, n=4).

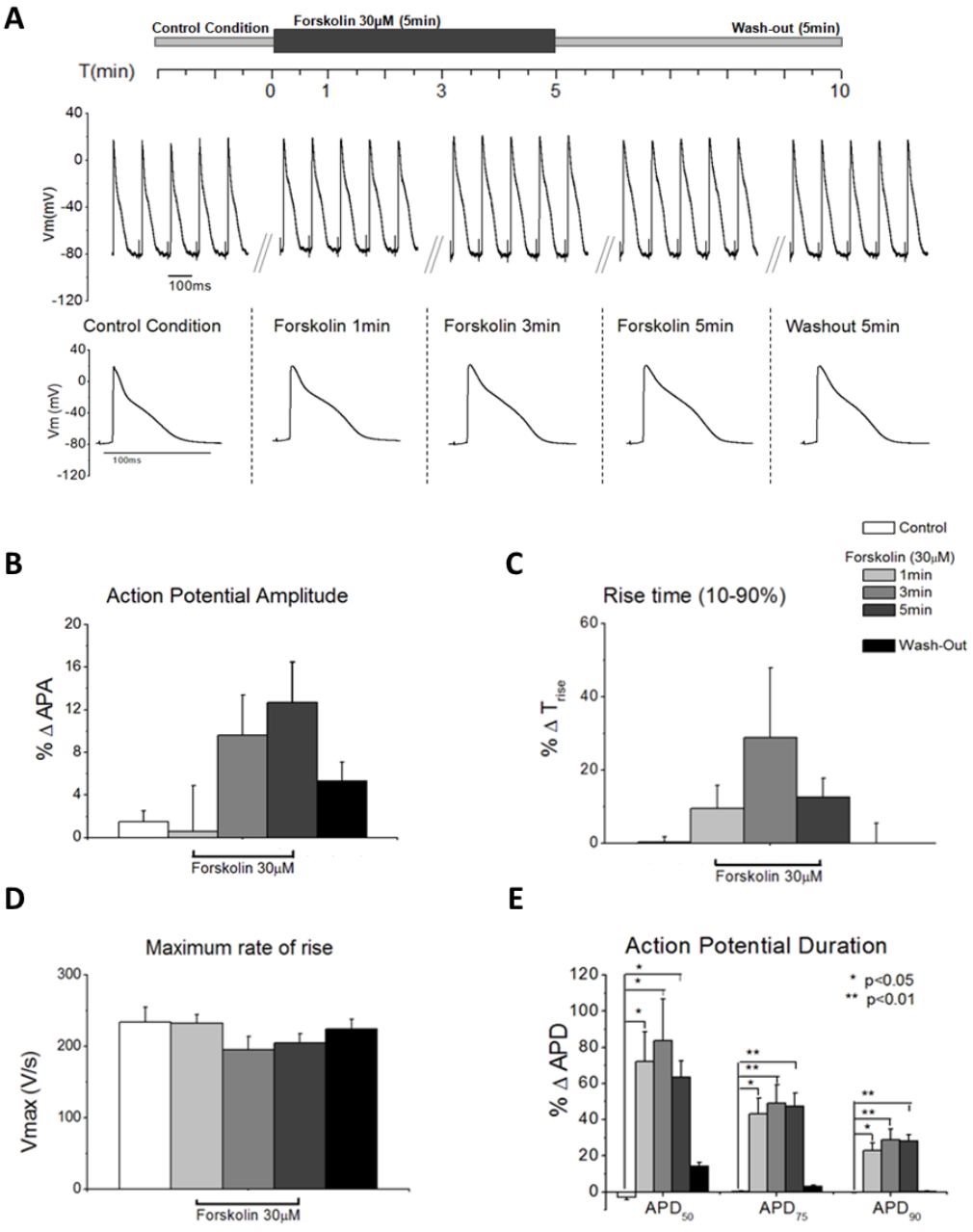

Figure 4.3.1 Raising cAMP prolongs APD in the intact rat heart

A) *Example APs from a single experiment. The top line shows sections of the original trace from the experiment at each of the recording points. Data is represented in bar graph as the mean response ± SEM. Below shows a single AP which is an average of 5s recording. White bars indicate the control recording taken prior to adding Fsk, grey indicates time-points at which recordings were taken during Fsk perfusion and black indicates the washout period.* ***B)*** *There was no significant increase in APA in response to Fsk (n=4).* ***C)*** *There was no significant change in AP rise time in response to Fsk (n=4).* ***D)*** *Maximum rate of rise of the AP (Vmax) was calculated by differentiating the AP with respect to time. Treatment with Fsk did not significantly change Vmax (n=4).* ***E)*** *Fsk significantly prolonged the rat AP at 50, 75 and 90% (n = 4 for everything except wash out, which n=2). (*=p<0.05; **=p<0.01).*

4.4 Optrode Recordings of the action potential show that β-AR stimulation prolongs APD and increases AP amplitude in the intact rat heart

A combination of 1µM Fsk and 100µM IBMX were perfused into the heart to raise cAMP. Fsk+IBMX significantly increased APA (AP amplitude) to a maximum of 8.2±3.2% and by 20.2±4.4% when compared to the DMSO control ($p<0.001$, control n=3, Fsk+IBMX n=6; Fig. 4.4.1 B). There was no significant difference in TRise between Fsk+IBMX and the DMSO control at any point during drug perfusion (Fig. 4.4.1 C).

Fsk+IBMX significantly increased APD at APD50, 75 and 90 (Fig 4.4.1 E-F). APD50 was increased by a maximum of 60.1±11.7% ($p<0.001$, control n=3, Fsk+IBMX n=6); APD75 was increased by a max of 53.2±4.6% ($p<0.001$ control n=3, Fsk+IBMX n=6); APD90 was increased by 32.6±4.7% ($p<0.001$ control n=3, Fsk+IBMX n=6). The change in APD was rapid with maximal values reached within 2min of drug perfusion.

The effect of 100nM isoproterenol on AP was also recorded. ISO significantly increased APA by 10.6±5.0% compared to a time control ($P<0.05$, n=4; Fig 4.4.2 A). As with Fsk + IBMX, there was no significant change in TRise in response to ISO (Fig. 4.4.2 B). ISO prolonged APD50 and 90, but to a lesser extent than Fsk+IBMX (Fig 4.4.2 C-E). APD50 was prolonged by a maximum of 18.1±7.9% ($p<0.05$, n=4). APD75 was slightly prolonged by perfusion with ISO but this change was not significant. Finally, APD90 was significantly prolonged by ISO to a maximum of 8.7±6.2% ($p<0.05$, n=4).

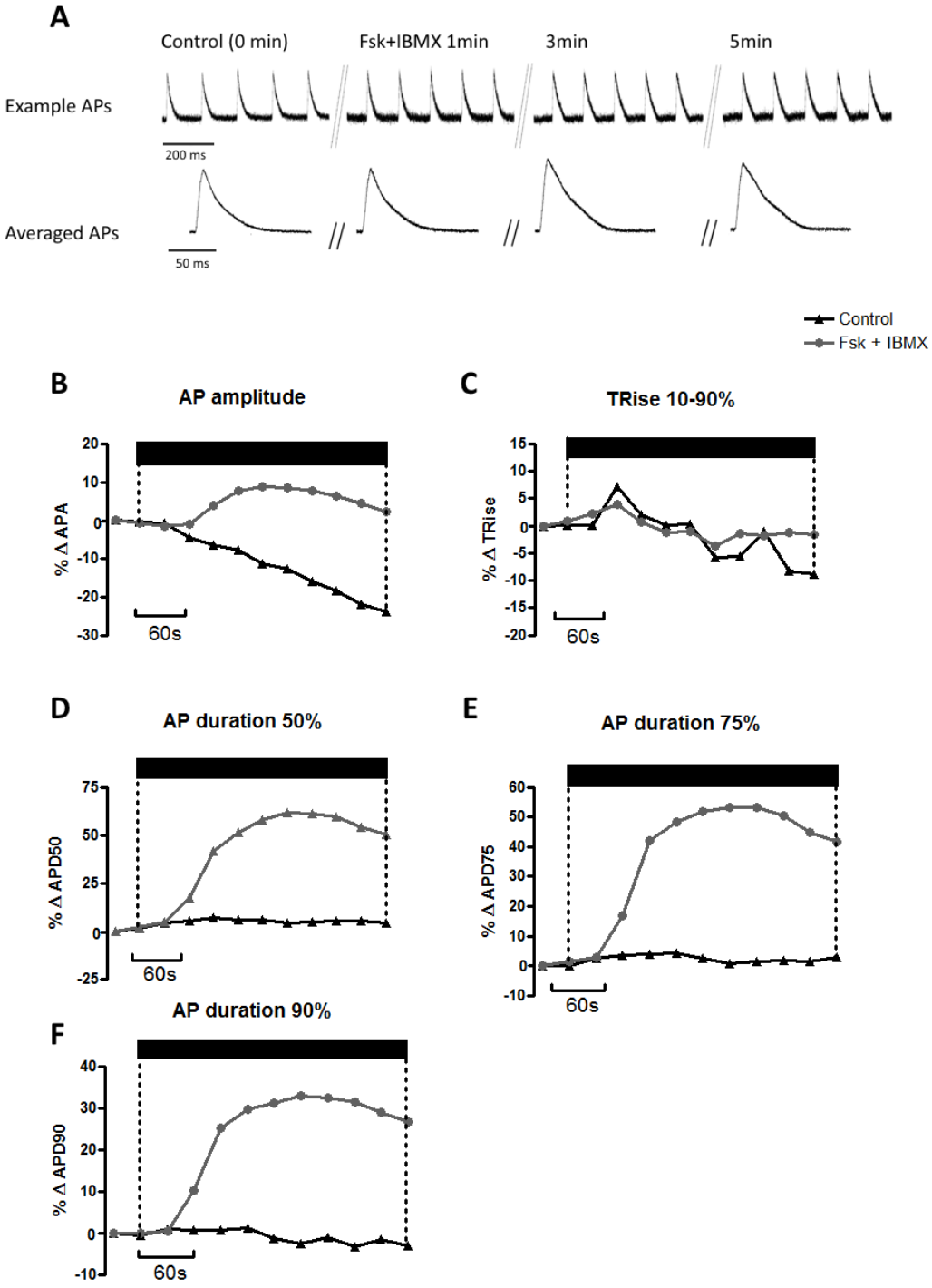

Figure 4.4.1 Raising cAMP increases action potential amplitude (APA) and prolongs action potential duration (APD) in the intact rat heart

A) *Example APs from a single experiment. The top line shows sections of the original trace from immediately prior to drug addition and at 1, 3 and 5min during drug perfusion. Below shows a single AP for each time point which is an average of 5s recording. Data are shown as the mean at individual time points* ***B)*** *Treatment with Fsk+IBMX significantly increased APA. 90s-300s p<0.001 (Control n=3, Fsk+IBMX n=6)* ***C)*** *There was no significant change in AP rise time in response to Fsk+IBMX (Control*

n=3, Fsk+IBMX n=6). ***D)*** *Fsk+IBMX significantly prolonged the rat AP at 50% (APD50). At 90s p<0.01. 120s-300s p< 0.001 (Control n=3, Fsk+IBMX n=6).* ***E)*** *Fsk+IBMX significantly prolonged the rat AP at 75% (APD75). 90s-300s p< 0.001 (Control n=3, Fsk+IBMX n=6).* ***F)*** *Fsk+IBMX significantly prolonged the rat AP at 90% (APD90). At 90s-300s p< 0.001 (Control n=3, Fsk+IBMX n=6).*

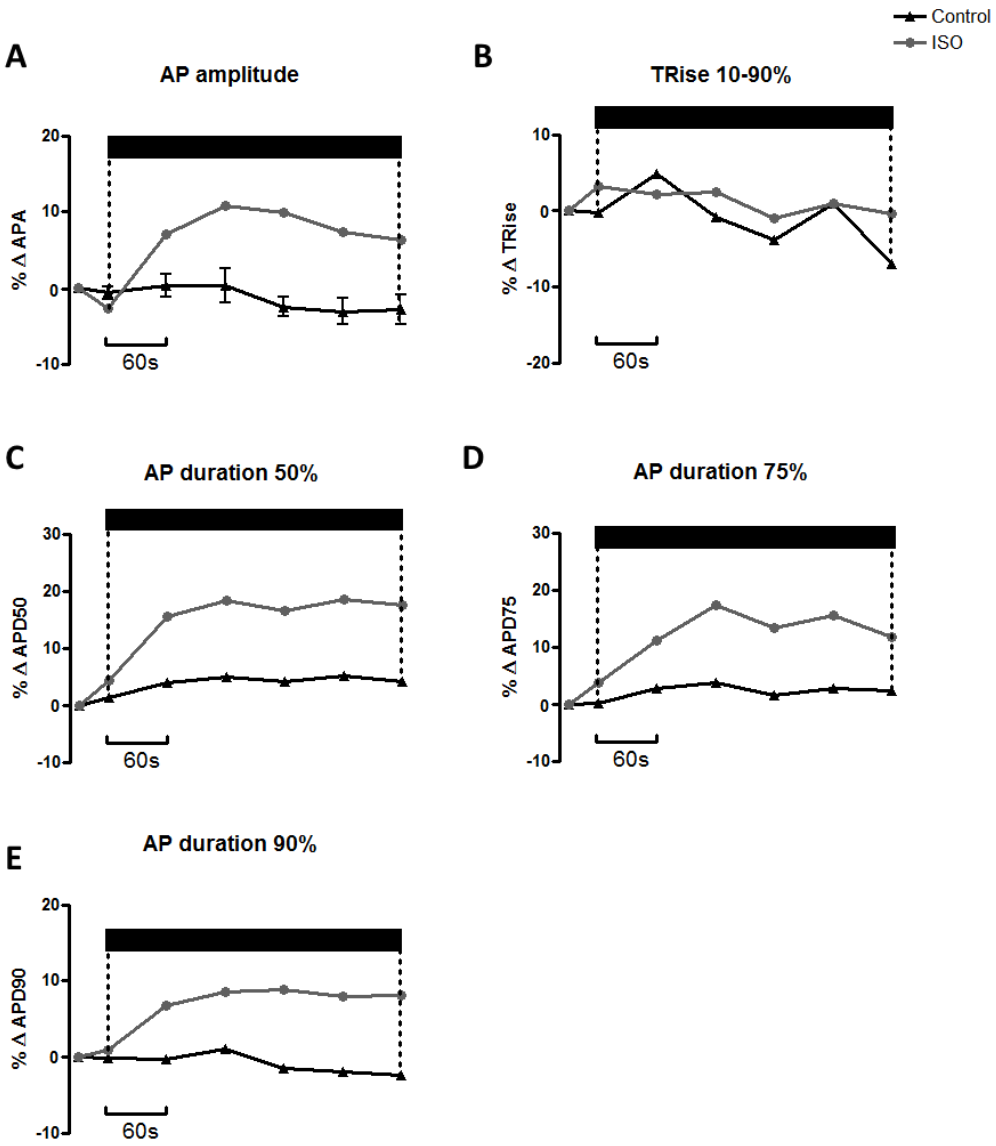

Figure 4.4.2 β-adrenergic stimulation with isoproterenol (ISO) increases action potential amplitude (APA) and prolongs action potential duration (APD) in the intact rat heart
Data shown as mean at individual time points. ***A)*** *Treatment with ISO significantly increased APA. 120s-240s p<0.05 (n=4)* ***B)*** *There was no significant change in AP rise time in response to ISO (n=4).* ***C)*** *ISO did not significantly prolong rat AP at 50% (APD50 (n=4)).* ***D)*** *ISO prolonged the rat AP at 75% (APD75) but the change was not significant (n=4).* ***E)*** *ISO significantly prolonged the rat AP at 90% (APD90). At 180s-300s p< 0.05 (n=4).*

4.5 β-AR increases calcium transient amplitude and shortens the later phases of the calcium transient

Using the Ca^{2+} sensitive dye, Fura-4, Ca^{2+} transients were recorded alongside the AP recordings. Fig. 4.5.1 A shows an example section of AP trace and the corresponding averaged AP, and below that is the averaged Ca^{2+} transient from the same time-point.

1µM Fsk + 100µM IBMX were again used to raise intracellular cAMP. Fsk+IBMX did not significantly affect the Ca^{2+} transient baseline and therefore diastolic Ca^{2+} (n=4; Fig.4.5.1 B). Fsk + IBMX significantly increased the Ca^{2+} transient amplitude, increasing it by 100.3±7.4% (n=4, Fig. 4.5.1C).

Fsk+IBMX also decreased the rise time of Ca^{2+}, suggesting an increase in rate of rise of the Ca^{2+} transient (Fig 4.5.1 D). TRise 10-90% was reduced by 11.9±3.0% at its lowest point ($p<0.05$, n=4). Raising cAMP did not significantly alter Ca^{2+} duration (CaD) at 50% (Fig.4.5.1 E), however it shortened Ca^{2+} transient duration at CaD75 and CaD90 (Fig 4.5.1 F-G). Fsk+IBMX shortened CaD75 by 11.1±1.4% ($p<0.05$, n=4) and CaD90 by 15.0±1.3% ($p<0.001$, n=4).

100nM ISO was used to measure the effect of β-AR stimulation on the Ca^{2+} transient (Fig. 4.5.2). ISO had no significant effect on diastolic Ca^{2+} (Fig. 4.5.2 A). As with raising intracellular cAMP, ISO significantly increased Ca^{2+} transient amplitude by 73.8±10.0% at its highest point ($p<0.001$, n=4; Fig. 4.5.2B). ISO also reduced TRise 10-90% to a maximum response of 9.0±1.8% ($p<0.001$, n=4; Fig.4.5.2 C), indicating an increase in the rate of rise of the Ca^{2+} upstroke. As with Fsk+IBMX, ISO had no effect of CaD50, but shortened the Ca^{2+} transient duration at 75 and 90% (Fig. 4.5.2 D-E). CaD75 was shortened by 11.6±1.3% ($p<0.05$, n=4) and CaD90 was shortened by 18.6±1.2% ($p<0.001$, n=4).

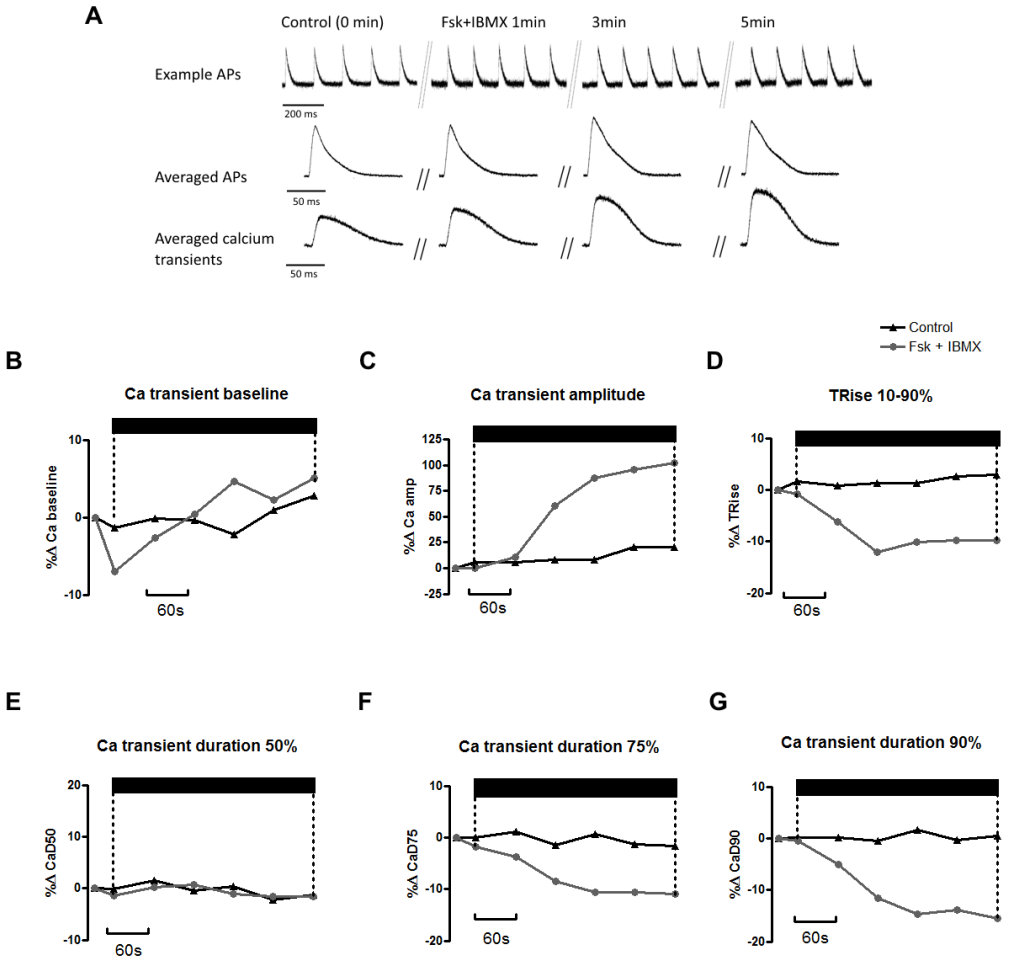

Figure 4.5.1 Raising cAMP increases calcium transient amplitude (CaA) and shortens the later stages of the calcium transient in the intact rat heart

A) *Example APs and Ca^{2+} transients from a single experiment. The top line shows sections of the ratioed AP trace from immediately prior to drug addition and at 1, 3 and 5min during drug perfusion. Below shows a single AP for each time point which is an average of 5s recording. The bottom row shows a single averaged Ca^{2+} from 5s of recording at the same time points as the APs.* ***B)*** *Fsk+IBMX had no significant effect on the baseline of the Ca^{2+} transient (n=4).* ***C)*** *Treatment with Fsk+IBMX significantly increased CaA. 120s-300s $p<0.001$ (n=4)* ***D)*** *Fsk+IBMX significantly shortened Ca^{2+} rise time. 90s-300s $p<0.05$ (n=4).* ***E)*** *Fsk+IBMX did not significantly affect Ca^{2+} transient duration (CaD) at 50% (CaD50) (n=4).* ***F)*** *Fsk+IBMX significantly shortened the Ca^{2+} transient duration at 75% (CaD75). 120s-300s $p< 0.05$ (n=4).* ***G)*** *Fsk+IBMX significantly shortened the Ca^{2+} transient duration at 90% (CaD90). At 60s, $p<0.05$ and at 120s-300s $p< 0.001$ (n=4).*

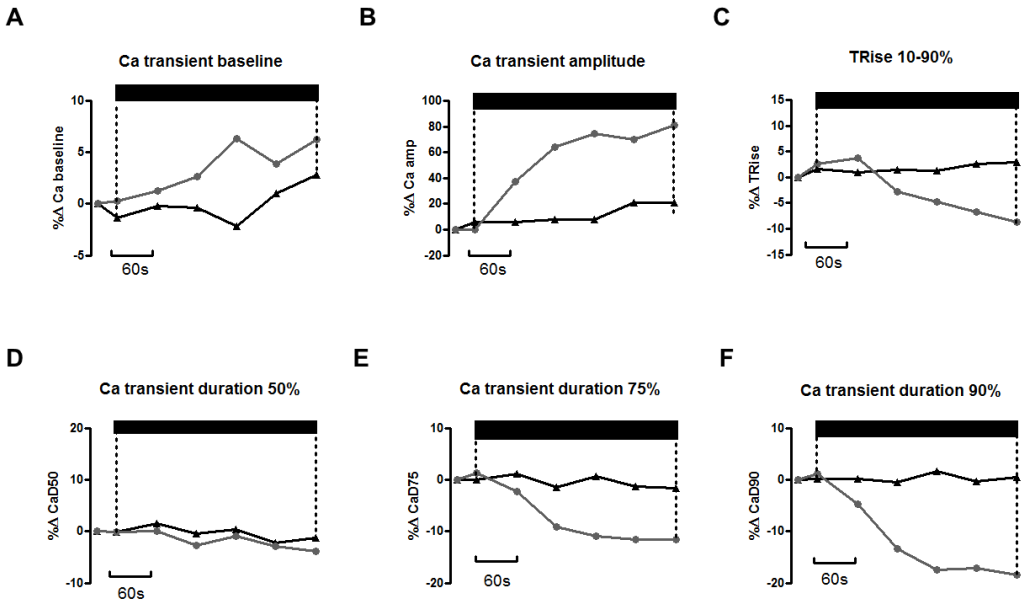

Figure 4.5.2 β-adrenergic stimulation with isoproterenol (ISO) increases calcium transient amplitude (CaA) and shortens the later stages of the calcium transient in the intact rat heart ***A)*** *ISO had no significant effect on the baseline of the Ca^{2+} transient. (n=4)* ***B)*** *Treatment with ISO significantly increased CaA. 120s-300s p<0.001 (n=4)* ***C)*** *ISO significantly shortened Ca^{2+} rise time. At 240s p<0.05 and at 300s p<0.001 (n=4).* ***D)*** *ISO did not significantly affect CaD at 50% (CaD50 (n=4)).* ***E)*** *ISO significantly shortened the Ca^{2+} transient duration at 75% (CaD75). 120s-300s p< 0.05 (n=4).* ***F)*** *ISO significantly shortened the Ca^{2+} transient duration at 90% (CaD90). At 120s-300s p< 0.001 (n=4).*

4.6 Discussion

4.6.1 β-AR Stimulation Increases AP Amplitude but Does Not Affect dV/dt_{max}

Phase 0 of the cardiac AP is the upstroke of the AP: in the ventricle, this upstroke is determined largely by the Na^+ current (I_{Na}) which is caused by the activation of voltage sensitive Na channels ($Na_v1.5$) (Levick, 2000). As previously discussed, the upstroke is a major determinant of CV: it is the source of the depolarising current which spreads between adjacent cells (Buchanan et al., 1985; Kléber and Rudy, 2004; Shaw and Rudy, 1997). It has been previously demonstrated the β-AR stimulation increases the magnitude of I_{Na} and increases the rate of rise of the AP, or dV/dt_{max} (Frohnwieser et al., 1997; Lu et al., 1999; Matsuda et al., 1992; Schreibmayer et al., 1994). However, I_{Na} is also indirectly influenced by β-AR stimulation through changes in diastolic interval, via influences on heart rate and APD (Ng et al., 2007; Taggart et al., 2003), therefore the effect of β-AR on I_{Na} and dV/dt_{max}, in the intact myocardium is complex.

Although it is possible to measure I_{Na} in the intact heart, these experiments are technically extremely challenging. Therefore, both AP amplitude and dV/dt_{max} were shown to represent changes in $g_{Na.}$ The relationship between g_{Na} and dV/dt_{max} is approximately linear, and theoretical and experimental studies have suggested that a 40% increase in g_{Na} would increase dV/dt_{max} by approximately 20% (Berecki et al., 2010, Buchanan et al., 1985; Cohen et al., 1984, 1981).

The microelectrode study showed an insignificant increase in APA and no change in the AP TRise (Fig. 4.3.1B and C). dV/dt_{max} was calculated and Fsk did not significantly affect dV/dt_{max}. This suggests that raising cAMP via Fsk did not affect g_{Na} and therefore was not the mechanism behind the previously recorded change in CV. However, it is important to note that APA is one of the more difficult parameters to record via sharp microelectode, as the slightest movement of the microelectrode would influence APA. Therefore, the trend towards an increase in APA may have become significant with further experiments.

This is supported by the significant increase in APA in response to both Fsk and ISO recorded in the optrode experiments. An increase in APA could suggest an increase I_{Na}, however this increase was not large enough to significantly affect dV/dt_{max} or TRise. The largest increase in APA recorded in these experiments was 10.6%, which would correspond to only a 5% increase in dV/dt_{max}. Again, it is important to consider the possible influence of Ca^{2+} on the AP amplitude – experiments in 4.5 show an increase in CaA in response to Fsk+IBMX. Therefore, the calculated dV/dt_{max} values are a better indicator of g_{Na} than APA.

Change in amplitude in response to Fsk may have been underestimated due to bleaching or wash-out of Di-4-ANEPPS - this is further discussed in 4.6.4.

The relationship between dV/dt_{max} and CV is also not clear. Darrow et al. reported increases in CV in cultured rat neonatal cardiac cells without any reported increase in dV/dt_{max} (Darrow et al., 1996), whereas De Boer et al. carried out a similar study in neonatal rat cells and found a corresponding increase in dV/dt_{max} (de Boer et al., 2007). Studies carried out in the intact ventricle have shown that dV/dt_{max} is proportional to CV^2 (Buchanan et al., 1985; Cohen et al., 1984). Therefore, if the recorded change in amplitude did correspond to approx. 5% increase in dV/dt_{max}, it would only produce an approx. 2% increase in CV. So, although these experiments indicate a possible increase in g_{Na}, this increase is not large enough to account for the full extent of the CV recorded. Using the square-law relationship, an increase in CV of 10% would require an increase dV/dt_{max} of 25%, a result not reported or observed in this study. It is also important to consider that the linear relationship between dV/dt_{max} and CV^2 exists in a uniform, linear cable (Buchanan et al, 1985), whereas in the intact myocardium the relationship will be more complex.

4.6.2 β-AR Stimulation Prolongs APD in the Rat Heart

It is well established that in larger mammals, β-AR causing shortening of the cardiac AP (Jost et al., 2005; Volders et al., 2003). However, in these experiments both Fsk+IBMX and ISO caused the opposite response: significant prolongation of action potential duration. The slow outward K^+ current (I_{Ks}) is a substrate for PKA and β-AR stimulation causes an increase in I_{Ks} (Walsh et al., 1988; Walsh and Kass, 1988), causing the shortening of the APD in larger mammals. However, in rats and mice, the amplitude of both I_{Ks} and I_{Kr} are both much lower than in larger mammals, with a smaller relative contribution to repolarisation (Varró et al., 1993). Therefore, an increase in I_{Ks} in response to β-AR stimulation would not be sufficient to shorten the rat APD. This means that the influence of $Ca^{2+}$and its reuptake by the SR has a greater influence on the repolarisation of the rat AP. As shown in Fig. 4.5.1 and 4.5.2, β-AR stimulation significantly increases the amplitude of the Ca^{2+} transient through a combination of increased I_{Ca}, increased SR Ca^{2+} uptake as discussed in 4.1.2. Although the Ca^{2+} transient is shortened at 75 and 90% by treatment with β-AR stimulation (Fig. 4.5.2 E&F), the large increase in CaA causes an increase in mean Ca^{2+}. The overall effect of these changes on the AP in larger mammals is to elevate the plateau phase of the AP (Bers, 2001). The rat AP is shorter and lacks the plateau phase, therefore the increase in systolic Ca^{2+} instead affects AP repolarisation and prolongs APD.

This changes the effect of β-AR on effective refractory period (or ERP) in rats compared with larger mammals, which - as previously discussed - is an important determinant of calculating 'wavelength' and therefore predicting the likelihood of arrhythmias. This highlights a need to carry out further work studying the effect of β-AR stimulation on CV in larger mammal hearts, for example rabbits, which have a more similar cardiac AP to humans than rats. However, the changes shown in these experiments are rate independent changes in the AP and ERP due to pacing continuously throughout the experiment. The increase in HR caused by β-AR stimulation shortens ERP, and this effect occurs across species (Erlij and Mendez, 1964; Ng et al., 2007).

4.6.3 β-AR Stimulation Increases Ca^{2+} Transient Amplitude and Shortens Transient Duration

The largest response to β-AR recorded in these experiments was the increase in Ca^{2+} transient amplitude (Fig 4.5.1, Fig. 4.5.2); Fsk+IBMX increased Ca^{2+} by as much as 100.3±7.4%. This is in line with previous studies, which suggest this increase is due to a combination of factors, including phophorylation of the LTCC and increase of I_{Ca} (Bers, 2001; Kamp and Hell, 2000), increased SR content via stimulation of SERCA due to PLB phosphorylation (Bers, 2001), and increased Ca^{2+} release from RyR2 (Bers, 2002). β-AR stimulation also shortened the Ca^{2+} at CaD75 and CaD90. This was also in line with previously studies, which suggest this is due phosphorylation of PLB by PKA which reduces the inhibitory effects of PLB on SERCA2, and due to faster Ca^{2+} mediated inactivation of the LTCC (Bers, 2002).

It is clear there is a large change in systolic Ca^{2+} during drug perfusion over the same time period as the changes in CV. Changes in Ca^{2+} have a number of effects in the cell: apart from the obvious positive inotropic and lusitropic effects previously discussed, Ca^{2+} is also involved in intracellular signaling through the calcium/calmodulin-dependent protein kinase (CaMKII) (Grimm and Brown, 2010).

Therefore, although Ca^{2+} is not typically considered as a factor which could increase CV it is important to consider the multiple potential roles of Ca^{2+} in intracellular signaling. Raised intracellular Ca^{2+} has previously been shown to decrease gap junctional conductance, though it has been described as a small response which is more dependent on changes in intracellular pH (De Mello, 1975; Loewenstein, 1981; Spray et al., 1985). Therefore, further study on the effect of raised Ca^{2+} on CV in the intact heart is required.

4.6.4 Limitations of Optical Recordings

Although optical recordings of APs and Ca^{2+} transients provided many advantages during this study, there were limitations to these techniques, particularly when studying both Ca^{2+} and voltage at the same time. Although a background recording was taken before each experiment, this background recording was made before the addition of either Di-4 or Fura-4-AM. For accurate measurements of [Ca^{2+}], background subtraction from the Ca^{2+} signal is required. Due to the fact perfusion of Fura-4-AM and cleaving of the ester groups took in total 20min, Di-4 ANEPPS needed to be added after Fura-4-AM to prevent it from being washed out before the experiment. Therefore, the background recordings had to be taken in the absence of Di-4-ANEPPS, which was less accurate than taking a background in the presence of Di-4-ANEPPS. This did not affect the recordings of the time-course of the Ca^{2+} transient or the relative changes in amplitude recorded, therefore its impact on these experiments was small.

Both V_m and Ca^{2+} results are taken from an area on the surface of the heart, rather than a single cell. Although this meant that a larger number of cells were being sampled, this meant that there was a degree of difference in the time until activation (T_{Act}) between cells. This could cause a 'smearing' of the action potential upstroke when averaging signals from a region of cells - the action potential upstroke would appear slower due to the range of APs being averaged. Due to the speed of the AP upstroke, this was the only measurement affected by this: APD, Ca^{2+} upstroke and Ca^{2+} transient duration would not be significantly affected by this due to their longer time-course. Reporting results as relative change reduced the impact of this, and our results were confirmed with the microelectrode recordings.

Recording from a region of cells would also make it impossible to quantify [Ca^{2+}]. Instead relative change in fluorescence was recorded, and changes in the Ca^{2+} reported as relative change.

Finally, there was also an issue with Di-4-ANEPPS bleaching and washing out during experiments. A decrease in APA was recorded over control conditions (Fig. 4.4.1 B). Although an increase in APA was recorded in response to Fsk+IBMX, it is possible a greater response was partially masked by this decrease in the control. The most likely cause for this decrease in APA is the bleaching of Di-4-ANEPPS or the washout of the dye during the experiment.

5. The Effect of Calcium on Ventricular Conduction Velocity

5.1 Introduction

Previous experiments have demonstrated an increase in CV of ~8% in response to treatment with the β-agonist ISO and of ~10% in response to treatment with the cAMP raising drugs Fsk and IBMX (Chapter 3). Experiments with both microelectrode and voltage-sensitive dyes suggested that changes in the AP were not sufficient to fully explain the mechanism behind these changes in CV in response to β-AR stimulation. These experiments also recorded the effects of β-AR stimulation on the Ca^{2+} transient. A large increase in the Ca^{2+} amplitude of ~100% was recorded in response to raising cAMP (Chapter 4) and this change occurred over the same time-course as the CV response to β-AR stimulation. A change in Ca^{2+} transient amplitude signifies at large increase in intracellular systolic [Ca^{2+}]. This change in Ca^{2+} may have had some impact on CV, and therefore the next step of this study was to examine the effect of Ca^{2+} alone on CV in the heart.

Increased intracellular [Ca^{2+}] is typically thought to have a negative impact on CV - previous studies have shown that increased intracellular Ca^{2+} decreases gap junctional conductance (GJC) (De Mello, 1975; Loewenstein, 1981; Spray et al., 1985), which would also decrease CV. However, Ca^{2+} also plays a role in intracellular signaling through activation of Ca^{2+} sensitive kinases and phosphatases, particularly the Ca^{2+}/calmodulin-dependent protein kinase (CaMKII), which has many diverse roles throughout the cell (Grimm and Brown, 2010) - this is further discussed in 6.1.3.

Initial experiments raised and lowered extracellular Ca^{2+} to measure the effect [Ca^{2+}] on CV. However, it was not clear if this change in extracellular concentration was enough to alter intracellular CV as no significant change in Ca^{2+} amplitude was recorded (5.3.2 D). Therefore, following experiments looked at the effect of the LTCC inhibitor Nifedipine on CV: the LTCC is a substrate for PKA and is phosphorylated in β-AR stimulation. This increases I_{Ca} and is the primary way β-AR increases the amplitude of the Ca^{2+}. Therefore, inhibition of LTCC would be expected to attentuate the CV response if it were mediated by Ca^{2+}.

5.2 Methods

CV measurements were recorded as described in 2.2. AP and Ca^{2+} recordings were made alongside CV using the 'optrode' setup described in 2.4. APs were recorded using the voltage sensitive dye: Di-4-ANEPPS. Ca^{2+} transients were recorded using the Ca^{2+} sensitive dye: Fura-4-AM.

5.2.1 Altering Extracellular Ca^{2+}

To raise extracellular Ca^{2+} for a 5min period, the heart was perfused with Tyrode's solution with (normal) 1.8mM Ca^{2+} as described in 2.1. A glass syringe was loaded with a high Ca^{2+} Tyrode's solution which, on mixing with the perfusate, would result in a final [Ca^{2+}] of 3.6mM. The high Ca^{2+} solution was delivered to the heart as described in 2.6. To reduce extracellular Ca^{2+}, Tyrode's with a [Ca^{2+}] of 1mM was perfused onto the heart. A glass syringe was loaded with high Ca^{2+} so that when the syringe driver was turned on, the final [Ca^{2+}] reaching the heart was 1.8mM. The syringe driver was switched on from the beginning of the experiment and switched off to lower Ca^{2+} perfusing the heart to 1mM during discrete period (5mins) before switching the perfusion syringe on again to restore 1.8mM Ca^{2+}.

5.2.2 Drug Delivery

1µM Nifedipine (Sigma Aldrich, UK) was used to inhibit the LTCC. In 5.3.3, Nifedipine was perfused into the heart using the syringe driver setup described in 2.6. In 5.4.1, 1µM Nifedipine was perfused onto the heart with Tyrode's solution for 10min prior to the experiment. Fsk+IBMX were perfused into the coronary vasculature using the syringe driver setup shown in 2.6

Results

5.3 Raising extracellular Ca^{2+} decreases Ventricular Conduction Velocity

To study the effect of raising or lowering Ca^{2+} on CV, extracellular Ca^{2+} was either increased to 3.6mM or reduced to 1mM for a 5min period. CV, AP and Ca^{2+} transients were recorded over this time. Fig.5.3.1 A shows example averaged Ca^{2+} transients from individual experiments: it shows the Ca^{2+} in normal [Ca^{2+}], followed by the Ca^{2+} transient after Ca^{2+} has been reduced to 1mM or increased to 3.6mM. Increasing extracellular [Ca^{2+}] to 3.6mM significantly decreased CV by 7.3±3.0% when compared with a time control ($p<0.05$, n=4; Fig. 5.3.1). Decreasing extracellular $[Ca]^{2+}$ to 1mM increased CV by 6.9±6.3%. This increases was not significant when compared to a time control (control n=4, Low Ca^{2+} n=3).

Changing extracellular [Ca^{2+}] did not significantly affect Ca^{2+} transient baseline - or diastolic Ca^{2+} - until 300s where high Ca^{2+} increased diastolic Ca^{2+} by 5.0±1.8% ($p<0.05$, Control and high Ca^{2+} n=4, low Ca^{2+} n=3; Fig 5.3.1 D). However, there was an upward drift in the control, and in both low and high [Ca^{2+}] traces. These experiments are shown without background subtraction in Fig. 5.3.1; Fig. 5.3.2 compares these data with the background subtracted data for diastolic Ca^{2+}. An increase in diastolic Ca^{2+} is seen in the example traces for high [Ca^{2+}]: this increase was seen in some but not all experiments, and is line with reported changes in the literature (Bers, 2002). The variability in diastolic Ca^{2+} recordings may be due to the sensitivity of Fura-4, and is further discussed in 5.5.2.

Increasing extracellular [Ca^{2+}] to 3.6mM significantly increased Ca^{2+} transient amplitude by 32.2±5.2% at its maximal point ($p<0.001$, n=4; Fig. 5.3.1 E). Decreasing extracellular [Ca^{2+}] to 1mM decreased Ca^{2+} transient amplitude but this change was not significant until 300s ($p<0.05$ control n=4, low Ca^{2+}n=3; Fig. 5.3.1 E). Altering extracellular Ca^{2+} did not significantly affect Ca^{2+} duration at 90% (control, high Ca^{2+} n=4, low Ca^{2+} n=3; Fig 5.3.1 F).

The change in extracellular Ca^{2+} did not significantly affect the cardiac AP, with no change in APA, TRise or APD90 between high or low Ca^{2+} when compared with the time control (Fig. 5.3.1 G, H and I). However, there was a downward drift in APA over time, which may be due to Di-4 bleaching or wash-out, as discussed in 4.6.4.

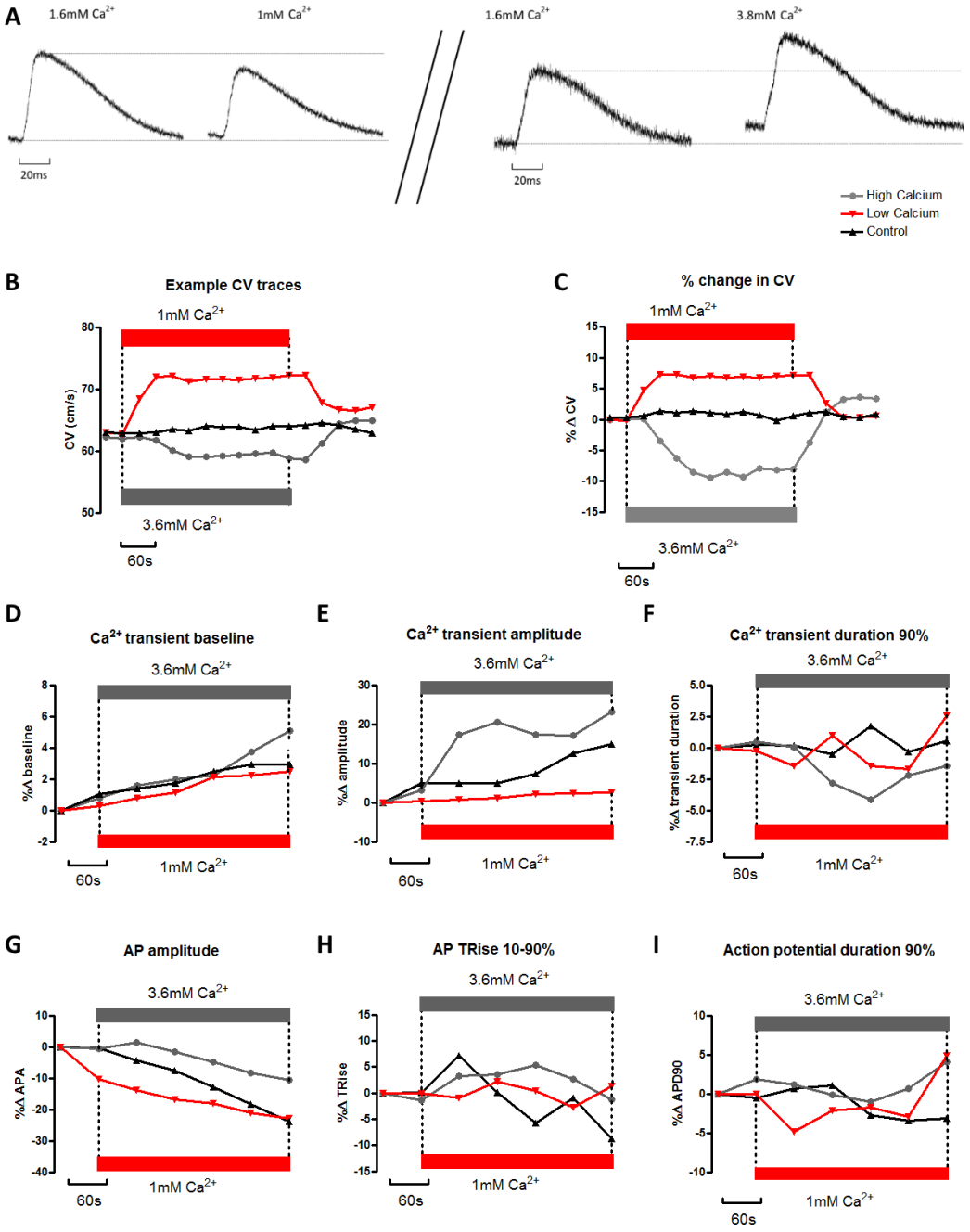

Figure 5.3.1 Raising extracellular Ca^{2+} decreases CV, while lowering extracellular Ca^{2+} increases CV in the intact rat heart.

A) *Example averaged Ca^{2+} transients from a single low Ca^{2+} (1mM) and a single high Ca^{2+} (3.6mM Ca^{2+}) experiment. Transients from pre-and post changing extracellular Ca^{2+} concentration are shown.* ***B)*** *Example CV traces from single experiments showing the effect of high extracellular Ca^{2+} and low extracellular Ca^{2+} on CV.* ***C)*** *Decreasing extracellular Ca^{2+} causes an increase in CV which is not significant when compared to a time control (low Ca^{2+} n=3, time control n=4). Increasing extracellular Ca^{2+}signficiantly decreases ventricular CV (120-270s $p<0.05$ or less, n=4) when compared to a time control. Low Ca^{2+} is significantly different from high Ca^{2+} (at 90s $p<0.01$, 120-300s $p<0.001$. High Ca^{2+} n=4, low Ca^{2+}n=3).* ***D)*** *The change in extracellular Ca^{2+} did not significantly affect the Ca^{2+} transient*

baseline (Control n=4, High Ca^{2+} n=4, low Ca^{2+}n=3) until 300s where 1mM Ca^{2+} was significantly higher vs. time control (P<0.05 Control n=4, low Ca^{2+}n=3). ***E)*** *Increasing extracellular Ca^{2+} to 3.6mM significantly increased Ca^{2+} transient amplitude (60-180s p<0.001, n=4; 300s p<0.001 n=4). Decreasing extracellular Ca^{2+} to 1mM decreased Ca^{2+} amplitude but this change was not significant until 300s (p<0.05 time control n=4, low Ca^{2+}n=3).* ***F)*** *The change in extracellular Ca^{2+} did not significantly affect the duration of the Ca^{2+} at 90% (CaD90) (Control n=4, High Ca^{2+} n=4, low Ca^{2+}n=3).* ***G, H, I)*** *The change in extracellular Ca^{2+} did not significantly affect the cardiac action potential (Control n=4, High Ca^{2+} n=4, low Ca^{2+}n=3).*

The Fura-4 ratio signals that represent intracellular Ca^{2+} concentration results shown in Fig 5.3.1 were measured without subtraction of background fluorescence: this means that the ratio signal is not purely due to Fura-4 fluoresence but also has contributions from backgroud light/intrinsic fluorescence. Thus, loss of Fura4 signal due to loss of dye or bleaching cannot be properly compensated by ratiometry since the significant fixed contribution of background fluorescence to both ordinate and abscissa would result in inappropriate ratio values. This may account for the apparent increase in fluoresence ratio baseline show in Fig. 5.3.1 C and again in Fig. 5.3.2A. Fig. 5.3.2 C and D show the same Ca^{2+} transient baseline and amplitude graphs as A and B, but a background recording - where fluorescence from the preparation has been recorded before the addition of Fura-4-AM - has been subtracted from the traces prior to analysis.

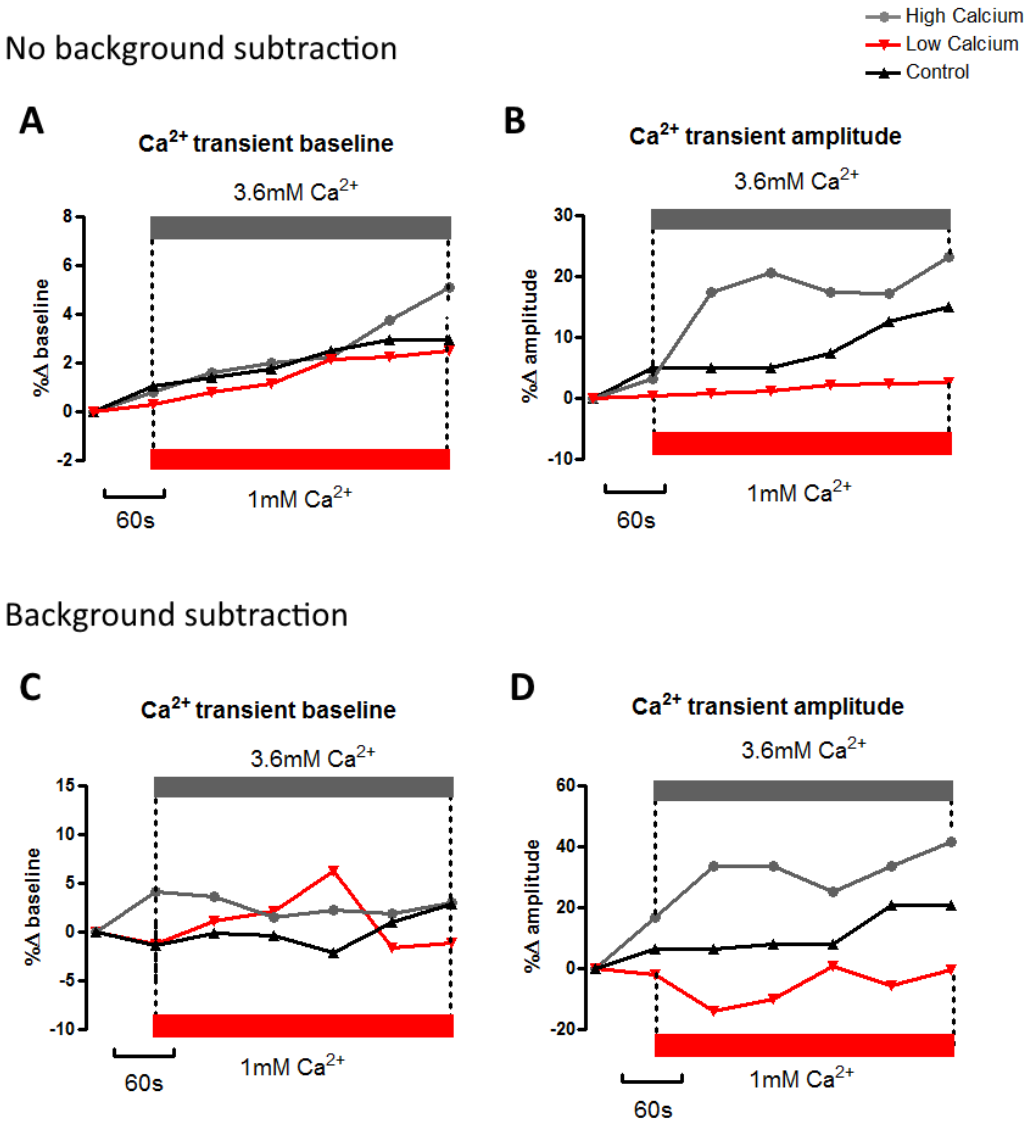

Fig. 5.3.2 Background subtraction gives a more accurate indication of Ca^{2+} transient baseline and amplitude.
A, B) *show the Ca^{2+} transient baseline and amplitude analysed from Ca^{2+} ratioed without background subtraction, as shown in fig. 5.3.1. C, D: show Ca^{2+} transient baseline and amplitude analysed from Ca^{2+} ratioed after background subtraction.* ***C)*** *The change in extracellular Ca^{2+} did not significantly affect the Ca^{2+} transient baseline (Control n=4, High Ca^{2+} n=4, low Ca^{2+}n=3).* ***D)*** *The change in extracellular Ca^{2+} did not significantly affect the Ca^{2+} transient amplitude (Control n=4, High Ca^{2+} n=4, low Ca^{2+}n=3).*

In the background subtracted experiments, there is no significant change in the Ca^{2+} transient baseline in response to raising extracellular [Ca^{2+}] to 3.6mM or reducing it to 1mM (control and high Ca^{2+} n=4, low Ca^{2+}n=3; Fig. 5.3.2 C). However, there is also no significant change in Ca^{2+} transient amplitude in response to high or low Ca^{2+} (control and

high Ca^{2+} n=4, low Ca^{2+}n=3). There is still a trend towards an increase in Ca^{2+} transient amplitude in response to high Ca^{2+} and a trend towards a decrease in Ca^{2+} amplitude in response to low Ca^{2+}, however these changes are small and not significant.

Therefore, it is not clear whether the changes in extracellular Ca^{2+} are also causing changes in intracellular Ca^{2+}. This may due to small changes being difficult to detect on this system or due to the sensitivity of Fura-4-AM - this is discussed further in 5.5.5. Regardless, the changes in amplitude recorded are much lower than the corresponding increase in systolic Ca^{2+} recorded in response to β-AR.

To study the effect of changing systolic Ca^{2+} on CV, the LTCC inhibitor Nifedipine was used, which would decrease systolic Ca^{2+} and therefore decrease Ca^{2+} transient amplitude. These experiments have a n=2, therefore individual traces fro these experiments are shown. 1µM Nifedipine was perfused into the heart for 5min. Nifedipine cause a small increase in CV of 5.6% at its maximal in one trace, but no increase in the second (Fig. 5.3.2 B). Nifedipine did not affect diastolic Ca^{2+} (Fig 5.3.2 C) or Ca^{2+} transient duration at 90% (Fig.5.3.2 E). However, Nifedipine did decrease Ca^{2+} transient amplitude by 45% at its maximal response (Fig 5.3.2 D).

There was no change in the amplitude or the TRise of the AP in response to Nifedipine (Fig 5.3.2 F and G). However, incubation with Nifedipine decreased APD90 by 27%.

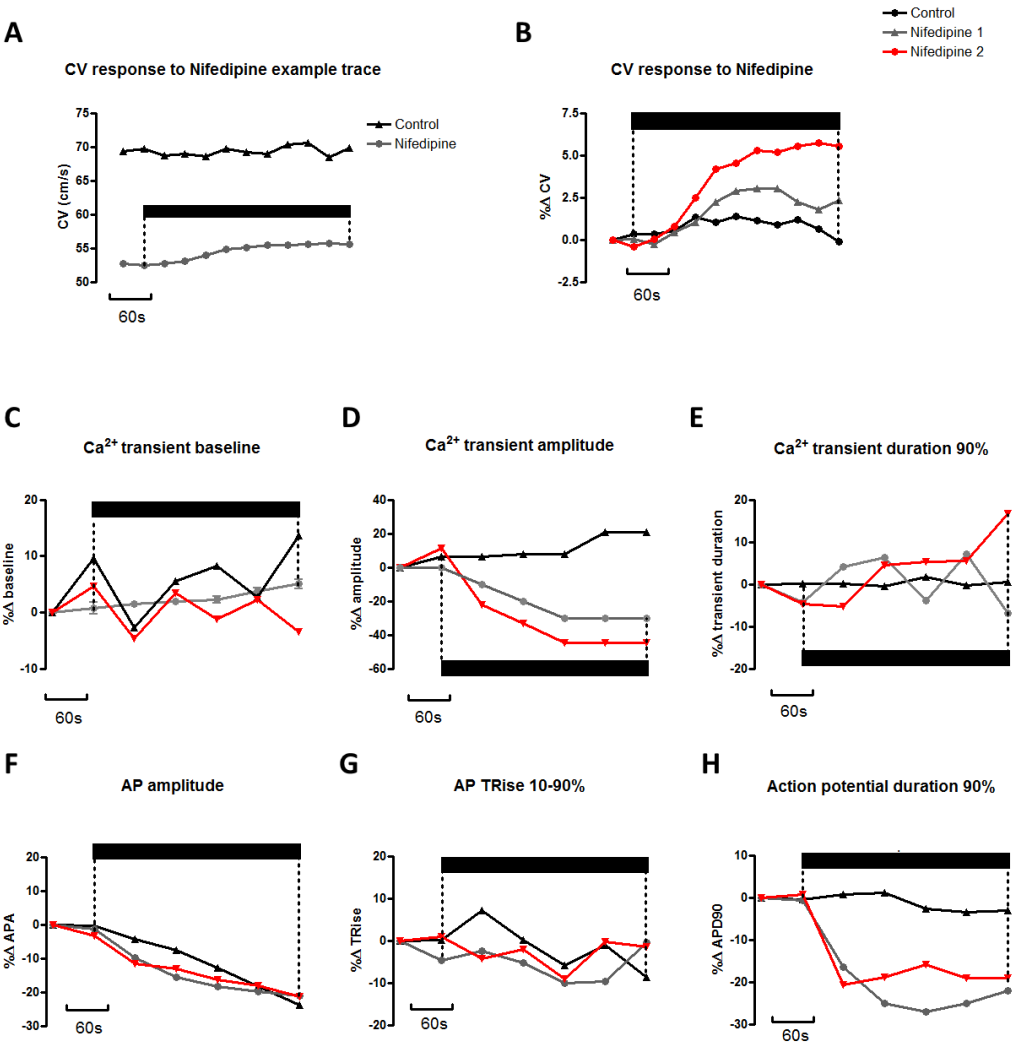

Fig. 5.3.3 Inhibition of L-type Ca^{2+} channel with 1µM Nifedipine increases CV but not to extent of cAMP response.

A) *Example trace showing the raw CV response to Nifedipine.* ***B)*** *% change in CV in response to treatment with Nifedipine. Traces show mean control (black), and the individual Nifedipine traces Nifedipine 1 (grey) and Nifedipine 2 (red). Nifedipine appears to increase CV in one experiment but not in the second. Stats could not be calculated due to the n=2.* ***C)*** *Nifedipine does not affect the Ca^{2+} transient baseline.* ***D)*** *Nifedipine decreases Ca^{2+} transient amplitude.* ***E)*** *Nifedipine does not affect Ca^{2+} transient duration at 90%.* ***F)*** *Nifedipine does not significantly affect AP amplitude.* ***G)*** *Nifedipine does not significantly affect the TRise of the AP.* ***H)*** *Nifedipine significantly decreases APD at 90%.*

5.4 Inhibiting the L-type Calcium Channel with Nifedipine does not Affect the Conduction Velocity Response to Forskolin and IBMX

Although increasing intracellular Ca^{2+} appears to decrease CV (Fig. 5.3.1 B), the opposite of the CV change which accompanies the increase of systolic Ca^{2+} in β-AR stimulation, β-AR signaling and its interaction with Ca^{2+} is complex. Therefore, to understand whether the increase in CV in response to β-AR stimulation is Ca^{2+} independent, the response to Fsk+IBMX was recorded in the presence of 1µM Nifedipine.

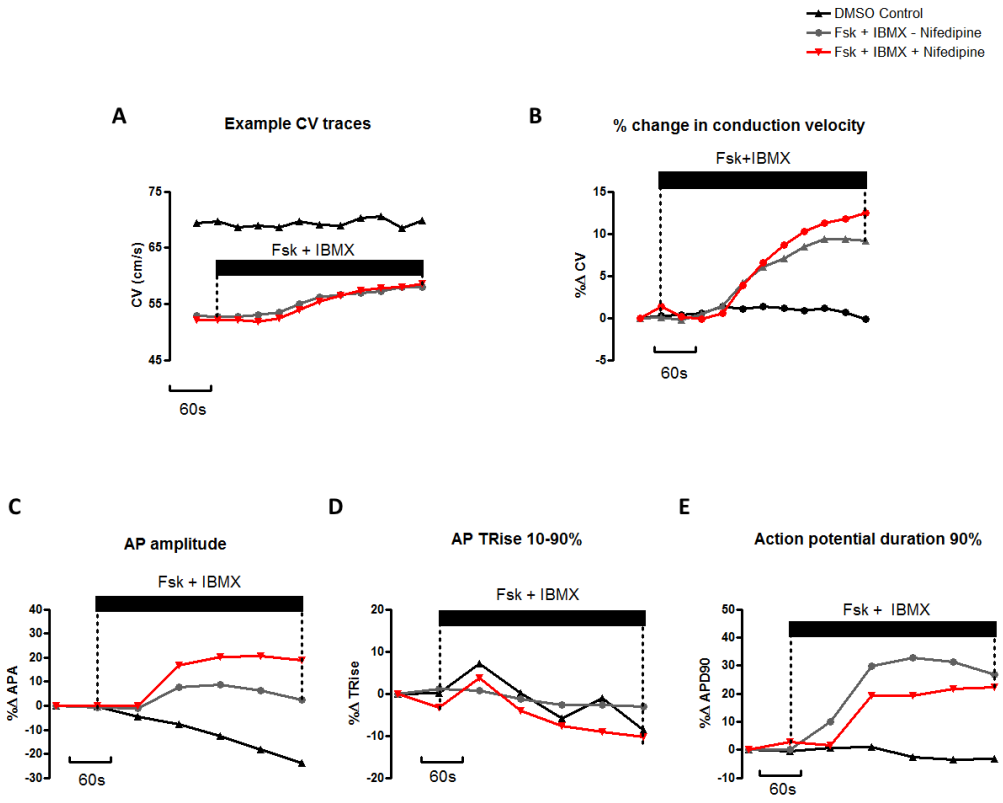

Fig. 5.3.4 CV increases significantly in response to Fsk+IBMX in the presence of the L-type Ca^{2+} inhibitor Nifedipine (1µM).

A) *Example CV traces from individual experiments showing a DMSO control (black), the CV response to Fsk+IBMX-Nifedipine (grey), and Fsk+IBMX+Nifedipine.* ***B)*** *% change in CV in response to fsk+IBMX ± Nifedipine. The CV response is not significantly different between Fsk + IBMX ± Nifedipine (n=4). Fsk+IBMX in the presence of Nifedipine significantly increased CV compared to the DMSO control (150-300s p<0.001, n=4).* ***C, D)*** *The APA and TRise response to Fsk+IBMX are also not significantly different ± Nifedipine (control n=3, Fsk+IBMX-Nifedipine n=6, Fsk+IBMX+Nifedipine n=4).* ***E)*** *Fsk+IBMX+Nifedipine significantly prolongs APD at 90% when compared to the control (240-300s p<0.05; control n=3, Fsk+IBMX-Nifedipine n=6, Fsk+IBMX+Nifedipine n=4). APD90 prolongation is not significantly different between Fsk+IBMX±Nifedipine (control n=3, Fsk+IBMX-Nifedipine n=6, Fsk+IBMX+Nifedipine n=4).*

Fsk+IBMX increased CV by 12.5±1.5% in the presence of Nifedipine ($p<0.001$, n=4; Fig 5.4.1 B). The increase in CV was not significantly different between Fsk+IBMX±Nifedipine (n=4). The APA and TRise response to Fsk+IBMX was not significantly different ±Nifedipine (Control, Fsk +IBMX+Nifediepine n=4, Fsk+IBMX-Nifedipine n=6; Fig 5.4.1 C and D). APD90 was significantly prolonged by Fsk+IBMX both in the presence and absence of Nifedipine ($p<0.001$ Control, Fsk +IBMX+Nifediepine n=4, Fsk+IBMX-Nifedipine n=6; Fig. 5.4.1 E). Although prolongation of the AP at APD90 was slightly reduced in the presence of Nifedipine, it was not significantly different from the Fsk+IBMX-Nifedipine results (Control, Fsk +IBMX+Nifediepine n=4, Fsk+IBMX-Nifedipine n=6).

5.5 Discussion

5.5.1 Raising Extracellular Ca^{2+} Decreases Ventricular Conduction Velocity, While Decreasing Extracellular Ca^{2+}Increases CV

As β-AR stimulation causes a large increase in systolic Ca^{2+} as well as an increase in CV, this study looked at the effects of raising intracellular Ca^{2+} independent of β-AR stimulation. This was achieved by raising extracellular Ca^{2+} from 1.8mM to 3.6mM. The effect of low Ca^{2+} on CV was also measured, by lowering extracellular Ca^{2+} to 1mM. The effect of raising extracellular Ca^{2+} on CV was the opposite of the effect of β-AR stimulation, where high Ca^{2+} significantly reduced CV compared to a time control (Fig. 5.3.1). Low Ca^{2+} also appeared to slightly increase CV, however this change was not significant. This results are in line with previous literature which suggests that raising intracellular Ca^{2+} decreases gap junctional conductance (GJC) (De Mello, 1975; Loewenstein, 1981; Spray et al., 1985). GJC is a major determinant of CV, and a decrease in GJC would correspond to a decrease in CV (Jongsma and Wilders, 2000; Shaw and Rudy, 1997).

5.5.2 Altering Extracellular Ca^{2+} Did Not Affect Ca^{2+} transient Baseline or Amplitude

Although it was expected that increasing extracellular Ca^{2+} would increase intracellular Ca^{2+} - which would be reflected in an increase in Ca^{2+} transient amplitude caused by both an increase in I_{Ca} and SR content (Bers, 2001, 2002) - no significant change was recorded in Ca^{2+} baseline - diastolic Ca^{2+} - or in Ca^{2+} transient amplitude (systolic Ca^{2+}). Although a significant increase in Ca^{2+} transient amplitude is reported in Fig. 5.3.1, the result reported in Fig. 5.3.2 - in which the increase in Ca^{2+} transient amplitude is not significant - following background subtraction is considered the more accurate value. There is, however, both a trend towards increase in Ca^{2+} amplitude in 3.8mM Ca^{2+} and a trend towards a decrease in Ca^{2+} amplitude in 1mM Ca^{2+}. The CV response to changing extracellular Ca^{2+} also suggests

that there is a change in intracellular Ca^{2+}. It is possible that the change was too small to be detected by this system: the use of 360nm LED when exciting Fura-4-AM has limitations which are further discussed in 5.5.5. Fura-4-AM has a lower affinity for Ca^{2+} than its counterpart Fura-2: this makes Fura-4 ideal to study changes in peak Ca^{2+} and for studying the large changes in Ca^{2+} seen after β-AR stimulation, however it is less able to detect small changes in diastolic Ca^{2+} and therefore was possibly not the ideal choice of Ca^{2+} sensitive dye for use in these experiments. The combination of these factors may have prevented detection of small fluctuations in intracellular Ca^{2+}.

It is also clear that changes in Ca^{2+} caused by varying extracellular [Ca^{2+}] are a great deal smaller than the large increase in Ca^{2+} transient amplitude (~100% increase) seen in response to β-AR stimulation.

It is also important to consider that changes in extracellular [Ca^{2+}] may affect the cardiac AP. Increased Ca^{2+} transient amplitude has been shown to increase APA in the guinea pig heart (Leitch and Brown, 1996). Also, increased Ca^{2+} could also alter intracellular Na^{+} via Na^{+}-Ca^{2+} exchange. However, no change was seen in AP morphology in response to altering extracellular [Ca^{2+}] (Fig. 5.3.1 G, H & I).

5.5.3 Treatment with the L-Type Ca^{2+} Channel Inhibitor, Nifedipine, Decreased Intracellular Ca^{2+} but Did Not Significantly Affect CV

The major contributor to the large increase in Ca^{2+} transient amplitude following β-AR stimulation is the increase in I_{Ca} caused by the phosphorylation of the LTCC (Bers, 2002; Kamp and Hell, 2000). Therefore, the LTCC inhibitor Nifedipine was used to lower systolic Ca^{2+} and determine whether this influenced CV; this also has the advantage of directly modifying intracellular Ca^{2+} without affecting extracellular Ca^{2+}. A significant decrease in Ca^{2+} transient Inhibition of LTCC with 1μM Nifedipine demonstrated that inhibition of the LTCC was successful ($P<0.001$, control n=4, Nifedipine n=2; Fig. 5.3.1). Inhibition of the LTCC had no significant effect on CV (control n=4, Nifedipine n=2), however there was a trend towards an increase in CV in response to treatment of Nifedipine. The n of the Nifedipine experiments was only 2, therefore on further experiments, the increase in CV may have been significant. These experiments further suggest that the increase in CV in response to β-AR is not due to increased systolic Ca^{2+} and that in fact a decrease Ca^{2+} may increase CV.

5.5.4 Inhibition of the LTCC with Nifedipine Did Not Affect the CV Response to Fsk+IBMX

Finally, to demonstrate that the β-AR mediated increase in CV was not mediated by increased I_{Ca}, Fsk+IBMX were perfused into the heart in the presence of 1µM Nifedipine. The CV response to Fsk+IBMX in presence of Nifedipine was not significantly different from the Fsk+IBMX alone (n=4). Although the change in APD90 suggests that the increase in I_{Ca} in response to Fsk+IBMX was not completely abolished, Fig. 5.3.1 demonstrated that 1µM was sufficient to reduce Ca^{2+} transient amplitude by ~40%. Therefore, it appears that β-AR mediated I_{Ca} is not a key event in the intracellular pathway responsible for increased CV.

Nifedipine is used at a concentration of 1µM in these experiments. It is clear from 5.4.1 that inhibition of the LTCC reduces Ca^{2+} amplitude. However, in 5.4.2, it does not significantly affect the APD90 response to Fsk+IBMX. Prolongation of APD90 is due in part to the affect of β-AR on the LTCC increasing $I_{Ca.}$. Therefore, it is clear that the LTCC is not completely inhibited by Nifedipine. Previous experiments carried out in isolated rabbit myocytes show that Nifedipine used at 1µM inhibits the LTCC at between 50-70% in the presence and absence of isoprenaline. So although the LTCC is significantly inhibited, the increase in intracellular Ca^{2+} is not blocked. Therefore, the increase in β-AR mediated increase in CV observed in Nifedipine does not eliminate a role for increased cellular Ca2+ as part of cAMP mediated response.

5.5.5 Limitations of Optical Ca^{2+} Recordings Using 360nm and 380nm LEDs

Fura dyes are made to be excited at 340nm and 380nm so that a ratio of the change in fluorescence at each of the wavelengths can be taken: taking a ratio allows for the reduction of artifact caused by movement and reduction of noise on the signal. In these experiments, the ratio of the 380nm signal and the 360nm signal are taken. The signal at 360nm is the isobestic point - or Ca^{2+} insensitive part of the excitation spectrum. Using the isobestic point to take the ratio still cancels the movement artifact on the signal, but reduces the dynamic range of the indicator.

Although the 360nm LED is more powerful than the 340nm equivalent, the maximum power of the 360nm LED is still low, resulting in small emission signals which are as much as 100x smaller than the 380 signal. This means that there is poor signal/noise ratio on the 360nm signal and therefore noise on the 360nm signal can introduce noise on the final ratio. These factors combined with the lower sensitivity of Fura-4 to small changes in $[Ca^{2+}]$ may explain why it was difficult to detect changes in intracellular Ca^{2+} in 5.3.

6.Investigating the Signaling Pathway Behind a cAMP Mediated Increase in Conduction Velocity

6.1 Introduction

6.1.1 Catecholamines Signal Through Multiple Families of β-receptors on the Heart

As previously discussed, the sympathetic nervous system acts on the heart through the release of epinephrine and norepinephrine, which bind to a group of receptors called β-adrenergic receptors. β-receptors are G-protein-coupled receptors (GPCRs) located at the plasma membrane of cardiac myocytes (Bristow et al., 1986). There are multiple types of β-AR expressed on the heart: β_1-AR, β_2-AR, β_3-AR and β_4-AR. β_1-AR are the dominant type of β-AR in the human heart, with β_1-AR expressed at a roughly 80:20 β_1:β_2/β_3-AR ratio (Brodde et al., 2006; Lohse et al., 2003). Stimulation of β_1 receptors generates positive chronotropic, isotropic and lusitropic effects on the heart. Stimulation of β_2 receptors also generates these effects, however specific stimulation of β_2 receptors cannot generate a max inotropic response at the same level of stimulation of β_1 receptors (Brodde et al., 2006). It is thought this due to β_1 signaling being able to generate a global rise in cAMP, whereas β_2 signaling does not, instead giving rise only to compartmentalised increases in cAMP (Brodde et al., 2006). It has also been shown that β_2-AR stimulation does not lead to PLB or RyR2 phosphorylation (Heijman et al., 2011; Xiao et al., 1995). β_2 receptors are jointly coupled to both a G_s G-protein - which leads to the positive inotropic and chronotropic responses - and also to a G_i G-protein (Xiao et al., 1999; Xiao and Lakatta, 1993). G_i-proteins - or inhibitory G-proteins - lead to activation of phosphodiesterases (or PDEs), which may also limit the magnitude of any response to β_2 stimulation (Berthouze et al., 2011).

This study has shown a β-AR mediated increase in CV, which occurs via an increase in cAMP. Therefore, it is likely that this response occurs through either β_1 or β_2-AR mediated signaling. Hearts were treated with ISO (as in previous experiments) in the presence of either β_1 or β_2-AR specific inhibitors to determine whether CV is increased by either β_1 or β_2-AR stimulation.

6.1.2 The β_1 and β_2-AR Stimulatory Pathways Signal through Protein Kinase A and Exchange Protein Activated by cAMP

β-ARs are GPCRs. Both β_1 and β_2-ARs signal through the G_s-protein. The G-protein is made up of the G_α, G_β and G_γ subunits. On activation of the GPCR, the G_α subunit dissociates from $G_{\beta\gamma}$; in the case of the G_s-protein, G_α activates adenylyl cyclase (AC). AC converts cytosolic ATP to the second messenger cAMP, increasing cytosolic cAMP which in turn activates a number of cAMP effector proteins. The main effector of cAMP is protein kinase A (PKA), which, on binding to cAMP, dissociates from inhibitory subunits, allows it to phosphorylate target proteins. As previously discussed, there are a number of PKA targets in the heart, including $Na_v1.5$ (Frohnwieser et al., 1997), the LTCC (Bers, 2001; Reuter, 1987), RyR2 (Bers, 2002) and PLB (Bers, 2001). Cx43 contains phosphorylation sites for multiple protein kinases, including PKA (Grosely et al., 2013; Lampe and Lau, 2004; Solan et al., 2007; TenBroek et al., 2001). As the CV response to ISO was found to be β1-AR mediated, we hypothethised that this increase may be PKA mediated and therefore a PKA activator and inhibitor were selected for the next step of this study.

cAMP also signals via exchange proteins directly activated by cAMP (EPAC). Epac is a guanine nucleotide exchange factor: on binding of cAMP to Epac, Epac undergoes a conformational change which leads to the activation of Rap (Ras-related protein), which is a small GTPase (reviewed in: Edwards et al., 2012). Small GTPases are considered 'cellular switches' which are inactive in their GDP bound form, but become active on binding GTP. Activation of Epac leads to the activation of phospholipase Cε (PLCε) and also of CaMKII (Oestreich et al., 2009, 2007; Pereira et al., 2007), though the mechanism of this is not fully understood. Epacs have been shown to be activated in response to β-AR stimulation and play a role in the regulation of Ca^{2+} release in the heart (Oestreich et al., 2009), including phosphorylation of RyR2 (Pereira et al., 2007).

Inhibitors of both PKA and Epac are used in this study to determine if the increase in CV observed is mediated by either PKA or Epac. However, inhibition studies have limitations due to difficulty in fully inhibiting effects at lower concentrations or potentially causing non-specific effects at higher concentrations. Therefore, further to the inhibitor studies, specific activators of PKA and Epac were used to discriminate between effects caused by activation of PKA and activation of Epac. Analogues of cAMP which interact specifically with either PKA or Epac have been developed and used in multiple studies in cardiac cells (Frohnwieser et al., 1997; Santillán and Boland, 1998; Somekawa et al., 2005). In this study, the PKA activator Adenosine- 3',5'-cyclic adenosine monophosphorothioate, Sp-isomer (Sp-

cAMPS-AM; BioLog: Life Science Institute, Germany), which is resistant to PDE breakdown was used. It also contains an AM group to increase cell permeability as Sp-cAMPS is not lipophilic (Sandberg et al., 1991).

The Epac specific activator used in this study was 8-Bromo-2'-O-methyladenosine-3',5'-cyclic monophosphate (8-Br-2'-O-Me-cAMP-AM; BioLog: Life Science Institute, Germany). 8-Br-2'-O-Me-cAMP-AM is a cell permeable variant of a cAMP analogue shown to specifically activate Epac without activating PKA. (Börner et al., 2011; Komai et al., 2014).

6.1.3 β-AR Mediated Activation of Ca^{2+}/Calmodulin-Dependent Protein Kinase II

β-AR stimulation has also been shown to activate the Ca^{2+}/Calmodulin-dependent protein kinase II (CaMKII). As previously discussed, a PKA independent mechanism of CaMKII by β-AR stimulation has been demonstrated to involve Epac, though the mechanism behind this is not fully understood (Oestreich et al., 2009, 2007; Pereira et al., 2007). CaMKII is also activated in a PKA dependent manner by β-AR stimulation: it has been demonstrated that specific activation of PKA causes activation of CaMKII and that PKA activation is required for phosphorylation by CaMKII at particular phosphorylation sites (Kuschel et al., 1999; Said et al., 2002).

It has been suggested that the systolic increase in Ca^{2+} caused by β-AR stimulation may be responsible for the activation of CaMKII. However, in their review, Brown and Grimm suggest that the phasic nature of CaMKII activity makes this unlikely (Grimm and Brown, 2010) and that CaMKII is activated by local and restricted increases in Ca^{2+} (Song et al., 2008).

CaMKII has multiple targets in EC-coupling: CaMKII has been shown to interact with PLB and the RyR (Currie et al., 2004; Ferrero et al., 2007) and to increase cardiac contractility (Wang et al., 2004) There have also been CaMKII phosphorylation sites identified on the C-terminus of Cx43 (Huang et al., 2011): Huang et al. identify 15 different phosphorylation sites for CaMKII on the C-terminus of Cx43, including previously identified CaMKII phosphorylation sites S306, S325, S328 and S330. It has been suggested that these may play a role in modulating GJC (Grosely et al., 2013).

This study looked at the effect of raising cAMP via Fsk+IBMX in the presence of the CaMKII inhibitor, KN-93.

6.2 Methods

6.2.1 Inhibitor Studies

To study the mechanism behind the increase in CV caused by β-AR, various inhibitors were used to block various components of the β-AR signaling pathway. 300nM CGP 20712A (Sigma Aldrich, UK) was used to block β_1-AR and 100nM ICI 118, 551 (Sigma Aldrich, UK) was used to block β_2-AR. The PKA inhibitor H-89 (Sigma Aldrich, UK) was used at 3μM to selectively inhibit PKA; 10μM of H-89 was used initially (data not shown), however this concentration of H-89 appeared to be damaging to the heart: at this concentration the heart became inexcitable. 5μM KN-93 ($C_{26}H_{29}ClN_2O_4S \cdot H3PO4$, Sigma Aldrich, UK) was used to inhibit CaMKII. Due to the known non-specific effects of KN-93, the control drug KN-92 was also used: KN-93 is the active form of the drug, whereas KN-92 ($C_{24}H_{25}ClN_2O_3S \cdot H_3O_4P$) lacks the active component of the molecule and does not inhibit CaMKII – this allows it to work as a negative control for KN93. Finally, a new inhibitor of Epac1, CE3F4 (Courilleau et al., 2012), was kindly donated by Professor Fischmeister, Université Paris-Sud. This was used at 40μM, as directed, however, this inhibitor had not previously been used in the intact heart.

Inhibitors were perfused onto the heart with Tyrode's solution at least 10min prior to β-AR stimulation. A control recording was taken immediately prior to drug addition and then Fsk+IBMX was perfused into the heart for 5 min, as in previous experiments.

6.2.3 Analogues of cAMP

As previously mentioned in 6.1.2, analogues of cAMP which are designed to specifically activate either PKA or Epac - without binding to other downstream effectors of cAMP - were used to determine whether the recorded increase in CV was PKA or Epac mediated. The PKA activator Sp-cAMPS-AM was used at 24μM in line with concentrations used in previous studies (Sandberg et al., 1991; Santillán and Boland, 1998), however this analogue of cAMP had not previously been used in the intact heart. The Epac activator, 8-Br-2'-O-Me-cAMP-AM, was used at 10μM. Studies site using 8-Br-2'-O-Me-cAM at a range of concentrations from between 20μM and 1mM (Börner et al., 2011; Komai et al., 2014). Due to the large volumes of drug needed in whole heart experiments, 10μM was used to allow the n numbers required for these experiments. Again, this drug had not previously been used on the intact heart.

As the cell permeable variants of these drugs require the removal of acetomethyl group by intracellular esterases, these drugs were perfused on for 10min rather than the 5min used

in previous experiments. They were perfused on using the same syringe driver setup described in 2.6.

Results

6.3 β-AR Mediated Increase in Conduction Velocity is via β_1 adrenoreceptors

The heart was pretreated with either 300nM CGP 20712A (CGP), an inhibitor of β_1-ARs, or 100nM ICI 118, 551 (ICI), an inhibitor of β_2-ARs. The heart was then treated with 100nM ISO as in previous experiments. In the presence of ICI, CV increased in response to ISO by 9.6±3.0%, which was not significantly different from the response to ISO without inhibitor (ISO n=6, ISO+β-inhibitors n=4; Fig 6.3.1 B). Treatment with CGP significantly reduced the CV response to ISO: ISO increased CV by only 2.6±3.6% in presence of CGP compared to 11.9±5.1 without CGP ($p<0.001$, ISO n=6, ISO+β-inhibitors n=4). Inhibition with ICI had no significant effect on the APA response to ISO: ISO increased APA by 5.1±6.5% in the presence of ICI vs. 10.3±5.6% without (n.s., n=4; Fig. 6.3.1 C). CGP completely abolished any increase in APA in response to ISO ($p<0.05$, n=4).

Inhibition with either ICI or CGP produced no effect on the TRise of the APD90 response to ISO (n=4, Fig. 6.3.1 D and E). The increase in Ca^{2+} transient amplitude in response to ISO was reduced in the presence of CGP ($p<0.05$, n=4; Fig. 6.3.1 G): ISO alone increased Ca^{2+} transient amplitude by 62.3±5.4% at its maximal response, whereas ISO in presence of CGP increased Ca^{2+} transient amplitude by only 22.3±17%. ICI appeared to slightly reduce the increase in Ca^{2+} transient amplitude, with Ca^{2+} amplitude reaching 53.3±15.8% at its max response, however the change is not significant (n=4). Shortening of the Ca^{2+}at 90% in response to ISO was significantly decreased by CGP, with Ca^{2+}duration being shortened by only 7.4±4.5% by ISO in the presence of CGP compared to 17.1±1.1% with ISO alone ($p<0.05$, n=4; Fig. 6.3.1 H). Again, ICI had no significant effect on Ca^{2+} duration shortening (n=4).

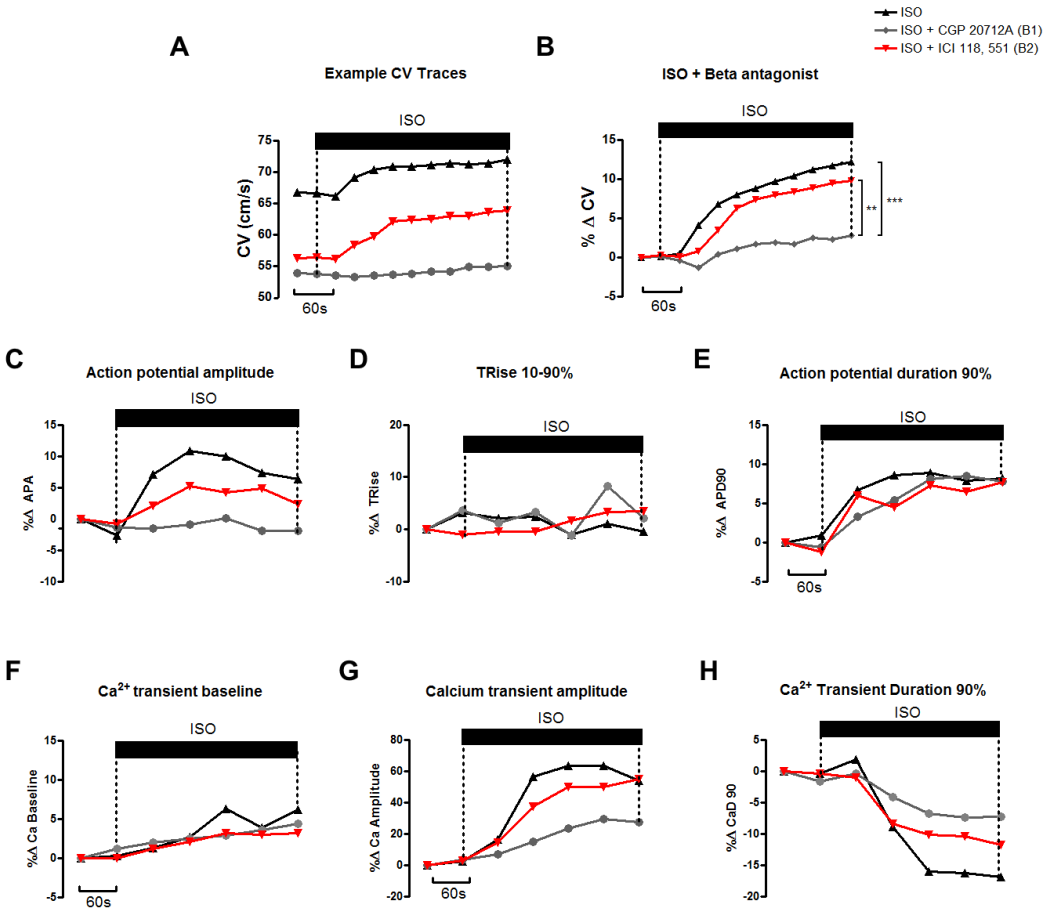

Fig. 6.3.1 β-AR mediated increase in CV is via β1-AR.
A) *Example CV traces taken from individual experiments. Traces show a heart treated with ISO alone (black), a heart treated with ISO after preincubation with 300nM CGP 20712A (grey), a β-1 inhibitor, and a heart treated with ISO after pre-incubation with 100nM ICI 118, 551 (red), a β-2 inhibitor.* ***B)*** *Pre-treatment with CGP 20712A significantly reduces the CV response to ISO (60-120s $p<0.05$ or less, 150-300s $p<0.001$; ISO n=6; ISO+β-inhibitors n=4). Pre-treatment with ICI 118, 551 does not significantly alter the CV response to ISO (ISO n=6, ISO+β-inhibitors n=4). The increase in CV in response to ISO is significantly greater in hearts pretreated with ICI 118, 551 vs hearts treated with CGP 20712A (150-300s $p<0.05$ or less, n=4).* ***C)*** *Inhibition with ICI 118, 551 appeared to reduce the effect of ISO on APA, however this difference was not significant (n=4). CGP 20712A significantly reduced the effect of ISO on APA (120s $p<0.05$, n=4).* ***D, E)*** *Pre-incubation with CGP 20712A or ICI 118, 551 had no effect on TRise or the effect of ISO on APD90.* ***F)*** *Pre-incubation with CGP 20712A or ICI 118, 551 had no effect on Ca^{2+} baseline.* ***G)*** *The increase in Ca^{2+} transient amplitude in response to ISO is reduced in the presence of CGP 20712A (120s $p<0.05$, n=4). ICI 118, 551 also appears to slight reduce the increase in Ca^{2+} transient amplitude, however the change is not significant.* ***H)*** *Shortening of the Ca^{2+}at 90% in response to ISO is significantly decreased by CGP 20712A (120-300s $p<0.05$, n=4). ICI 118, 551 does not significantly alter the CaD response to ISO.*

6.4 Inhibition with the PKA Inhibitor H-89 Does Not Affect the CV Response to Forskolin and IBMX

Hearts were pre-treated with the PKA inhibitor H-89 and then treated with Fsk+IBMX to raise intracellular cAMP to determine if the β-AR mediated increase in CV occurred via PKA. Inhibition of H-89 had no significant effect on the CV response to raising cAMP (Fsk+IBMX-H-89 n=6, Fsk+IBMX+H-90 n=5; Fig. 6.4.1 B).

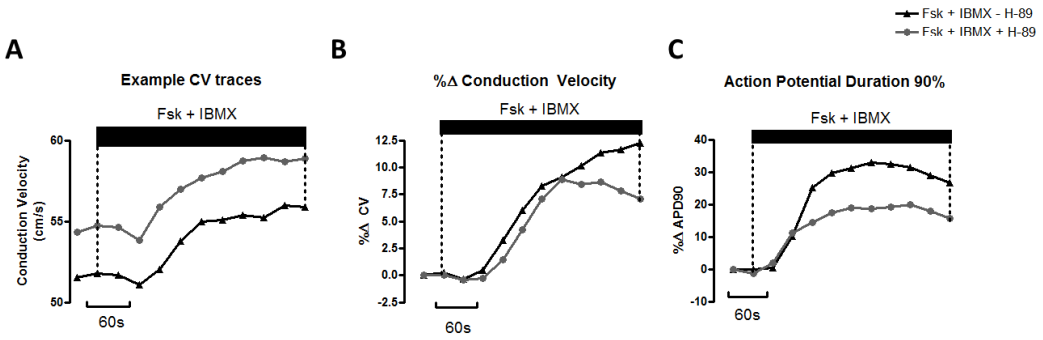

Fig. 6.4.1 Inhibition of PKA via H-89 does not alter the CV response to raised cAMP via Fsk+IBMX. ***A)*** *Example CV traces taken from individual experiments**.** Traces show a heart treated with Fsk+IBMX alone (black) and a heart treated with Fsk+IBMX after preincubation with 3μM H-89 (grey).* ***B)*** *Pre-treatment with 3μM H-89 does not significantly affect the CV response to Fsk+IBMX (Fsk+IBMX-H-89 n=6, Fsk+IBMX+H-89 n=5).* ***C)*** *Pre-incubation with H-89 significantly reduced APD90 prolongation by Fsk+IBMX (p<0.01 Fsk+IBMX-H-89 n=6, Fsk+IBMX+H-89 n=5).*

Incubation with H-89 reduced APD90 prolongation in response to raising cAMP: APD90 was prolonged by 18.6±6.4% in the presence of H-89 and by 31.9±6.9% by Fsk+IBMX alone (p<0.01 Fsk+IBMX-H-89 n=6, Fsk+IBMX+H-89 n=5; Fig. 6.4.1 C).

6.5 Inhibition with the CaMKII Inhibitor KN-93 Reduces the CV Response to Forskolin and IBMX

Hearts were pre-incubated with either the CaMKII inhibitor KN-93 or the control drug KN-92: KN-93 ($C_{26}H_{29}ClN_2O_4S \cdot H3PO4$) is the active form of the drug, whereas KN-92 ($C_{24}H_{25}ClN_2O_3S \cdot H_3O_4P$) lacks the active component of the molecule and does not inhibit CaMKII – this allows it to work as a negative control for KN93. Inhibition with KN-93 significantly reduced the CV response to Fsk+IBMX: Fsk+IBMX increased CV by 12.1±5%, whereas CV was only increased by 3.2±1.8% in the presence of KN-93 (p<0.001 Fsk+IBMX±KN-93 n=6, Fsk+IBMX+KN-92 n=5; Fig. 6.5.1). There was no significant difference

between KN-92 and Fsk+IBMX alone (p<0.001 Fsk+IBMX±KN-93 n=6, Fsk+IBMX+KN-92 n=5). KN-93 also significantly reduced the prolongation of the APD at 90% in response to Fsk+IBMX: Fsk+ IBMX alone prolong the APD90 by 31.9±6%, whereas APD is prolonged by 21.1±10.5% in the presence of KN-93 (p<0.05 Fsk+IBMX±KN-93 n=6, Fsk+IBMX+KN-92 n=5; Fig. 6.5.1). However, KN-92 also reduced APD prolongation in response to Fsk+IBMX, prolonging APD90 by only 12.1±3.7% (p<0.01 Fsk+IBMX±KN-93 n=6, Fsk+IBMX+KN-92 n=5). This suggests that there was a non-specific interaction between KN-92 - and therefore likely also KN-93 - and APD.

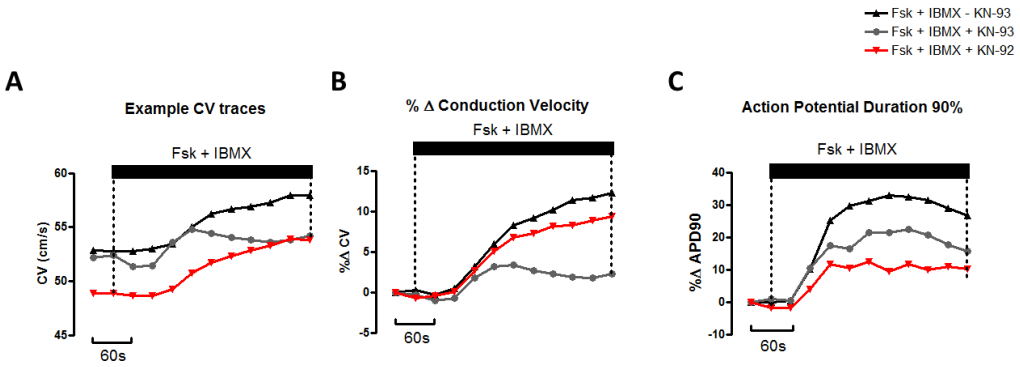

Fig. 6.5.1 Inhibition of CaMKII via KN-93 significantly reduces the CV response to raised cAMP via Fsk+IBMX.

A) *Example CV traces taken from individual experiments. Traces show a heart treated with Fsk+IBMX alone (black) and a heart treated with Fsk+IBMX after preincubation with 5μM KN-93 (grey), and a heart treated with Fsk+IBMX after pre-incubation with the control peptide KN-92 (red).* ***B)*** *Pre-treatment with 5μM KN-93 significantly decreases the CV response to Fsk+IBMX (150-180 p<0.05 or less, 210-300s p<0.001; Fsk+IBMX±KN-93 n=6, Fsk+IBMX+KN-92 n=5). KN-92 did not significantly affect the CV response to Fsk+IBMX.* ***C)*** *Pre-incubation with KN-93 significantly reduced APD90 prolongation by Fsk+IBMX (120s p<0.05, Fsk+IBMX±KN-93 n=6, Fsk+IBMX+KN-92 n=5). However, the control peptide KN-92 also significantly decreased the APD90 response to Fsk+IBMX (90-300 p<0.05or less; Fsk+IBMX±KN-93 n=6, Fsk+IBMX+KN-92 n=5).*

6.6 Inhibition with the Epac1 Inhibitor CE3F4 Does Not Affect the CV Response to Forskolin and IBMX

Hearts were pretreated with the Epac1 inhibitor CE3F4 and then treated with Fsk+IBMX over 5min. Incubation with the Epac1 inhibitor had no effect on the CV response to Fsk+IBMX (Fsk+IBMX- CE3F4 n=6, Fsk+IBMX+ CE3F4 n=3; Fig.6.6.1 B). Pre-incubation with CE3F4 appeared to reduce APD prolongation at 90%: Fsk+IBMX alone prolonged APD90 by 12.6±8, whereas APD90 was prolonged 5.6±4.3% in the presence of CE3F4, however this difference was not significant (Fsk+IBMX- CE3F4 n=6, Fsk+IBMX+ CE3F4 n=3; Fig. 6.6.1 C).

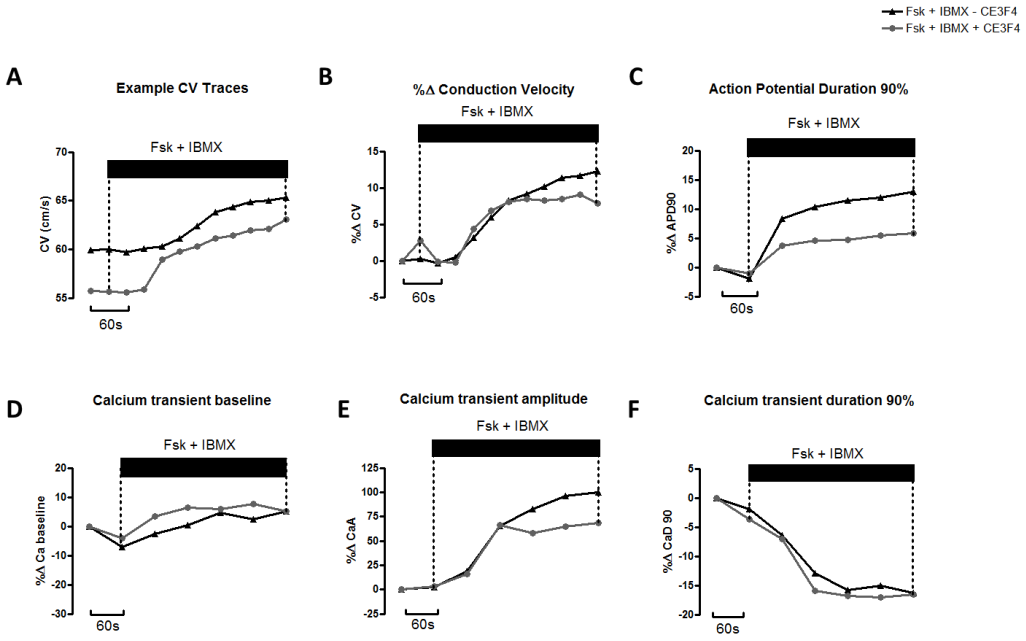

Fig. 6.6.1 Inhibition of Epac1 via CE3F4 does not alter the CV response to raised cAMP via Fsk+IBMX.

A) *Example CV traces taken from individual experiments**.*** *Traces show a heart treated with Fsk+IBMX alone (black) and a heart treated with Fsk+IBMX after preincubation with 40µM CE3F4 (grey).* ***B)*** *Pre-treatment with 40µM CE3F4 does not significantly affect the CV response to Fsk+IBMX (Fsk+IBMX- CE3F4 n=6, Fsk+IBMX+ CE3F4 n=3).* ***C)*** *Pre-incubation with CE3F4 appears to reduce APD90 prolongation by Fsk+IBMX, however the change was not significant (Fsk+IBMX- CE3F4 n=6, Fsk+IBMX+ CE3F4 n=3).* ***D)*** *Pre-treatment with 40µM CE3F4 does not significantly affect the baseline of the Ca^{2+} transient (Fsk+IBMX- CE3F4 n=6, Fsk+IBMX+ CE3F4 n=3).* ***E)*** *Pre-incubation with CE3F4 appears to reduce the increase in Ca^{2+} transient amplitude by Fsk+IBMX, however the change was not significant (Fsk+IBMX- CE3F4 n=6, Fsk+IBMX+ CE3F4 n=3).* ***F))*** *Pre-treatment with CE3F4 does not significantly affect Ca^{2+} duration at 90% (Fsk+IBMX- CE3F4 n=6, Fsk+IBMX+ CE3F4 n=3).*

6.7 PKA specific cAMP analogue SpcAMPS-AM Increases Conduction Velocity in the Intact Rat Heart

Analogues of cAMP which specifically activate either PKA (Sp-cAMPS) or Epac (8-Br-2'-O-Me-cAMP-AM - referred to as 8-Br-AM from this point) were perfused into the heart to determine whether the increase in CV in response to β-AR was a PKA or Epac1 mediated response. The analogues of cAMP used in these experiments were -AM cell permeable variants of the drugs, therefore they were perfused on for 10min - rather than 5min - as cleavage of the acetomethyl group would mean these drugs would take longer to work. The Fsk+IBMX trace shown for comparison contains only 5min of drug incubation. The DMSO control trace also shows only 5min of addition of DMSO, however a further 5min washout period is displayed as a time-control.

CV was significantly increased by the PKA specific analogue, SpcAMPS (Fig. 6.7.1 B). SpcAMPS showed a maximal increase in CV of 10.9±3.5% ($p<0.001$ Fsk+IBMX n=6, DMSO, SPcAMPS-AM, 8-Br-AM n=4). This increase was comparable to the increase of 12.1±2.5% seen in response to Fsk+IBMX. 8-Br-AM had no effect on CV (Fsk+IBMX n=6, DMSO, SPcAMPS-AM, 8-Br-AM n=4). SpcAMPS significantly prolonged APD90 by 8.9±4.4% ($p<0.05$ Fsk+IBMX n=6, DMSO, SPcAMPS-AM, 8-Br-AM n=4; Fig. 6.7.1 C), though APD90 by SpcAMPS was significantly less than APD90 prolongation by Fsk+IBMX ($p<0.1$ Fsk+IBMX n=6, DMSO, SPcAMPS-AM, 8-Br-AM n=4). 8-Br-AM showed no significant difference from the DMSO control (Fsk+IBMX n=6, DMSO, SPcAMPS-AM, 8-Br-AM n=4).

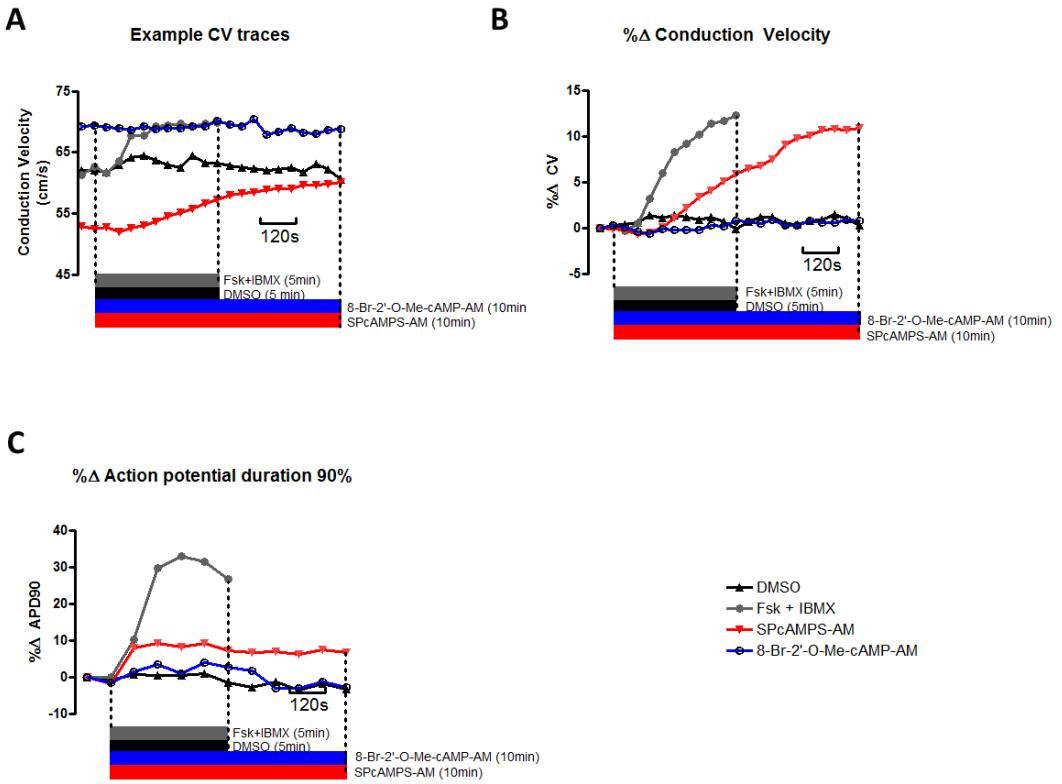

Fig. 6.7.1 Treatment with the PKA-specific cAMP analogue, SPcAMPS-AM, significantly increases CV over 10 minutes

A) *Example CV traces taken from individual experiments**.** Traces show DMSO control in black, a heart treated with Fsk+IBMX in grey, a heart treated with the PKA specific cAMP analogue SPcAMPS in red, and a heart treated with the Epac specific cAMP analogue 8-Br-2'-O-Me-cAMP-AM (8-Br-AM) in blue . **B)** 24µM SPcAMPS-AM significantly increases CV. 10µM 8-Br-AM was not significantly different from the DMSO control. (270s-330s p<0.05 or less, 330-600s p<0.001; Fsk+IBMX n=6, DMSO, SPcAMPS-AM, 8-Br-AM n=4). **C)** SPcAMPS significantly prolonged APD90, though not to the same extent as Fsk+IBMX. 8-Br-AM was not significantly different from the DMSO control (360s, 480-600s p<0.05, Fsk+IBMX n=6, DMSO, SPcAMPS-AM, 8-Br-AM n=4).*

6.8 Discussion

6.8.1 β_1-AR stimulation Increases Ventricular CV

Inhibition with the β_1-AR inhibitor CGP almost completely abolished the CV response to ISO (Fig. 6.3.1). β_2-AR inhibition has no significant impact on the CV response to ISO. This suggests that CV is modulated by β-AR specifically through β_1-ARs. However, β_2-AR inhibition also had no effect on the AP or Ca^{2+} transient. Although the inotropic effects of β_2-AR stimulation are less than β_1-AR stimulation, it is expected that β_2 inhibition would lead to a slight decrease in Ca^{2+} amplitude and a slight reduction in APD prolongation. In these experiments, no significant difference was observed, suggesting it is possible that β_2-AR were not successfully being inhibited.

Therefore, although this study demonstrates that CV is regulated by β-AR through β_1-AR, it does not show that CV is not regulated through β_2-AR.

6.8.2 β-AR Stimulation Increases CV by a PKA Mediated Response

The PKA specific activator SpcAMPS significantly increased CV to a similar magnitude to Fsk+IBMX (Fig. 6.7.1). This cAMP anologue has been shown to be highly specific to PKA activation (Sandberg et al., 1991). Therefore, it is possible to conclude that β-AR stimulation increases ventricular CV via a cAMP and PKA mediated pathway. Although inhibition with the PKA inhibitor H-89 had no effect on the CV response to Fsk+IBMX, using inhibitors is a less accurate way to study the mechanism behind this response than using a specific activator of PKA: it is not possible to ensure that PKA is entirely inhibited by H-89 in this intact preparation, and it is also not known to which extent PKA would need to be inhibited to prevent the CV response. Although it is clear from the APD90 response that H-89 is having an effect on the heart, it was clearly not to a high enough extent to block PKA mediated changes in AP characteristics, this suggests there is a significant remnant PKA activity that couple mediate the CV response observed.

As previously discussed, PKA interacts with numerous targets in EC-coupling, including $Na_v1.5$, which is phosphorylated to increase I_{Na} (Frohnwieser et al., 1997; Lu et al., 1999; Matsuda et al., 1992). This may account for some of the increase in CV, however - as previously discussed in 4.6.1 - the magnitude of change recorded in APA is not sufficient to explain the full increase in CV.

Cx43 has been shown to contain phosphorylation sites for PKA (reviewed by Lampe and Lau, 2004; Solan et al., 2007; TenBroek et al., 2001). Phosphorylation by PKA at S365 has

been suggested to cause an increase in GJC and also to prevent the down-regulation of GJC through phosphorylation by PKC (Solan et al., 2007). This is in line with previous studies which suggest that β-AR increases GJC (Burt and Spray, 1988; Mehta et al., 1992; Salameh et al., 2006) and studies which suggest that PKA activation increases GJC (Somekawa et al., 2005).

6.8.3 Epac activator 8-Br-2'-O-Me-cAMP-AM Did Not Increase CV

The Epac activator 8-Br-2'-O-Me-cAMP-AM did not have any effect on CV (Fig. 6.7.1). The Epac activator also had no effect on APD90. A low concentration of this drug was used and it has never been used in the intact heart before, therefore it is difficult to ascertain whether 8-Br-AM successfully reached the cardiac myocytes at a concentration to have an effect. There are conflicting reports suggesting that Epac has no effect on APD (Hothi et al., 2008) and also that Epac prolongs APD in the rat heart (Brette et al., 2013), therefore it is difficult to ascertain if 8-Br-AM had any effect via other likely EPAC targets.

The inhibitor of Epac1, CE3F4, also had no impact on the CV response to Fsk+IBMX (Fig. 6.6.1), supporting that this is not an Epac1 mediated response. It also had no significant impact on the APD90 prolongation. CE3F4 also had no significant impact on the Ca^{2+} transient. Epac is known to have a role in Ca^{2+} regulation in the heart. Literature suggests that activation of Epac decreases the Ca^{2+} transient amplitude (Hothi et al., 2008; Pereira et al., 2007), meaning that inhibition of Epac would cause an increase in Ca^{2+} amplitude. However, it is possible this increase was masked by the already large increase in Ca^{2+} amplitude caused by Fsk+IBMX and PKA mediated effects. So it is again difficult to ascertain if CE3F4 was having any effect on the heart.

Due to the magnitude of the PKA mediated CV response, it seems probable that this response is PKA and not Epac mediated. However, to fully investigate the role of Epac in this response, further experiments are required. For example, experiments using higher concentrations of the Epac activator while also taking Ca^{2+} transient recordings may give a better indication of whether the Epac activator is reaching the heart.

6.8.4 CaMKII May Play a Role in the β-AR Mediated Increase in CV

Inhibition with the CaMKII inhibitor KN-93 greatly reduced the CV response to Fsk+IBMX. This suggests that CaMKII is involved in the regulation of CV by β-AR stimulation. Recent studies have identified CaMKII phosphorylation sites on the C-terminus of Cx43 (Huang et al., 2011), however the role of CaMKII phosphorylation of Cx43 is unknown. Based on the

results of this study, CaMKII could be activated in a PKA dependent manner and both CaMKII and PKA phosphorylate targets which increase CV.

However, although the control peptide KN-92 had no effect on the CV response to Fsk+IBMX, KN-92 significantly reduced APD90 prolongation by Fsk+IBMX. These results suggest that there are non-specific effects of KN-92 - and therefore KN-93 - occurring. Although these don't appear to affect CV, it would be important to verify these results in further experiments using a different CaMKII inhibitor, such as Autocamtide 2-related inhibitory peptide (AIP).

In summary, attempts to modulate the cAMP mediated CV response using specific inhibitors of A-kinase and CaMkinase pathways proved equivocal. However, strong evidence for an A-kinase mediated changes was obtained using an A kinase specific cAMP analogue which strongly suggests that this is the dominant pathways used to modulate β1-mediated changes in myocardial CV.

7. Discussion

7.1 Conclusions

This study aimed to investigate the effect of β-AR stimulation on ventricular CV. It found that β-AR stimulation via ISO caused an increase in left ventricular CV of approximately 8%. This increase in CV was found to be cAMP mediated, with Fsk+IBMX increasing CV by between 8-12%. This effect was not due to changes in Ca^{2+} handling and, although an increase in action potential amplitude (APA) was recorded, it was determined that changes in I_{Na} were likely not sufficient to explain the change in CV. This suggested a potential role for GJC in mediating these changes in CV. The role for GJC needs to be further investigated: methods by which this could be done are discussed in 7.3.

β_1AR stimulation was shown to be responsible for the increase in CV, though the role of β_2-AR signaling could not be completely ruled out. The β_1AR signals through raising cAMP, and the increase in CV was shown to be mediated through the cAMP sensitive kinase, PKA. This was demonstrated using the PKA activator SP-cAMPS, whereas the inhibitor of PKA – H-89 – had no effect. We suggest that the use of a specific activator is a more accurate way to assess the involvement of PKA in this pathway, as it is not possible to tell if PKA was fully inhibited by H-89. Epac was not shown to have a role in this pathway. The increase in CV in response to β-AR stimulation was also shown to be at least partially CaMKII dependent: inhibition of CaMKII significantly reduced the CV response to raising cAMP. However, this change was accompanied by non-specific effects of KN-92/93 on APD and therefore further experiments are required to validate this.

7.2 PKA Phosphorylation Sites Which Modulate CV

As the increase in CV in response to β-AR stimulation has been demonstrated to be mediated by PKA, it is important to discuss PKA phosphorylation sites which may affect CV and the mechanisms by which PKA may regulate CV.

As previously discussed, $Na_V1.5$ is known to be phosphorylated by PKA. The phosphorylation of $Na_V1.5$ increases I_{Na}, which would be seen in these experiments as an increase in APA and dV/dt_{max}. An increase in APA of 11% was recorded but no change in dV/dt_{max} or TRise was recorded in these experiments. As previously discussed, APA is not an ideal method by which to estimate I_{Na}, as literature has suggests that it may also be influenced by increased Ca^{2+} transient amplitude (Leitch and Brown, 1996; Niedergerke and Orkand, 1966). However, if it is assumed the 11% increase in APA does correspond to an

equivalent increase in I_{Na}, this would increase dV/dt_{max} by approximately 5%. Since dV/dt_{max} is proportional to CV^2, the effect of β-AR stimulation on I_{Na} would only increase CV by approximately 2%. Therefore, the estimated change in I_{Na} caused by acute β-AR stimulation over this time-period is insufficient to explain the ~10% increase in CV. The literature has not come to a consensus on this point, e.g. recordings from neonatal cardiomyocytes suggest that the increase on CV is caused entirely by an increase in dV/dt_{max} (de Boer et al., 2007), while in a separate study on the same preparation (Darrow et al., 1996), increased CV was independent of increased in dV/dt_{max}.

Therefore, the role of other PKA phosphorylation targets must be considered. Cx43 is the dominant Cx in the ventricle. Cx43 has been demonstrated to be a phosphoprotein, which has multiple phosphorylation sites for multiple different kinases. This includes multiple phosphorylation sites for PKA in the C-terminal tail of the protein: S373, S369, S365 and S364 (Lampe and Lau, 2004; Solan et al., 2007; TenBroek et al., 2001). Cx43 turnover is highly dynamic in the heart, as Cx43 has a half-life of only 1-2 hours (Beardslee et al., 1998; Laird et al., 1991) and Cx43 has shown to be variably phosphorylated throughout its lifetime (Chen et al., 2013). cAMP has been shown both to upregulate the amount of Cx43 at the intercalated disc (Somekawa et al., 2005; TenBroek et al., 2001); this could be due to increased transcription of Cx43, as shown in neonatal rat cardiac myocytes (Salameh et al., 2006) or through trafficking of Cx43 to the intercalated disc (Paulson et al., 2000b).

Phosphorylation of Cx43 has also been shown to increase GJ permeability. Solen et. al demonstrated that phosphorylation of S365 on Cx43 not only increased conductance of GJs, but also that S365 phosphorylation prevented phosphorylation of Cx43 by PKC at a site which decreased GJC (Solan et al., 2007). Somekawa et al. showed that activation of PKA using a cAMP specific analogue (6Bnz) led to an increase in GJC without changing the levels of Cx43 at the intercalated disc, suggestion an increase in GJ permeability (Somekawa et al., 2005).

There has been very little work looking at Cx43 and its phosphorylation state following β-AR in adult cells. Western blotting with the use of phospho-specific antibodies could be carried out on tissue which is snap frozen immediately following drug addition. Western blots could also be carried out on isolated cardiac myocytes treated with specific activators of PKA. Further to this, studying the localisation of both Cx43 and phospho-Cx43 following β-AR stimulation, using confocal microscopy and fluorescent antibodies, could give an

indication of whether any change in CV is due to GJ open probability or changes in GJ plaque size.

7.2.1 The Role of CaMKII

Activation of PKA can also lead to the activation of Ca^{2+}/calmodulin-dependent protein kinase II (CaMKII) (Kuschel et al., 1999; Said et al., 2002). This study demonstrated that inhibition of CaMKII by KN-93 significantly reduced the CV response to raising cAMP, however there were concerns about the non-specific effects of KN-93/92, therefore further experiments are required. Recently, 15 CaMKII phosphorylation sites have been identified on Cx43 by mass spectroscopy (Huang et al., 2011), but the function of phosphorylation of Cx43 by CaMKII is unknown.

7.3 β-AR May Regulate CV Via GJC

One possible mechanism by which to explain the change in CV in response to β-AR is changes in GJC. Though these experiments have not measured GJC, the lack of a sufficient increase in dV/dt_{max} to explain this change presents GJC as a likely candidate to explain these changes. However, it is important to consider that the relationship between GJC and CV is not linear: at low levels of GJC, there is a far greater effect on CV than at GJC under normal conditions, as demonstrated by computer simulations by Jongsma and Wilders (Jongsma and Wilders, 2000). Fig. 7.3.1 shows the relationship between CV and GJC (represented as g_j below) (Jongsma and Wilders, 2000). This simulation suggests that to increase CV from 60cm/s to 70cm/s - values within the normal range of CV in mammals - would take an increase in GJC of ~50%.

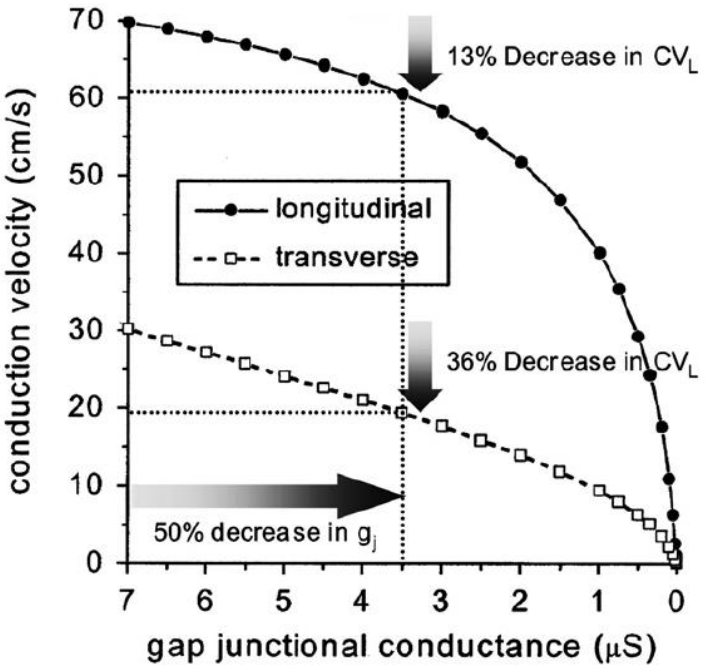

Fig. 7.3.1 Simulations of the effect of gap junctional conductance (g_j) on conduction velocity (Jongsma and Wilders, 2000).
Directional changes in CV shown as a function of gj. Annotated by Valderrábano et al. to highlight the difference in gj modulation of CV between longitudinal and transverse CV: a 50% decrease in gj generates a 13% decrease in longitudinal CV vs. a 36% decrease in transverse CV (Valderrábano, 2007).

It also shows that changes in GJC do not affect transverse conduction velocity (CV_T) and longitudinal (CV_L) equally. Longitudinal conduction velocity is conduction along the fibre orientain - ie. along the long axis of the cell. This has a higher proportion of cytoplasmic conduction vs. conduction across the intercalated disc and is overall lower resistance than in the transverse direction. With transverse conduction, conduction crosses a higher proportion of intercalated discs vs. cytoplasm. This is a higher resistance path - demonstrated by lower CV - but also a path which is more influenced by GJC. This is also demonstrated by computational modeling carried out by Martin Bishop, King's College, UK (Fig. 7.3.2). His modeling demonstrates that increasing GJC has a greater influence of CV_T than CV_L, whereas varying intracellular conductance has a greater influence on CV_L than CV_T.

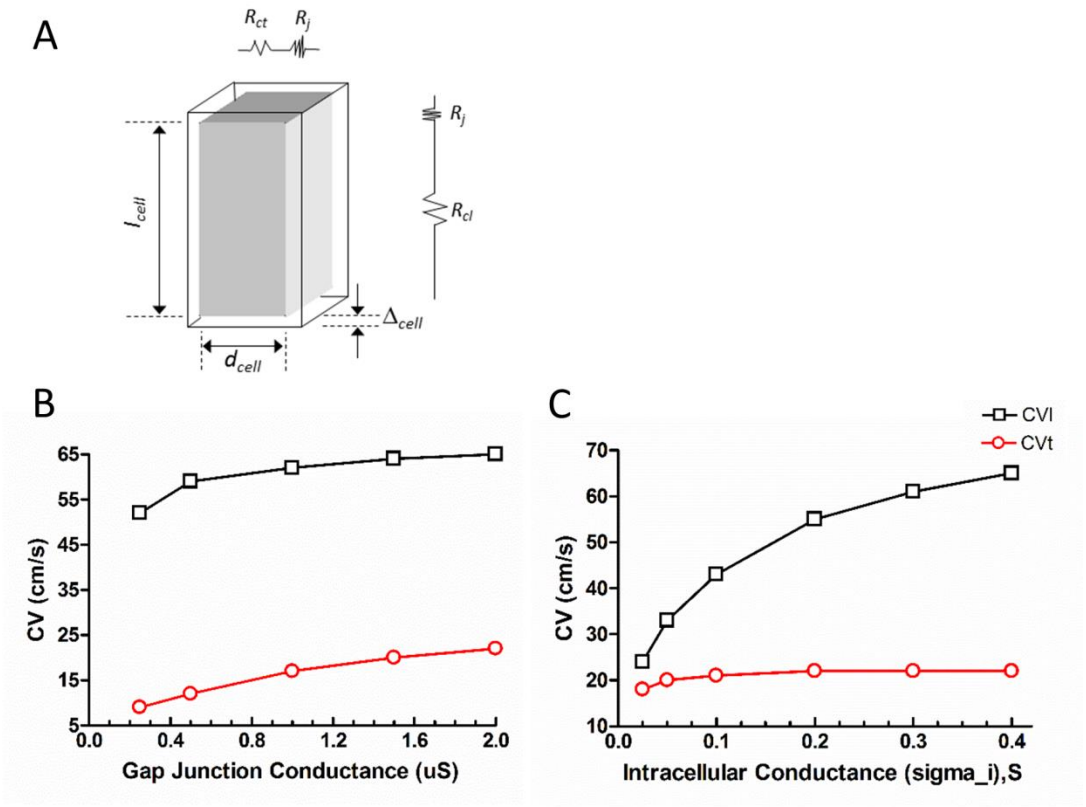

Figure 7.3.2: Computational modelling of longitudinal and transverse conduction (Dr. Martin Bishop, King's College, UK).
A.) *Schematic representation of an idealised cuboid cell of length l_{cell}, width d_{cell}, showing resistance to current flow along and transverse to the cell's length where R_{cl} is the cytoplasmic resistance along the cell, R_{ct} is the cytoplasmic resistance transverse to the cell and R_j is the resistance of the gap junction.* ***B.)*** *Variation in CV as gap junction conductivity is varied and* ***C.)*** *Variation in CV as intracellular conductivity is varied.*

This suggests that if CV was recorded in a transverse direction rather than a longitudinal direction, then a greater increase in CV in response to β-AR would be recorded. Some initial experiments were carried out during this study to investigate this. Fig.7.3.3 shows CV response to 5min of ISO, carried out as described in previous experiments. Recordings were made in the transverse direction rather than the longitudinal - this was achieved by first locating the point of highest CV (CV_L) and then rotating the electrode 90^o. Initial experiments show an increase in CV_T of 23±7.9% compared to the 8-10% response recorded in the longitudinal direction (Fig. 7.3.3 B). However, locating the angle at which CV_T is completely transverse to the electrode is more difficult than locating the direction of longitudinal conduction, and therefore the transverse response to β-AR was highly variable and the difference between CV_L and CV_T was not significant (n=4), though further experiments are required to account for variability.

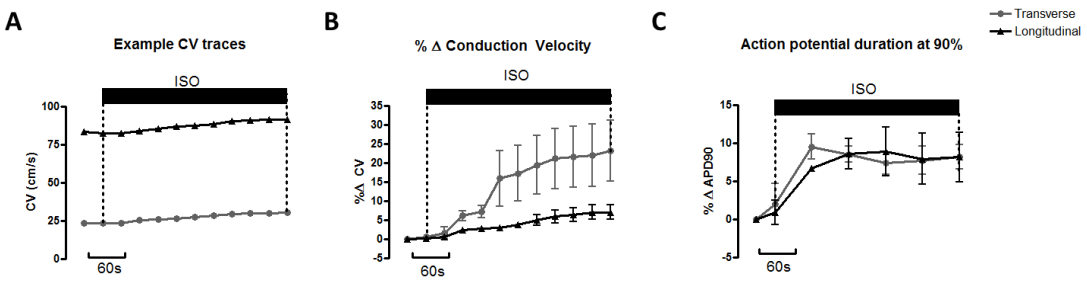

Fig. 7.3.3 The ISO CV response is greater in the transverse vs. longitudinal direction, but the difference is not significant.
A) *Example CV traces taken from individual experiments. Traces show a heart treated with ISO where CV was measured in line with fibre orientation, longitudinally (black), and a heart treated with ISO where CV was measured at right angles to the fibre orientation, transversely (grey).* ***B)*** *The increase in transverse CV in response to ISO appears greater than the increase in CV in the longitudinal direction, however this difference is not significant (n=4)* ***C)*** *Recording APD90 in the longitudinal or transverse direction has no effect on APD90 (n=4).*

The next logical step in this study would be to find a way to measure the effect of β-AR stimulation on GJC. Though this has been carried out in isolated pairs of cells or in monolayers of neonatal rat cardiac myocytes, this has not been carried out in the intact heart.

One way to approach this would be to measure space constant: recording the distance a DC electrical signal can travel through the myocardium. This would involve using a subthreshold pulse at one point on the surface of the myocardium, and then measuring the rate at which this pulse degrades as it travels away from the point of stimulation. This would give an indication of the resistance of the myocardium and therefore GJC. Experiments could be carried out in more linear models – such as trabeculae – to simplify the study and allow the application of linear cable theory.

Another possible technique has been used in the myocardium to measure myocardial impedance and calculate GJ resistivity (Dhillon et al., 2013): in this technique, cardiac myocardium was coated with mineral-oil gel and an electrical current was passed through both the myocardium and an extracellular shunt. The impedance of the entire system was measured, and resistance was measured using two electrodes in the myocardium which were a known distance apart. The impedance of the extracellular shunt was known, and from this it was possible to calculate impedance of the myocardium. Longitudinal impedance was calculated as both sarcoplasmic resistance and GJ impedance, and from

this it was possible to calculate GJ resistance. Use of a method such as this would allow the study of the effect of β-AR on GJC while still studying the intact myocardium, which is essential when looking at the effect on CV in the adult heart.

Substances that modulate GJC – such as the gap junction inhibitors heptanol and carbenoxolone – could also be used to inhibit GJC. If the increase in CV in response to β-AR stimulation were GJ mediated, it is possible that inhibition of GJC would attenuate the CV response. However, there are few compounds that modulate purely GJC without also altering the electrophysiology of the heart.

Although it is important to study CV in intact tissue, this work could also be supported by experiments carried out in pairs of cells or cell monolayers (Burt and Spray, 1988; Somekawa et al., 2005). This would also allow the use of drugs which we were unable to use in the intact heart, either due to cost constraints or due to the drug appearing not to reach the tissue: these include the specific inhibitor of CaMKII, AIP, and other cAMP analogues which specifically activate PKA or EPAC.

Investigating both the effect of β-AR stimulation on Cx43 itself and also how this affects GJC would give a better idea of how the β-AR pathway regulates CV.

7.4 Regulation of CV in Heart Failure

As previously discussed, understanding the regulation of CV is an important part of understanding both arrhythmogenesis and how re-entrant circuit arrhythmias are maintained. A key model for understanding this is the 'wavelength' theory. CV x ERP is defined as the cardiac wavelength. A lower wavelength promotes the generation and maintenance of re-entrant circuit arrhythmias. Therefore, a lower CV could contribute to arrhythmogenesis and in principle, a higher CV could be anti-arrhythmic.

Uncoupling of GJs has been demonstrated to occur in ischaemic regions of the heart (Kléber et al., 1987), which profoundly reduces CV. In surviving regions of the heart, remodeling of gap junctions has been shown to occur in heart failure in humans (Severs et al., 2004; J. Smith et al., 1991) and in animal models (Matsushita et al., 1999). Alongside this, β-AR signaling, particular β_1ARs, has also been demonstrated to be down-regulated in heart failure (Lohse et al., 2003a; Nikolaev et al., 2010). Therefore, understanding the regulation of CV by β-AR stimulation in heart failure could be key to understanding the changes in disease which lead to the generation of arrhythmias.

In addition to experiments on normal myocardium, experiments looking at the effect of β-AR stimulation in heart failure models would be an interesting next step. A routine observation in failing hearts is β-AR desensitization within the ventricle: this occurs through multiple mechanisms in which β-ARs are uncoupled from G_s protein. Phosphorylation of the GPCR by PKA and G receptor kinases (GRKs) lead to decreased association of G_s and increased association with the inhibitory G protein (G_i) and also increases recruitment of β-arrestin (Ungerer 1994, 1993). This is more pronounced in β_2AR signaling and therefore the decreased ratio of β_1:β_2 in heart failure amplifies this effect (Lohse et al., 2003b). Lower levels of G_s and higher levels of G_i are expressed in heart failure (Ping et al., 1997). Therefore, β-AR signaling is greatly altered in the ventricle in heart failure. Potentially, if the modified β-AR response in HF has a lowered or absent CV compoenent, the absence of a higher CV may contribute to the pro-arrhythmic status of the myocardium. As explained elsewhere (Section 3.6.2) decreased electrical wavelength increases the opportunity for re-entrant arrhythmias, a pathological β-AR response that involved a decreased APD without an increased CV may result in a critically reduced electrical wavelength. Further work is required to investigate whether this novel mechanism applies in HF. The study would involve direct measurements of ECG *in vivo*, electrophysiology and CV *in vitro* and Western Blot analysis of tissue to determine the phosphorylation state of Cx43 in heart failure models.

8. Bibliography

Aidley, D.J., 2008. Ion Channels: Molecules in Action, 1st edition edition. ed. Cambridge University Press, Cambridge ; New York.

Aistrup, G.L., Shiferaw, Y., Kapur, S., Kadish, A.H., Wasserstrom, J.A., 2009. Mechanisms underlying the formation and dynamics of subcellular calcium alternans in the intact rat heart. Circ. Res. 104, 639–649. doi:10.1161/CIRCRESAHA.108.181909

Baillie, G.S., 2009. Compartmentalized signalling: spatial regulation of cAMP by the action of compartmentalized phosphodiesterases. FEBS J. 276, 1790–1799. doi:10.1111/j.1742-4658.2009.06926.x

Baillie, G.S., Adams, D.R., Bhari, N., Houslay, T.M., Vadrevu, S., Meng, D., Li, X., Dunlop, A., Milligan, G., Bolger, G.B., Klussmann, E., Houslay, M.D., 2007. Mapping binding sites for the PDE4D5 cAMP-specific phosphodiesterase to the N- and C-domains of beta-arrestin using spot-immobilized peptide arrays. Biochem. J. 404, 71–80. doi:10.1042/BJ20070005

Beardslee, M.A., Laing, J.G., Beyer, E.C., Saffitz, J.E., 1998. Rapid turnover of connexin43 in the adult rat heart. Circ. Res. 83, 629–635.

Berecki, G., Wilders, R., Jonge, B. de, Ginneken, A.C.G. van, Verkerk, A.O., 2010. Re-Evaluation of the Action Potential Upostroke Velocity as a Measure of the Na^+ in Cardiac Myocytes at Physiological Conditions. PLOS ONE 5, e15772. doi:10.1371/journal.pone.0015772Beblo, D.A., Wang, H.Z., Beyer, E.C., Westphale, E.M., Veenstra, R.D., 1995. Unique conductance, gating, and selective permeability properties of gap junction channels formed by connexin40. Circ. Res. 77, 813–822.

Bedner, P., Niessen, H., Odermatt, B., Willecke, K., Harz, H., 2003. A method to determine the relative cAMP permeability of connexin channels. Exp. Cell Res. 291, 25–35.

Bers, D., 2001. Excitation-Contraction Coupling and Cardiac Contractile Force (Developments in Cardiovascular Medicine): Second Edition, 2 edition. ed. Springer, Dordrecht.

Bers, D.M., 2002. Cardiac excitation-contraction coupling. Nature 415, 198–205. doi:10.1038/415198a

Berthouze, M., Laurent, A.-C., Breckler, M., Lezoualc'h, F., 2011. New perspectives in cAMP-signaling modulation. Curr. Heart Fail. Rep. 8, 159–167. doi:10.1007/s11897-011-0062-8

Börner, S., Schwede, F., Schlipp, A., Berisha, F., Calebiro, D., Lohse, M.J., Nikolaev, V.O., 2011. FRET measurements of intracellular cAMP concentrations and cAMP analog permeability in intact cells. Nat. Protoc. 6, 427–438. doi:10.1038/nprot.2010.198

Bos, J.L., 2006. Epac proteins: multi-purpose cAMP targets. Trends Biochem. Sci. 31, 680–686. doi:10.1016/j.tibs.2006.10.002

Bos, J.L., 2003. Epac: a new cAMP target and new avenues in cAMP research. Nat. Rev. Mol. Cell Biol. 4, 733–738. doi:10.1038/nrm1197

Brack, K.E., Narang, R., Winter, J., Ng, G.A., 2013a. The mechanical uncoupler blebbistatin is associated with significant electrophysiological effects in the isolated rabbit heart. Exp. Physiol. 98, 1009–1027. doi:10.1113/expphysiol.2012.069369

Brack, K.E., Winter, J., Ng, G.A., 2013b. Mechanisms underlying the autonomic modulation of ventricular fibrillation initiation--tentative prophylactic properties of vagus nerve stimulation on malignant arrhythmias in heart failure. Heart Fail. Rev. 18, 389–408. doi:10.1007/s10741-012-9314-2

Brette, F., Blandin, E., Simard, C., Guinamard, R., Sallé, L., 2013. Epac activator critically regulates action potential duration by decreasing potassium current in rat adult ventricle. J. Mol. Cell. Cardiol. 57, 96–105. doi:10.1016/j.yjmcc.2013.01.012

Bristow, M., Ginsburg, R., Umans, V., Fowler, M., Minobe, W., Rasmussen, R., Zera, P., Menlove, R., Shah, P., Jamieson, S., 1986. Beta 1- and beta 2-adrenergic-receptor subpopulations in nonfailing and failing human ventricular myocardium: coupling of both receptor subtypes to muscle contraction and selective beta 1-receptor down- regulation in heart failure. Circ. Res. 59, 297–309.

Brodde, O.-E., Bruck, H., Leineweber, K., 2006. Cardiac adrenoceptors: physiological and pathophysiological relevance. J. Pharmacol. Sci. 100, 323–337.

Bruzzone, R., White, T.W., Paul, D.L., 1996. Connections with Connexins: the Molecular Basis of Direct Intercellular Signaling. Eur. J. Biochem. 238, 1–27. doi:10.1111/j.1432-1033.1996.0001q.x

Buchanan, J., Saito, T., Gettes, L., 1985. The effects of antiarrhythmic drugs, stimulation frequency, and potassium-induced resting membrane potential changes on conduction velocity and dV/dtmax in guinea pig myocardium. Circ. Res. 56, 696–703. doi:10.1161/01.RES.56.5.696

Bukauskas, F.F., Weingart, R., 1993. Temperature dependence of gap junction properties in neonatal rat heart cells. Pflüg. Arch. Eur. J. Physiol. 423, 133–139.

Burt, J.M., Spray, D.C., 1988. Inotropic agents modulate gap junctional conductance between cardiac myocytes. Am. J. Physiol. - Heart Circ. Physiol. 254, H1206–H1210.

Cabo, C., Yao, J., Boyden, P.A., Chen, S., Hussain, W., Duffy, H.S., Ciaccio, E.J., Peters, N.S., Wit, A.L., 2006. Heterogeneous gap junction remodeling in reentrant circuits in the epicardial border zone of the healing canine infarct. Cardiovasc. Res. 72, 241–249. doi:10.1016/j.cardiores.2006.07.005

Catterall, W.A., 2012. Voltage-gated sodium channels at 60: structure, function and pathophysiology. J. Physiol. 590, 2577–2589. doi:10.1113/jphysiol.2011.224204

Catterall, W.A., 1988. Structure and function of voltage-sensitive ion channels. Science 242, 50–61.

Chen, V.C., Gouw, J.W., Naus, C.C., Foster, L.J., 2013. Connexin multi-site phosphorylation: Mass spectrometry-based proteomics fills the gap. Biochim. Biophys. Acta BBA - Biomembr. 1828, 23–34. doi:10.1016/j.bbamem.2012.02.028

Cheng, D.K., Tung, L., Sobie, E.A., 1999. Nonuniform responses of transmembrane potential during electric field stimulation of single cardiac cells. Am. J. Physiol. 277, H351-362.

Choi, B.R., Salama, G., 2000. Simultaneous maps of optical action potentials and calcium transients in guinea-pig hearts: mechanisms underlying concordant alternans. J. Physiol. 529 Pt 1, 171–188.

Cohen, C., Bean, B., Tsien, R., 1984. Maximal upstroke velocity as an index of available sodium conductance. Comparison of maximal upstroke velocity and voltage clamp measurements of sodium current in rabbit Purkinje fibers. Circ. Res. 54, 636–651. doi:10.1161/01.RES.54.6.636

Cohen, I., Attwell, D., Strichartz, G., 1981. The Dependence of the Maximum Rate of Rise of the Action Potential Upstroke on Membrane Properties. Proc. R. Soc. Lond. B Biol. Sci. 214, 85–98. doi:10.1098/rspb.1981.0083

Courilleau, D., Bisserier, M., Jullian, J.-C., Lucas, A., Bouyssou, P., Fischmeister, R., Blondeau, J.-P., Lezoualc'h, F., 2012. Identification of a tetrahydroquinoline analog as a pharmacological inhibitor of the cAMP-binding protein Epac. J. Biol. Chem. 287, 44192–44202. doi:10.1074/jbc.M112.422956

Currie, S., Loughrey, C.M., Craig, M.-A., Smith, G.L., 2004. Calcium/calmodulin-dependent protein kinase IIdelta associates with the ryanodine receptor complex and regulates channel function in rabbit heart. Biochem. J. 377, 357–366. doi:10.1042/BJ20031043

Darrow, B.J., Fast, V.G., Kleber, A.G., Beyer, E.C., Saffitz, J.E., 1996. Functional and Structural Assessment of Intercellular Communication: Increased Conduction Velocity and Enhanced Connexin Expression in Dibutyryl cAMP–Treated Cultured Cardiac Myocytes. Circ. Res. 79, 174–183. doi:10.1161/01.RES.79.2.174

de Boer, T.P., van Rijen, H.V.M., Van der Heyden, M.A.G., Kok, B., Opthof, T., Vos, M.A., Jongsma, H.J., de Bakker, J.M.T., van Veen, T.A.B., 2007. Beta-, Not Alpha-Adrenergic Stimulation Enhances Conduction Velocity in Cultures of Neonatal Cardiomyocytes. Circ. J. 71, 973–981. doi:10.1253/circj.71.973

De Mello, W.C., 1975. Effect of intracellular injection of calcium and strontium on cell communication in heart. J. Physiol. 250, 231–245.

Dhillon, P.S., Gray, R., Kojodjojo, P., Jabr, R., Chowdhury, R., Fry, C.H., Peters, N.S., 2013. Relationship between gap-junctional conductance and conduction velocity in mammalian myocardium. Circ. Arrhythm. Electrophysiol. 6, 1208–1214. doi:10.1161/CIRCEP.113.000848

DiFrancesco, D., Tortora, P., 1991. Direct activation of cardiac pacemaker channels by intracellular cyclic AMP. Nature 351, 145–147. doi:10.1038/351145a0

Draper, M.H., Mya-Tu, M., 1959. A comparison of the conduction velocity in cardiac tissues of various mammals. Q. J. Exp. Physiol. Cogn. Med. Sci. 44, 91–109.

Dunn, C.A., Su, V., Lau, A.F., Lampe, P.D., 2012. Activation of Akt, Not Connexin 43 Protein Ubiquitination, Regulates Gap Junction Stability. J. Biol. Chem. 287, 2600–2607. doi:10.1074/jbc.M111.276261

Edwards, H.V., Christian, F., Baillie, G.S., 2012. cAMP: novel concepts in compartmentalised signalling. Semin. Cell Dev. Biol. 23, 181–190. doi:10.1016/j.semcdb.2011.09.005

Ek-Vitorín, J.F., Calero, G., Morley, G.E., Coombs, W., Taffet, S.M., Delmar, M., 1996. PH regulation of connexin43: molecular analysis of the gating particle. Biophys. J. 71, 1273–1284. doi:10.1016/S0006-3495(96)79328-1

Erlij, D., Mendez, C., 1964. Adrenergic actions on heart rate, atrio-ventricular refractory period and intraventricular conduction in dogs. Arch. Int. Physiol. Biochim. 72, 44–65.

Fedorov, V.V., Lozinsky, I.T., Sosunov, E.A., Anyukhovsky, E.P., Rosen, M.R., Balke, C.W., Efimov, I.R., 2007. Application of blebbistatin as an excitation-contraction uncoupler for electrophysiologic study of rat and rabbit hearts. Heart Rhythm Off. J. Heart Rhythm Soc. 4, 619–626. doi:10.1016/j.hrthm.2006.12.047

Ferrero, P., Said, M., Sánchez, G., Vittone, L., Valverde, C., Donoso, P., Mattiazzi, A., Mundiña-Weilenmann, C., 2007. Ca2+/calmodulin kinase II increases ryanodine binding and Ca2+-induced sarcoplasmic reticulum Ca2+ release kinetics during beta-adrenergic stimulation. J. Mol. Cell. Cardiol. 43, 281–291. doi:10.1016/j.yjmcc.2007.05.022

Fischmeister, R., Castro, L.R.V., Abi-Gerges, A., Rochais, F., Jurevičius, J., Leroy, J., Vandecasteele, G., 2006. Compartmentation of Cyclic Nucleotide Signaling in the Heart. Circ. Res. 99, 816–828. doi:10.1161/01.RES.0000246118.98832.04

Fluhler, E., Burnham, V.G., Loew, L.M., 1985. Spectra, membrane binding, and potentiometric responses of new charge shift probes. Biochemistry (Mosc.) 24, 5749–5755. doi:10.1021/bi00342a010

Frohnwieser, B., Chen, L.Q., Schreibmayer, W., Kallen, R.G., 1997. Modulation of the human cardiac sodium channel alpha-subunit by cAMP-dependent protein kinase and the responsible sequence domain. J. Physiol. 498, 309–318.

Ghouri, I.A., Kelly, A., Burton, F.L., Smith, G.L., Kemi, O.J., 2015. 2-Photon excitation fluorescence microscopy enables deeper high-resolution imaging of voltage and Ca(2+) in intact mice, rat, and rabbit hearts. J. Biophotonics 8, 112–123. doi:10.1002/jbio.201300109

Giepmans, B.N.., 2004. Gap junctions and connexin-interacting proteins. Cardiovasc. Res. 62, 233–245. doi:10.1016/j.cardiores.2003.12.009

Gilbert, S.H., Benoist, D., Benson, A.P., White, E., Tanner, S.F., Holden, A.V., Dobrzynski, H., Bernus, O., Radjenovic, A., 2011. Visualization and quantification of whole rat heart laminar structure using high-spatial resolution contrast enhanced MRI. Am. J. Physiol. - Heart Circ. Physiol. doi:10.1152/ajpheart.00824.2011

Gintant, G.A., Liu, D.W., 1992. Beta-adrenergic modulation of fast inward sodium current in canine myocardium. Syncytial preparations versus isolated myocytes. Circ. Res. 70, 844–850. doi:10.1161/01.RES.70.4.844

Goldberger, J.J., Ahmed, M.W., Parker, M.A., Kadish, A.H., 1994. Assessment of effects of autonomic stimulation and blockade on the signal-averaged electrocardiogram. Circulation 89, 1656–1664.

Goodenough, D.A., Gilula, N.B., 1974. The splitting of hepatocyte gap junctions and zonulae occludentes with hypertonic disaccharides. J. Cell Biol. 61, 575–590.

Grimm, M., Brown, J.H., 2010. Beta-adrenergic receptor signaling in the heart: role of CaMKII. J. Mol. Cell. Cardiol. 48, 322–330. doi:10.1016/j.yjmcc.2009.10.016

Gros, D.B., Jongsma, H.J., 1996. Connexins in mammalian heart function. BioEssays News Rev. Mol. Cell. Dev. Biol. 18, 719–730. doi:10.1002/bies.950180907

Grosely, R., Kopanic, J.L., Nabors, S., Kieken, F., Spagnol, G., Al-Mugotir, M., Zach, S., Sorgen, P.L., 2013. Effects of phosphorylation on the structure and backbone dynamics of the intrinsically disordered connexin43 C-terminal domain. J. Biol. Chem. 288, 24857–24870. doi:10.1074/jbc.M113.454389

Grynkiewicz, G., Poenie, M., Tsien, R.Y., 1985. A new generation of Ca2+ indicators with greatly improved fluorescence properties. J. Biol. Chem. 260, 3440–3450.

Han, J., Jalon, P.G.D., Moe, G.K., 1964. Adrenergic Effects on Ventricular Vulnerability. Circ. Res. 14, 516–524. doi:10.1161/01.RES.14.6.516

Hayes, J.S., Brunton, L.L., Brown, J.H., Reese, J.B., Mayer, S.E., 1979. Hormonally specific expression of cardiac protein kinase activity. Proc. Natl. Acad. Sci. U. S. A. 76, 1570–1574.

Heijman, J., Volders, P.G.A., Westra, R.L., Rudy, Y., 2011. Local control of β-adrenergic stimulation: Effects on ventricular myocyte electrophysiology and Ca2+-transient. J. Mol. Cell. Cardiol. 50, 863–871. doi:10.1016/j.yjmcc.2011.02.007

Hicks, M.J., Shigekawa, M., Katz, A.M., 1979. Mechanism by which cyclic adenosine 3':5'-monophosphate-dependent protein kinase stimulates calcium transport in cardiac sarcoplasmic reticulum. Circ. Res. 44, 384–391.

Holm, I., Mikhailov, A., Jillson, T., Rose, B., 1999. Dynamics of gap junctions observed in living cells with connexin43-GFP chimeric protein. Eur. J. Cell Biol. 78, 856–866. doi:10.1016/S0171-9335(99)80087-9

Hothi, S.S., Gurung, I.S., Heathcote, J.C., Zhang, Y., Booth, S.W., Skepper, J.N., Grace, A.A., Huang, C.L.-H., 2008. Epac activation, altered calcium homeostasis and ventricular arrhythmogenesis in the murine heart. Pflüg. Arch. Eur. J. Physiol. 457, 253–270. doi:10.1007/s00424-008-0508-3

Huang, R.Y.-C., Laing, J.G., Kanter, E.M., Berthoud, V.M., Bao, M., Rohrs, H.W., Townsend, R.R., Yamada, K.A., 2011. Identification of CaMKII phosphorylation sites in Connexin43 by high-resolution mass spectrometry. J. Proteome Res. 10, 1098–1109. doi:10.1021/pr1008702

Hutter, O.F., Trautwein, W., 1956. Vagal and sympathetic effects on the pacemaker fibers in the sinus venosus of the heart. J. Gen. Physiol. 39, 715–733.

Hutter, O.F., Trautwein, W., 1955. Effect of vagal stimulation on the sinus venosus of the frog's heart. Nature 176, 512–513.

Jalife, J., Delmar, M., Anumonwo, J., Berenfeld, O., Kalifa, J., 2009. Basic Cardiac Electrophysiology for the Clinician, 2nd Edition. ed. Wiley-Blackwell

Johnstone, S., Isakson, B., Locke, D., 2009. Biological and Biophysical Properties of Vascular Connexin Channels. Int. Rev. Cell Mol. Biol., International Review Of Cell and Molecular Biology Volume 278, 69–118.

Johnstone, S.R., Billaud, M., Lohman, A.W., Taddeo, E.P., Isakson, B.E., 2012. Posttranslational Modifications in Connexins and Pannexins. J. Membr. Biol. 245, 319–332. doi:10.1007/s00232-012-9453-3

Jongsma, H.J., van Rijen, H.V.M., Kwak, B.R., Chanson, M., 1999. Chapter 6: Phosphorylation of Connexins: Consequences for Permeability, Conductance, and Kinetics of Gap Junction Channels, in: Gap Junctions Molecular Basis of Cell Communication in Health and Disease. Academic Press, pp. 131–144.

Jongsma, H.J., Wilders, R., 2000. Gap Junctions in Cardiovascular Disease. Circ. Res. 86, 1193–1197. doi:10.1161/01.RES.86.12.1193

Jost, N., Virág, L., Bitay, M., Takács, J., Lengyel, C., Biliczki, P., Nagy, Z., Bogáts, G., Lathrop, D.A., Papp, J.G., Varró, A., 2005. Restricting excessive cardiac action potential and QT prolongation: a vital role for IKs in human ventricular muscle. Circulation 112, 1392–1399. doi:10.1161/CIRCULATIONAHA.105.550111

Jozwiak, J., Dhein, S., 2008. Local effects and mechanisms of antiarrhythmic peptide AAP10 in acute regional myocardial ischemia: electrophysiological and molecular findings. Naunyn. Schmiedebergs Arch. Pharmacol. 378, 459–470. doi:10.1007/s00210-008-0317-4

Kääb, S., Nuss, H.B., Chiamvimonvat, N., O'Rourke, B., Pak, P.H., Kass, D.A., Marban, E., Tomaselli, G.F., 1996. Ionic mechanism of action potential prolongation in ventricular myocytes from dogs with pacing-induced heart failure. Circ. Res. 78, 262–273.

Kaneshiro, E. (Ed.), 2011. Cell Physiology Source Book: Essentials of Membrane Biophysics, 4 edition. ed. Academic Press

Kamp, T.J., Hell, J.W., 2000. Regulation of cardiac L-type calcium channels by protein kinase A and protein kinase C. Circ. Res. 87, 1095–1102.

Kanter, H.L., Laing, J.G., Beau, S.L., Beyer, E.C., Saffitz, J.E., 1993. Distinct patterns of connexin expression in canine Purkinje fibers and ventricular muscle. Circ. Res. 72, 1124–1131. doi:10.1161/01.RES.72.5.1124

Kelly, A., Ghouri, I.A., Kemi, O.J., Bishop, M.J., Bernus, O., Fenton, F.H., Myles, R.C., Burton, F.L., Smith, G.L., 2013. Subepicardial action potential characteristics are a function of depth and activation sequence in isolated rabbit hearts. Circ. Arrhythm. Electrophysiol. 6, 809–817. doi:10.1161/CIRCEP.113.000334

Kettlewell, S., Walker, N.L., Cobbe, S.M., Burton, F.L., Smith, G.L., 2004. The electrophysiological and mechanical effects of 2,3-butane-dione monoxime and cytochalasin-D in the Langendorff perfused rabbit heart. Exp. Physiol. 89, 163–172. doi:10.1113/expphysiol.2003.026732

Kléber, A.G., Riegger, C.B., Janse, M.J., 1987. Electrical uncoupling and increase of extracellular resistance after induction of ischemia in isolated, arterially perfused rabbit papillary muscle. Circ. Res. 61, 271–279.

Kléber, A.G., Rudy, Y., 2004. Basic Mechanisms of Cardiac Impulse Propagation and Associated Arrhythmias. Physiol. Rev. 84, 431–488. doi:10.1152/physrev.00025.2003

Kojodjojo, P., Kanagaratnam, P., Segal, O.R., Hussain, W., Peters, N.S., 2006. The Effects of Carbenoxolone on Human Myocardial Conduction: A Tool to Investigate the Role of Gap Junctional Uncoupling in Human Arrhythmogenesis. J Am Coll Cardiol 48, 1242–1249. doi:10.1016/j.jacc.2006.04.093

Komai, A.M., Brännmark, C., Musovic, S., Olofsson, C.S., 2014. PKA-independent cAMP stimulation of white adipocyte exocytosis and adipokine secretion: modulations by Ca2+ and ATP. J. Physiol. 592, 5169–5186. doi:10.1113/jphysiol.2014.280388

Krayer, O., Mandoki, J.J., Mendez, C., Rubio, G.R., 1951. Studies on veratrum alkaloids. XVI. The action of epinephrine and of veratramine on the functional refractory period of the auriculo-ventricular transmission in the heart-lung preparation of the dog. J. Pharmacol. Exp. Ther. 103, 412–419.

Kucera, J.P., Rohr, S., Rudy, Y., 2002. Localization of sodium channels in intercalated disks modulates cardiac conduction. Circ. Res. 91, 1176–1182.

Kuschel, M., Karczewski, P., Hempel, P., Schlegel, W.P., Krause, E.G., Bartel, S., 1999. Ser16 prevails over Thr17 phospholamban phosphorylation in the beta-adrenergic regulation of cardiac relaxation. Am. J. Physiol. 276, H1625-1633.

Kwak, B.R., Hermans, M.M., De Jonge, H.R., Lohmann, S.M., Jongsma, H.J., Chanson, M., 1995. Differential regulation of distinct types of gap junction channels by similar phosphorylating conditions. Mol. Biol. Cell 6, 1707–1719.

Laird, D.W., Puranam, K.L., Revel, J.P., 1991. Turnover and phosphorylation dynamics of connexin43 gap junction protein in cultured cardiac myocytes. Biochem. J. 273, 67–72.

Lampe, P.D., Lau, A.F., 2004. The effects of connexin phosphorylation on gap junctional communication. Int. J. Biochem. Cell Biol. 36, 1171–1186. doi:10.1016/S1357-2725(03)00264-4

Lehnart, S., Marks, A.R., 2007. Regulation of Ryanodine Receptors in the Heart. Circ. Res. 101, 746–749. doi:10.1161/CIRCRESAHA.107.162479

Leitch, S.P., Brown, H.F., 1996. Effect of raised extracellular calcium on characteristics of the guinea-pig ventricular action potential. J. Mol. Cell. Cardiol. 28, 541–551. doi:10.1006/jmcc.1996.0050

Lera Ruiz de, M., Kraus, R.L., 2015. Voltage-Gated Sodium Channels: Structure, Function, Pharmacology, and Clinical Indications. J. Med. Chem. 58, 7093–7118

Levick, J., 2000. Introduction to Cardiovascular Physiology, 3Ed. Taylor & Francis.

Lewis, S.T., 1920. The Mechanism and Graphic Registration of the Heart Beat. Shaw & Sons.

Liu, S., Taffet, S., Stoner, L., Delmar, M., Vallano, M.L., Jalife, J., 1993. A structural basis for the unequal sensitivity of the major cardiac and liver gap junctions to intracellular acidification: the carboxyl tail length. Biophys. J. 64, 1422–1433. doi:10.1016/S0006-3495(93)81508-X

Liu, Y., Cabo, C., Salomonsz, R., Delmar, M., Davidenko, J., Jalife, J., 1993. Effects of diacetyl monoxime on the electrical properties of sheep and guinea pig ventricular muscle. Cardiovasc. Res. 27, 1991–1997.

Loewenstein, W.R., 1981. Junctional intercellular communication: the cell-to-cell membrane channel. Physiol. Rev. 61, 829–913.

Lohse, M.J., Andexinger, S., Pitcher, J., Trukawinski, S., Codina, J., Faure, J.P., Caron, M.G., Lefkowitz, R.J., 1992. Receptor-specific desensitization with purified proteins. Kinase dependence and receptor specificity of beta-arrestin and arrestin in the beta 2-adrenergic receptor and rhodopsin systems. J. Biol. Chem. 267, 8558–8564.

Lohse, M.J., Engelhardt, S., Eschenhagen, T., 2003a. What Is the Role of β-Adrenergic Signaling in Heart Failure? Circ. Res. 93, 896 –906. doi:10.1161/01.RES.0000102042.83024.CA

Lohse, M.J., Engelhardt, S., Eschenhagen, T., 2003b. What Is the Role of β-Adrenergic Signaling in Heart Failure? Circ. Res. 93, 896–906. doi:10.1161/01.RES.0000102042.83024.CA

Lu, T., Lee, H.-C., Kabat, J.A., Shibata, E.F., 1999. Modulation of rat cardiac sodium channel by the stimulatory G protein α subunit. J. Physiol. 518, 371–384. doi:10.1111/j.1469-7793.1999.0371p.x

Lue, W.M., Boyden, P.A., 1992. Abnormal electrical properties of myocytes from chronically infarcted canine heart. Alterations in Vmax and the transient outward current. Circulation 85, 1175–1188.

Maeda, S., Tsukihara, T., 2011. Structure of the gap junction channel and its implications for its biological functions. Cell. Mol. Life Sci. CMLS 68, 1115–1129. doi:10.1007/s00018-010-0551-z

Márquez-Rosado, L., Solan, J.L., Dunn, C.A., Norris, R.P., Lampe, P.D., 2012. Connexin43 phosphorylation in brain, cardiac, endothelial and epithelial tissues. Biochim. Biophys. Acta BBA - Biomembr. 1818, 1985–1992. doi:10.1016/j.bbamem.2011.07.028

Marx, S.O., Reiken, S., Hisamatsu, Y., Jayaraman, T., Burkhoff, D., Rosemblit, N., Marks, A.R., 2000. PKA Phosphorylation Dissociates FKBP12.6 from the Calcium Release Channel (Ryanodine Receptor): Defective Regulation in Failing Hearts. Cell 101, 365–376. doi:10.1016/S0092-8674(00)80847-8

Matsuda, J.J., Lee, H., Shibata, E.F., 1992. Enhancement of rabbit cardiac sodium channels by beta-adrenergic stimulation. Circ. Res. 70, 199–207.

Matsushita, T., Oyamada, M., Fujimoto, K., Yasuda, Y., Masuda, S., Wada, Y., Oka, T., Takamatsu, T., 1999. Remodeling of cell-cell and cell-extracellular matrix interactions at the border zone of rat myocardial infarcts. Circ. Res. 85, 1046–1055.

Mehta, P.P., Yamamoto, M., Rose, B., 1992. Transcription of the gene for the gap junctional protein connexin43 and expression of functional cell-to-cell channels are regulated by cAMP. Mol. Biol. Cell 3, 839–850.

Mendez, C., Erlij, D., Moe, G.K., 1964. Indirect Action of Epinephrine on Intraventricular Conduction Time. Circ. Res. 14, 318–326. doi:10.1161/01.RES.14.4.318

Métrich, M., Lucas, A., Gastineau, M., Samuel, J.-L., Heymes, C., Morel, E., Lezoualc'h, F., 2008. Epac mediates beta-adrenergic receptor-induced cardiomyocyte hypertrophy. Circ. Res. 102, 959–965. doi:10.1161/CIRCRESAHA.107.164947

Mongillo, M., McSorley, T., Evellin, S., Sood, A., Lissandron, V., Terrin, A., Huston, E., Hannawacker, A., Lohse, M.J., Pozzan, T., Houslay, M.D., Zaccolo, M., 2004. Fluorescence Resonance Energy Transfer–Based Analysis of cAMP Dynamics in Live Neonatal Rat Cardiac Myocytes Reveals Distinct Functions of Compartmentalized Phosphodiesterases. Circ. Res. 95, 67–75. doi:10.1161/01.RES.0000134629.84732.11

Munger, T., Johnson, S., Packer, D., 1994. Voltage dependence of beta-adrenergic modulation of conduction in the canine Purkinje fiber. Circ. Res. 75, 511–519. doi:10.1161/01.RES.75.3.511

Musil, L.S., Le, A.C., VanSlyke, J.K., Roberts, L.M., 2000. Regulation of connexin degradation as a mechanism to increase gap junction assembly and function. J. Biol. Chem. 275, 25207–25215.

Näbauer, M., Beuckelmann, D.J., Uberfuhr, P., Steinbeck, G., 1996. Regional differences in current density and rate-dependent properties of the transient outward current in subepicardial and subendocardial myocytes of human left ventricle. Circulation 93, 168–177.

Neyton, J., Trautmann, A., 1985. Single-channel currents of an intercellular junction. Nature 317, 331–335.

Ng, G.A., Brack, K.E., Patel, V.H., Coote, J.H., 2007. Autonomic modulation of electrical restitution, alternans and ventricular fibrillation initiation in the isolated heart. Cardiovasc. Res. 73, 750–760. doi:10.1016/j.cardiores.2006.12.001

Niedergerke, R., Orkand, R.K., 1966. The dependence of the action potential of the frog's heart on the external and intracellular sodium concentration. J. Physiol. 184, 312–334. doi:10.1113/jphysiol.1966.sp007917Nikolaev, V.O., Moshkov, A., Lyon, A.R., Miragoli, M., Novak, P., Paur, H., Lohse, M.J., Korchev, Y.E., Harding, S.E., Gorelik, J., 2010. β2-Adrenergic Receptor Redistribution in Heart Failure Changes cAMP Compartmentation. Science 327, 1653–1657. doi:10.1126/science.1185988

Nishizawa, H., Suzuki, T., Shioya, T., Nakazato, Y., Daida, H., Kurebayashi, N., 2009. Causes of abnormal Ca2+ transients in Guinea pig pathophysiological ventricular muscle revealed by Ca2+ and action potential imaging at cellular level. PloS One 4, e7069. doi:10.1371/journal.pone.0007069

Nygren, A., Kondo, C., Clark, R.B., Giles, W.R., 2003. Voltage-sensitive dye mapping in Langendorff-perfused rat hearts. Am. J. Physiol. - Heart Circ. Physiol. 284, H892–H902. doi:10.1152/ajpheart.00648.2002

Oestreich, E.A., Malik, S., Goonasekera, S.A., Blaxall, B.C., Kelley, G.G., Dirksen, R.T., Smrcka, A.V., 2009. Epac and phospholipase Cepsilon regulate Ca2+ release in the heart by activation of protein kinase Cepsilon and calcium-calmodulin kinase II. J. Biol. Chem. 284, 1514–1522. doi:10.1074/jbc.M806994200

Oestreich, E.A., Wang, H., Malik, S., Kaproth-Joslin, K.A., Blaxall, B.C., Kelley, G.G., Dirksen, R.T., Smrcka, A.V., 2007. Epac-mediated activation of phospholipase C(epsilon) plays a critical role in beta-adrenergic receptor-dependent enhancement of Ca2+ mobilization in cardiac myocytes. J. Biol. Chem. 282, 5488–5495. doi:10.1074/jbc.M608495200

O'Quinn, M.P., Palatinus, J.A., Harris, B.S., Hewett, K.W., Gourdie, R.G., 2011. A Peptide Mimetic of the Connexin43 Carboxyl Terminus Reduces Gap Junction Remodeling and Induced Arrhythmia Following Ventricular Injury. Circ. Res. 108, 704–715. doi:10.1161/CIRCRESAHA.110.235747

Palatinus, J.A., Rhett, J.M., Gourdie, R.G., 2012. The Connexin43 Carboxyl Terminus and Cardiac Gap Junction Organization. Biochim. Biophys. Acta 1818, 1831–1843. doi:10.1016/j.bbamem.2011.08.006

Paulson, A.F., Lampe, P.D., Meyer, R.A., TenBroek, E., Atkinson, M.M., Walseth, T.F., Johnson, R.G., 2000a. Cyclic AMP and LDL trigger a rapid enhancement in gap junction assembly through a stimulation of connexin trafficking. J. Cell Sci. 113, 3037–3049.

Paulson, A.F., Lampe, P.D., Meyer, R.A., TenBroek, E., Atkinson, M.M., Walseth, T.F., Johnson, R.G., 2000b. Cyclic AMP and LDL trigger a rapid enhancement in gap junction assembly through a stimulation of connexin trafficking. J. Cell Sci. 113, 3037 –3049.

Pereira, L., Métrich, M., Fernández-Velasco, M., Lucas, A., Leroy, J., Perrier, R., Morel, E., Fischmeister, R., Richard, S., Bénitah, J.-P., Lezoualc'h, F., Gómez, A.M., 2007. The cAMP binding protein Epac modulates Ca2+ sparks by a Ca2+/calmodulin kinase signalling pathway in rat cardiac myocytes. J. Physiol. 583, 685–694. doi:10.1113/jphysiol.2007.133066

Peters, N.S., 2006. Gap Junctions Clarifying the Complexities of Connexins and Conduction. Circ. Res. 99, 1156–1158. doi:10.1161/01.RES.0000251936.26233.0d

Peters, N.S., Coromilas, J., Severs, N.J., Wit, A.L., 1997. Disturbed connexin43 gap junction distribution correlates with the location of reentrant circuits in the epicardial border zone of healing canine infarcts that cause ventricular tachycardia. Circulation 95, 988–996.

Pilhall, M., Riha, M., Jern, S., 1993. Changes in the QRS segment during exercise: effects of acute beta-blockade with propranolol. Clin. Physiol. Oxf. Engl. 13, 113–131.

Ping, P., Anzai, T., Gao, M., Hammond, H.K., 1997. Adenylyl cyclase and G protein receptor kinase expression during development of heart failure. Am. J. Physiol. 273, H707-717.

Potter, E.K., 1988. Neuropeptide Y as an autonomic neurotransmitter. Pharmacol. Ther. 37, 251–273.

Pu, J., Balser, J.R., Boyden, P.A., 1998. Lidocaine action on Na+ currents in ventricular myocytes from the epicardial border zone of the infarcted heart. Circ. Res. 83, 431–440.

Reuter, H., 1987. Calcium channel modulation by beta-adrenergic neurotransmitters in the heart. Experientia 43, 1173–1175.

Roberts, D., Hersh, L., Scher, A., 1979. Influence of cardiac fiber orientation on wavefront voltage, conduction velocity, and tissue resistivity in the dog. Circ. Res. 44, 701–712. doi:10.1161/01.RES.44.5.701

Rohr, S., 2004. Role of gap junctions in the propagation of the cardiac action potential. Cardiovasc. Res. 62, 309–322. doi:10.1016/j.cardiores.2003.11.035

Rossie, S., Catterall, W.A., 1987. Cyclic-AMP-dependent phosphorylation of voltage-sensitive sodium channels in primary cultures of rat brain neurons. J. Biol. Chem. 262, 12735–12744.

Saffitz, J.E., Laing, J.G., Yamada, K.A., 2000. Connexin expression and turnover: implications for cardiac excitability. Circ. Res. 86, 723–728.

Said, M., Mundiña-Weilenmann, C., Vittone, L., Mattiazzi, A., 2002. The relative relevance of phosphorylation of the Thr(17) residue of phospholamban is different at different levels of beta-adrenergic stimulation. Pflüg. Arch. Eur. J. Physiol. 444, 801–809. doi:10.1007/s00424-002-0885-y

Salameh, A., Dhein, S., 2011. Adrenergic control of cardiac gap junction function and expression. Naunyn. Schmiedebergs Arch. Pharmacol. 383, 331–346. doi:10.1007/s00210-011-0603-4

Salameh, A., Frenzel, C., Boldt, A., Rassler, B., Glawe, I., Schulte, J., Mühlberg, K., Zimmer, H.-G., Pfeiffer, D., Dhein, S., 2006. Subchronic alpha- and beta-adrenergic regulation of cardiac gap junction protein expression. FASEB J. 20, 365–367. doi:10.1096/fj.05-4871fje

Sandberg, M., Butt, E., Nolte, C., Fischer, L., Halbrügge, M., Beltman, J., Jahnsen, T., Genieser, H.G., Jastorff, B., Walter, U., 1991. Characterization of Sp-5,6-dichloro-1-beta-D-ribofuranosylbenzimidazole- 3',5'-monophosphorothioate (Sp-5,6-DCl-cBiMPS) as a potent and specific activator of cyclic-AMP-dependent protein kinase in cell extracts and intact cells. Biochem. J. 279, 521–527.

Santillán, G.E., Boland, R.L., 1998. Studies suggesting the participation of protein kinase A in 1, 25(OH)2-vitamin D3-dependent protein phosphorylation in cardiac muscle. J. Mol. Cell. Cardiol. 30, 225–233. doi:10.1006/jmcc.1997.0577

Schreibmayer, W., Frohnwieser, B., Dascal, N., Platzer, D., Spreitzer, B., Zechner, R., Kallen, R.G., Lester, H.A., 1994. Beta-adrenergic modulation of currents produced by rat cardiac Na+ channels expressed in Xenopus laevis oocytes. Receptors Channels 2, 339–350.

Segretain, D., Falk, M.M., 2004. Regulation of connexin biosynthesis, assembly, gap junction formation, and removal. Biochim. Biophys. Acta BBA - Biomembr. 1662, 3–21. doi:10.1016/j.bbamem.2004.01.007

Severs, N.J., Coppen, S.R., Dupont, E., Yeh, H.-I., Ko, Y.-S., Matsushita, T., 2004. Gap junction alterations in human cardiac disease. Cardiovasc. Res. 62, 368–377. doi:10.1016/j.cardiores.2003.12.007

Shaw, R.M., Rudy, Y., 1997. Ionic mechanisms of propagation in cardiac tissue. Roles of the sodium and L-type calcium currents during reduced excitability and decreased gap junction coupling. Circ. Res. 81, 727–741.

Siebens, A.A., Hoffman, B.F., Enson, Y., Farrell, J.E., Brooks, C.M., 1953. Effects of l-Epinephrine and l-Nor-Epinephrine on Cardiac Excitability. Am. J. Physiol. -- Leg. Content 175, 1–7.

Smeets, J., Allessie, M., Lammers, W., Bonke, F., Hollen, J., 1986. The wavelength of the cardiac impulse and reentrant arrhythmias in isolated rabbit atrium. The role of heart rate, autonomic transmitters, temperature, and potassium. Circ. Res. 58, 96–108. doi:10.1161/01.RES.58.1.96

Smith, J., Green, C., Peters, N., Rothery, S., Severs, N., 1991. Altered patterns of gap junction distribution in ischemic heart disease. An immunohistochemical study of human myocardium using laser scanning confocal microscopy. Am. J. Pathol. 139, 801.

Smith, J.H., Green, C.R., Peters, N.S., Rothery, S., Severs, N.J., 1991. Altered patterns of gap junction distribution in ischemic heart disease. An immunohistochemical study of human myocardium using laser scanning confocal microscopy. Am. J. Pathol. 139, 801–821.

Solan, J.L., Lampe, P.D., 2009. Biochemistry of Connexins, in: Harris, A.L., Locke, D. (Eds.), Connexins. Humana Press, Totowa, NJ, pp. 263–286.

Solan, J.L., Marquez-Rosado, L., Sorgen, P.L., Thornton, P.J., Gafken, P.R., Lampe, P.D., 2007. Phosphorylation at S365 is a gatekeeper event that changes the structure of Cx43 and prevents down-regulation by PKC. J. Cell Biol. 179, 1301–1309. doi:10.1083/jcb.200707060

Somekawa, S., Fukuhara, S., Nakaoka, Y., Fujita, H., Saito, Y., Mochizuki, N., 2005. Enhanced Functional Gap Junction Neoformation by Protein Kinase A–Dependent and Epac-Dependent Signals Downstream of cAMP in Cardiac Myocytes. Circ. Res. 97, 655–662. doi:10.1161/01.RES.0000183880.49270.f9

Song, Q., Saucerman, J.J., Bossuyt, J., Bers, D.M., 2008. Differential integration of Ca2+-calmodulin signal in intact ventricular myocytes at low and high affinity Ca2+-calmodulin targets. J. Biol. Chem. 283, 31531–31540. doi:10.1074/jbc.M804902200

Spach, M.S., Dolber, P.C., 1986. Relating extracellular potentials and their derivatives to anisotropic propagation at a microscopic level in human cardiac muscle. Evidence for electrical uncoupling of side-to-side fiber connections with increasing age. Circ. Res. 58, 356–371.

Spray, D.C., White, R.L., Mazet, F., Bennett, M.V., 1985. Regulation of gap junctional conductance. Am. J. Physiol. 248, H753-764.

Straight, A.F., Cheung, A., Limouze, J., Chen, I., Westwood, N.J., Sellers, J.R., Mitchison, T.J., 2003. Dissecting temporal and spatial control of cytokinesis with a myosin II Inhibitor. Science 299, 1743–1747. doi:10.1126/science.1081412

Swain, H.H., Weidner, C.L., 1957. A study of substances which alter intraventricular conduction in the isolated dog heart. J. Pharmacol. Exp. Ther. 120, 137–146.

Taggart, P., Sutton, P., Chalabi, Z., Boyett, M.R., Simon, R., Elliott, D., Gill, J.S., 2003. Effect of adrenergic stimulation on action potential duration restitution in humans. Circulation 107, 285–289.

TenBroek, E.M., Lampe, P.D., Solan, J.L., Reynhout, J.K., Johnson, R.G., 2001. Ser364 of connexin43 and the upregulation of gap junction assembly by cAMP. J. Cell Biol. 155, 1307–1318. doi:10.1083/jcb.200102017

Ungerer, M., Böhm, M., Elce, J.S., Erdmann, E., Lohse, M.J., 1993. Altered expression of beta-adrenergic receptor kinase and beta 1-adrenergic receptors in the failing human heart. Circulation 87, 454–463.

Ungerer, M., Parruti, G., Böhm, M., Puzicha, M., DeBlasi, A., Erdmann, E., Lohse, M.J., 1994. Expression of beta-arrestins and beta-adrenergic receptor kinases in the failing human heart. Circ. Res. 74, 206–213.

Unwin, P.N.T., Zampighi, G., 1980. Structure of the junction between communicating cells. Publ. Online 07 Febr. 1980 Doi101038283545a0 283, 545–549. doi:10.1038/283545a0

Valderrábano, M., 2007. Influence of anisotropic conduction properties in the propagation of the cardiac action potential. Prog. Biophys. Mol. Biol. 94, 144–168. doi:10.1016/j.pbiomolbio.2007.03.014

van Kempen, M.J., ten Velde, I., Wessels, A., Oosthoek, P.W., Gros, D., Jongsma, H.J., Moorman, A.F., Lamers, W.H., 1995. Differential connexin distribution accommodates cardiac function in different species. Microsc. Res. Tech. 31, 420–436. doi:10.1002/jemt.1070310511

Vanslyke, J.K., Naus, C.C., Musil, L.S., 2009. Conformational maturation and post-ER multisubunit assembly of gap junction proteins. Mol. Biol. Cell 20, 2451–2463. doi:10.1091/mbc.E09-01-0062

Varró, A., Lathrop, D.A., Hester, S.B., Nánási, P.P., Papp, J.G.Y., 1993. Ionic currents and action potentials in rabbit, rat, and guinea pig ventricular myocytes. Basic Res. Cardiol. 88, 93–102. doi:10.1007/BF00798257

Veeraraghavan, R., Gourdie, R.G., Poelzing, S., 2014. Mechanisms of cardiac conduction: a history of revisions. Am. J. Physiol. Heart Circ. Physiol. 306, H619-627. doi:10.1152/ajpheart.00760.2013

Veeraraghavan, R., Salama, M.E., Poelzing, S., 2012. Interstitial volume modulates the conduction velocity-gap junction relationship. Am. J. Physiol. Heart Circ. Physiol. 302, H278-286. doi:10.1152/ajpheart.00868.2011

Verheule, S., van Kempen, M.J., te Welscher, P.H., Kwak, B.R., Jongsma, H.J., 1997. Characterization of gap junction channels in adult rabbit atrial and ventricular myocardium. Circ. Res. 80, 673–681.

Vila Petroff, M.G., Egan, J.M., Wang, X., Sollott, S.J., 2001. Glucagon-like peptide-1 increases cAMP but fails to augment contraction in adult rat cardiac myocytes. Circ. Res. 89, 445–452.

Volders, P.G.A., Stengl, M., van Opstal, J.M., Gerlach, U., Spätjens, R.L.H.M.G., Beekman, J.D.M., Sipido, K.R., Vos, M.A., 2003. Probing the contribution of IKs to canine ventricular repolarization: key role for beta-adrenergic receptor stimulation. Circulation 107, 2753–2760. doi:10.1161/01.CIR.0000068344.54010.B3

Vozzi, C., Dupont, E., Coppen, S.R., Yeh, H.-I., Severs, N.J., 1999. Chamber-related Differences in Connexin Expression in the Human Heart. J. Mol. Cell. Cardiol. 31, 991–1003. doi:10.1006/jmcc.1999.0937

Wallace, A.G., Sarnoff, S.J., 1964. Effects of Cardiac Sympathetic Nerve Stimulation on Conduction in the Heart. Circ. Res. 14, 86–92. doi:10.1161/01.RES.14.1.86

Walsh, K.B., Begenisich, T.B., Kass, R.S., 1988. Beta-adrenergic modulation in the heart. Independent regulation of K and Ca channels. Pflüg. Arch. Eur. J. Physiol. 411, 232–234.

Walsh, K.B., Kass, R.S., 1988. Regulation of a heart potassium channel by protein kinase A and C. Science 242, 67–69.

Wang, Q., Li, Z., Shen, J., Keating, M.T., 1996. Genomic organization of the human SCN5A gene encoding the cardiac sodium channel. Genomics 34, 9–16. doi:10.1006/geno.1996.0236

Wang, W., Zhu, W., Wang, S., Yang, D., Crow, M.T., Xiao, R.-P., Cheng, H., 2004. Sustained beta1-adrenergic stimulation modulates cardiac contractility by Ca2+/calmodulin

kinase signaling pathway. Circ. Res. 95, 798–806. doi:10.1161/01.RES.0000145361.50017.aa

Wang, X., Gerdes, A.M., 1999. Chronic Pressure Overload Cardiac Hypertrophy and Failure in Guinea Pigs: III. Intercalated Disc Remodeling. J. Mol. Cell. Cardiol. 31, 333–343. doi:10.1006/jmcc.1998.0886

Wei, C.-J., Xu, X., Lo, C.W., 2004. Connexins and cell signaling in development and disease. Annu. Rev. Cell Dev. Biol. 20, 811–838. doi:10.1146/annurev.cellbio.19.111301.144309

Weingart, R., Imanaga, I., Weidmann, S., 1975. Low resistance pathways between

Myocardial cells. Recent Adv. Stud. Cardiac Struct. Metab. 5, 227-232Weiss, J.N., Chen, P.-S., Qu, Z., Karagueuzian, H.S., Garfinkel, A., 2000. Ventricular Fibrillation How Do We Stop the Waves From Breaking? Circ. Res. 87, 1103–1107. doi:10.1161/01.RES.87.12.1103

Williams, R.L., Vick, R.L., Riopel, D.A., 1972. Intraventricular propagation time: Biphasic effect of epinephrine. J. Electrocardiol. 5, 111–118. doi:10.1016/S0022-0736(72)80026-8

Xiao, R.P., Avdonin, P., Zhou, Y.Y., Cheng, H., Akhter, S.A., Eschenhagen, T., Lefkowitz, R.J., Koch, W.J., Lakatta, E.G., 1999. Coupling of beta2-adrenoceptor to Gi proteins and its physiological relevance in murine cardiac myocytes. Circ. Res. 84, 43–52.

Xiao, R.P., Ji, X., Lakatta, E.G., 1995. Functional coupling of the beta 2-adrenoceptor to a pertussis toxin-sensitive G protein in cardiac myocytes. Mol. Pharmacol. 47, 322–329.

Xiao, R.P., Lakatta, E.G., 1993. Beta 1-adrenoceptor stimulation and beta 2-adrenoceptor stimulation differ in their effects on contraction, cytosolic Ca2+, and Ca2+ current in single rat ventricular cells. Circ. Res. 73, 286–300.

Yao, J.-A., Hussain, W., Patel, P., Peters, N.S., Boyden, P.A., Wit, A.L., 2003. Remodeling of gap junctional channel function in epicardial border zone of healing canine infarcts. Circ. Res. 92, 437–443. doi:10.1161/01.RES.0000059301.81035.06

Yeager, M., 1998. Structure of Cardiac Gap Junction Intercellular Channels. J. Struct. Biol. 121, 231–245. doi:10.1006/jsbi.1998.3972

Yue, D.T., Herzig, S., Marban, E., 1990. Beta-adrenergic stimulation of calcium channels occurs by potentiation of high-activity gating modes. Proc. Natl. Acad. Sci. 87, 753–757.

Zaccolo, M., Filippin, L., Magalhães, P., Pozzan, T., 2001. Heterogeneity of Second Messenger Levels in Living Cells 85–95. doi:10.1002/0470846674.ch8

Zhai, K., Hubert, F., Nicolas, V., Ji, G., Fischmeister, R., Leblais, V., 2012. β-Adrenergic cAMP Signals Are Predominantly Regulated by Phosphodiesterase Type 4 in Cultured Adult Rat Aortic Smooth Muscle Cells. PLoS ONE 7. doi:10.1371/journal.pone.0047826